AD-A038 628 ROCKWELL INTERNATIONAL CANOGA PARK CALIF ROCKETDYNE DIV F/G 20/5
PRESSURE DAMPING FOR PULSED ELECTRIC DISCHARGE LASER.(U)
APR 76 R KESSELRING, R MARCH F29601-73-A-0034
UNCLASSIFIED R-9739 AFWL-TR-75-170 NL

1 OF 2
AD A038628

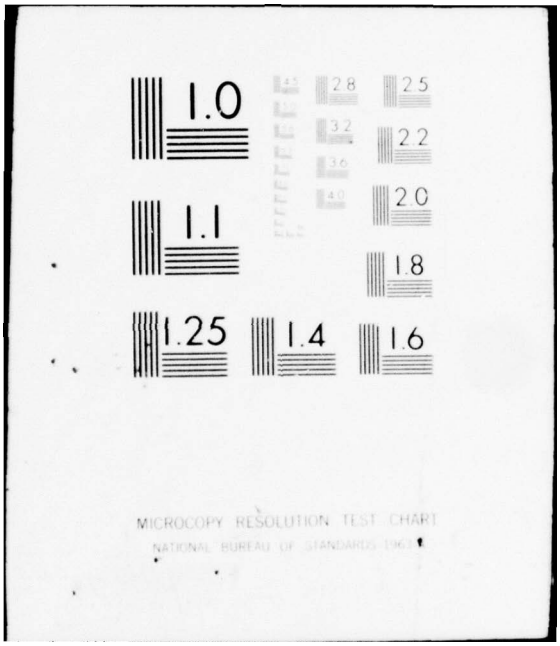
1.0
1.1
1.25
1.4
1.6
2.8
2.5
3.2
2.2
3.6
2.0
4.0
1.8
MICROCOPY RESOLUTION TEST CHART
NATIONAL BUREAU OF STANDARDS 1963

AFWL-TR-75-170

AFWL-TR-
75-170

(2)

PRESSURE DAMPING FOR PULSED ELECTRIC DISCHARGE LASER

R. Kesselring
R. March

Rockwell International
6633 Canoga Avenue
Canoga Park, CA 91304

April 1976

Final Report

AIR FORCE WEAPONS LABORATORY
Air Force Systems Command
Kirtland Air Force Base, NM 87117

AFWL-TR-75-170

This final report was prepared by the Rockwell International, Canoga Park, California, under Contract F29601-73-A-0034-0006, Job Order 317J0516 with the Air Force Weapons Laboratory, Kirtland Air Force Base, New Mexico. Mr. Roy Gene Autry (ALE) was the Laboratory Project Officer-in-Charge.

When US Government drawings, specifications, or other data are used for any purpose other than a definitely related Government procurement operation, the Government thereby incurs no responsibility nor any obligation whatsoever, and the fact that the Government may have formulated, furnished, or in any way supplied the said drawings, specifications, or other data, is not to be regarded by implication or otherwise, as in any manner licensing the holder or any other person or corporation, or conveying any rights or permission to manufacture, use, or sell any patented invention that may in any way be related thereto.

This report has been reviewed by the Information Office (OI) and is releasable to the National Technical Information Service (NTIS). At NTIS, it will be available to the general public, including foreign nations.

This technical report has been reviewed and is approved for publication.

Roy Gene Autry

ROY GENE AUTRY
Project Officer

FOR THE COMMANDER

Peter D. Tannen

PETER D. TANNEN
Lt Colonel, USAF
Chief, Electrical Laser Branch

Robert D. Rose

ROBERT D. ROSE
Colonel, USAF
Chief, Advanced Laser Technology Division

DO NOT RETURN THIS COPY. RETAIN OR DESTROY.

UNCLASSIFIED

SECURITY CLASSIFICATION OF THIS PAGE *(When Data Entered)*

REPORT DOCUMENTATION PAGE

READ INSTRUCTIONS BEFORE COMPLETING FORM

1. REPORT NUMBER: AFWL-TR-75-170
2. GOVT ACCESSION NO.:
3. RECIPIENT'S CATALOG NUMBER:
4. TITLE *(and Subtitle)*: PRESSURE DAMPING FOR PULSED ELECTRIC DISCHARGE LASER.
5. TYPE OF REPORT & PERIOD COVERED: Final Report.
6. PERFORMING ORG. REPORT NUMBER: R-9739
7. AUTHOR(s): R. Kesselring, R. March
8. CONTRACT OR GRANT NUMBER(s): F29601-73-A-0034-0006
9. PERFORMING ORGANIZATION NAME AND ADDRESS: Rockwell International, Rocketdyne Div, 6633 Canoga Avenue, Canoga Park, CA 91304 — 390 199
10. PROGRAM ELEMENT, PROJECT, TASK AREA & WORK UNIT NUMBERS: 63605F; 317J/05/16
11. CONTROLLING OFFICE NAME AND ADDRESS: Air Force Weapons Laboratory, Kirtland Air Force Base, NM 87117
12. REPORT DATE: April 1976
13. NUMBER OF PAGES: 128
14. MONITORING AGENCY NAME & ADDRESS *(if different from Controlling Office)*: 143p.
15. SECURITY CLASS. *(of this report)*: UNCLASSIFIED
15a. DECLASSIFICATION/DOWNGRADING SCHEDULE:

16. DISTRIBUTION STATEMENT *(of this Report)*

Approved for public release; distribution unlimited.

17. DISTRIBUTION STATEMENT *(of the abstract entered in Block 20, if different from Report)*

18. SUPPLEMENTARY NOTES

19. KEY WORDS *(Continue on reverse side if necessary and identify by block number)*

Electric Discharge Laser	Plexiglass Model
Acoustic Absorber	CERCOR
Damp Time	Explosive Charge
Pressure Oscillation	Analog Model

20. ABSTRACT *(Continue on reverse side if necessary and identify by block number)*

The electric discharge in a pulsed electric discharge laser (EDL) produces density disturbances in the gaseous medium which significantly alter the refractive index of the medium and seriously degrade laser beam quality. The use of acoustic absorbers and honeycomb flow conditioners to quickly damp the disturbances in the EDL has shown promise. An experimental study was conducted to further investigate the use of acoustic absorbers and honeycomb flow conditioners as attenuation devices in pulsed EDLs. A plexiglass model of a typical EDL, full scale in two cavity dimensions, was used for the experimental (OVER)

DD FORM 1 JAN 73 1473 EDITION OF 1 NOV 65 IS OBSOLETE 390 199 UNCLASSIFIED

SECURITY CLASSIFICATION OF THIS PAGE *(When Data Entered)*

ABSTRACT (Cont'd)

evaluations. This model was readily varied to provide for: (1) various aperture area and resonator volume acoustic absorbers behind the "anode" area, (2) the addition of CERCOR (glass ceramic) thicknesses of 0.5 inch and 3.0 inches in the flow channels immediately upstream and downstream of the cavity, and (3) various types of flow duct terminations (i.e., open, closed, partially closed, and plenum closed). The discharge was simulated with an explosive charge, and pressure oscillation damp times were determined for various model configurations. A total of 200 pulse tests was conducted on various model configurations. An analysis of AFWL data and the Rocketdyne acoustic model data led to the conclusion that laser cavity modes (2 to 3 kHz) exert relatively little influence in the attenuation of the pressure oscillation. The predominant frequency apparent in the data (≤1 kHz) is related to flow channel modes. The effect of cavity throughflow on damping characteristics was investigated, and no effect of cavity throughflow on the damping characteristics was found over a Mach number range of 0 to 0.10. An acoustic resonator having an aperture open-area of 20 percent and a piston position of about 2 inches appeared optimum from a damping standpoint over the range of EDL flow duct terminations. In some cases, however, such an absorber was not as effective as the use of 3.0-inch CERCOR inserts in the flow channel immediately upstream and downstream of the lasing cavity. An analog model was developed which incorporated the results of the acoustic model testing. This model was used to analytically evaluate high frequency pressure and temperature oscillations in a subsonic, pulsed wave EDL, closed-cycle fluid supply system.

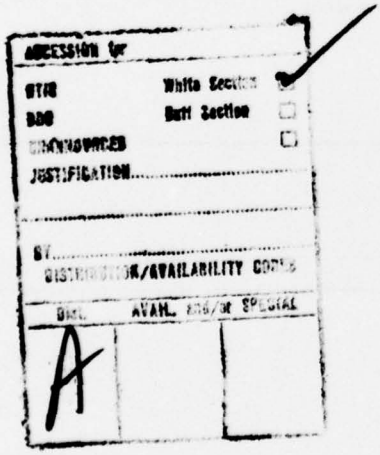

SUMMARY

An experimental study was conducted to further investigate the use of acoustic absorbers and honeycomb flow conditioners to quickly attenuate the oscillations resulting from the discharge in a pulsed electric discharge laser (EDL) device.

A plexiglass EDL model, full scale in two dimensions, was employed in the experimental testing. This model, which consisted of a total channel length of 13 inches with a 8 by 10 cm cavity in its center, was readily varied to provide for: (1) various aperture area and resonator volume acoustic absorbers behind the "anode" area, (2) the addition of CERCOR (glass ceramic) thicknesses of 0.5 inch and 3.0 inches in the flow channels immediately upstream and downstream of the cavity, and (3) various types of flow duct terminations (i.e., open, closed, partially closed, and plenum closed). An explosive device was used to simulate the brisance and amplitude of disturbances resulting from discharge in the AFWL 50-kW device. Measurement of the pressure response subsequent to a "pulse" was made using a Kistler pressure transducer and was recorded on magnetic tape.

A total of 200 pulse tests was conducted on various model configurations. An analysis of the AFWL data and the Rocketdyne acoustic model data led to the conclusion that laser cavity modes (2 to 3 kHz) exert relatively little influence in the attenuation of the pressure oscillation. The predominant frequency apparent in the data (>1kHz) is related to flow channel modes. The effect of cavity throughflow on damping characteristics was investigated, and no effect of cavity throughflow on the damping characteristics was found over a Mach No. range of 0 to 0.10.

For an open-ended, 13-inch-long EDL acoustic model with a predominant frequency of 484 Hz, optimum damping of the pressure oscillation following the pulse was achieved using a 20 percent aperture and a 2-inch piston position in the resonator volume. A factor of 8 reduction in damp time (from 33 msec to 4 msec) was noted. The addition of CERCOR in the flow channel did not improve the damping characteristics of the 20 percent aperture absorber. Simultaneous use of the

optimum absorber configuration and CERCOR also did not result in an improvement over the absorber alone, nor did the addition of CERCOR directly behind the aperture in the resonator volume itself.

For a close-ended 13-inch-long EDL acoustic model with a predominant frequency of 1044 Hz, optimum pressure damping was achieved with a 20 percent aperture and 0-inch piston position. A factor of 2.3 reduction in damp time (from 27 msec to 12 msec) was noted. The acoustic absorber alone is much less effective in this case than a CERCOR thickness of 3.0 inches in damping the pressure oscillation. The 3.0-inch CERCOR results in a factor of 13 reduction in damp time (from 27 to 2 msec). Simultaneous use of 3-inch CERCOR and absorber shows no improvement over the use of CERCOR alone.

For an open-ended 13-inch-long EDL acoustic model containing an array of rods partially blocking the flow area and having a predominant frequency of 304 Hz, optimum damping with a 20 percent aperture was achieved at a piston position of 2 inches. A factor of 1.6 reduction in damp time (from 9.5 to 6 msec) was noted. Use of 3.0-inch CERCOR resulted in an identical amplitude reduction.

The fact that neither optimization of the acoustic absorber nor use of the CERCOR flow conditioner improved damp time by any more than 4 to 5 msec led to the conclusion that the solid rods in the duct inserts (heat exchanger tube simulants) provide a very significant amount of damping by themselves.

A plenum duct termination in the EDL acoustic model resulted in simultaneously occurring frequencies of 570 Hz and 318 Hz which appeared as a predominant frequency of 694 Hz. Optimization of the acoustic absorber occurred with a 20 percent aperture area and a 3-inch piston position. A factor of 5 reduction in damp time (from 73 to 14.5 msec) was noted. A factor of 9 reduction in damp time (from 73 to 8 msec) was achieved, however, through use of a 3.0-inch CERCOR without acoustic resonators.

Summarizing these results, an acoustic resonator having an aperture open-area of 20 percent and a piston position of about 2 inches appeared optimum from a damping standpoint over a range of EDL duct geometry variations. In some cases, however, such an absorber was not as effective as the use of 3.0-inch CERCOR inserts in the flow channel immediately upstream and downstream of the lasing cavity. The use of such inserts involves a pressure drop penalty though that may be undesirable. Such use of flow conditioners may, however, be unnecessary unless it is clearly shown that the damping provided by the acoustic resonator itself is insufficient to acceptably damp the density oscillations.

An analog model was developed which incorporated the results of the acoustic model testing. This model was used to analytically evaluate high frequency pressure and temperature oscillations in a subsonic, pulsed wave EDL, closed-cycle fluid supply system.

PREFACE

This effort was funded under AFWL Contract F29601-75-A-0034-0006. The purpose was to apply acoustic damping techniques and devices to the internal aero-acoustics of pulsed electric discharge lasers. The period of performance was 12 November 1974 through 25 April 1975.

This program was conducted by the Combustion Technology Unit of the Rocketdyne Advanced Programs Department, M. T. Constantine and R. S. Siegler serving as Program Manager and Project Manager, respectively. The project engineer was J. A. Nestlerode and the principal engineer was Dr. R. C. Kesselring. R. D. Marcy and R. L. Nelson performed the analog model analysis. The contract monitor for the Air Force Weapons Laboratory was R. Gene Autry.

CONTENTS

ILLUSTRATIONS

TABLES

SECTION I: INTRODUCTION

The density disturbances produced in the gas laser medium resulting from the discharge in a pulsed electric discharge laser (EDL) significantly alter the refractive index of the medium and seriously degrade the laser beam quality. Propagation of the acoustic disturbances in the gas flow channel could cause laser beam degradation unless the disturbances are sufficiently attenuated.

Rocketdyne, during performance of Contract F29601-73-A-0034-0003, determined that the use of acoustic resonating cavities and honeycomb flow conditioning material could improve pressure damping times up to a factor of six in a non-flowing medium. This work was done using a plexiglass two-dimensional model of a typical EDL, with cavity dimensions full scale to the AFWL 50 kW device (8 by 10 cm). Air was employed as the working fluid in the model. The discharge was simulated with an explosive charge, and damp times were determined for various model configurations.

The objective of this program was to further investigate the use of acoustic resonating cavities and honeycomb flow conditioners as attenuation devices for acoustic disturbances occurring in pulsed EDLs. Experimental studies were limited to flow-damping interaction studies, acoustic resonator optimization studies and duct geometry studies all of which were performed on the existing two-dimensional model of the AFWL EDL lasing cavity. Analytical studies were limited to an analysis of the AFWL EDL acoustic data and to a dynamic analysis of cavity designs on an existing analog model.

SECTION II: EDL MODEL

LUCITE MODEL

A Lucite acoustic model of a typical EDL lasing cavity, and its immediately adjacent flow-channel, was designed and fabricated on Contract F29601-73-A-0034-0003. This design is shown in Fig. 1. The acoustic model provides for the full-scale modeling of both the 10-cm dimension (electrode length or distance between porous glass ceramic plates) and the 8-cm dimension (distance between electrodes). The size of the acoustic model in the remaining (optical path) direction was arbitrarily set at 1 inch (because pressure is assumed to be uniform in that direction in the EDL).

The acoustic model provides for the inclusion of acoustic absorbers (modified Helmholtz resonators) the geometry of which may be easily varied by the adjustment of a piston-type restraint plate at the rear of both anode and cathode absorbers. The length of the absorber cavity may thus be effectively varied between zero (no absorber) and 11 inches on each side of the laser cavity.

A "window" between the laser cavity and the absorber cavity permits investigation of the effect of fractional open area (based on laser cavity cross-sectional area in the discharge direction) of the aperture.

The 10-cm electrode length may be bounded on each end by a plate of CERCOR porous glass ceramic (which could serve in the EDL as a flow conditioner) if desired. The acoustic model accepts two thicknesses (1/2 and 3 inches) of type T2038 CERCOR (Fig. 2).

Flow ducts adjacent to the laser cavity may be modeled acoustically by the insertion of appropriate duct models into the tapered opening on each side of the basic EDL cavity model (see Fig. 1 and 2).

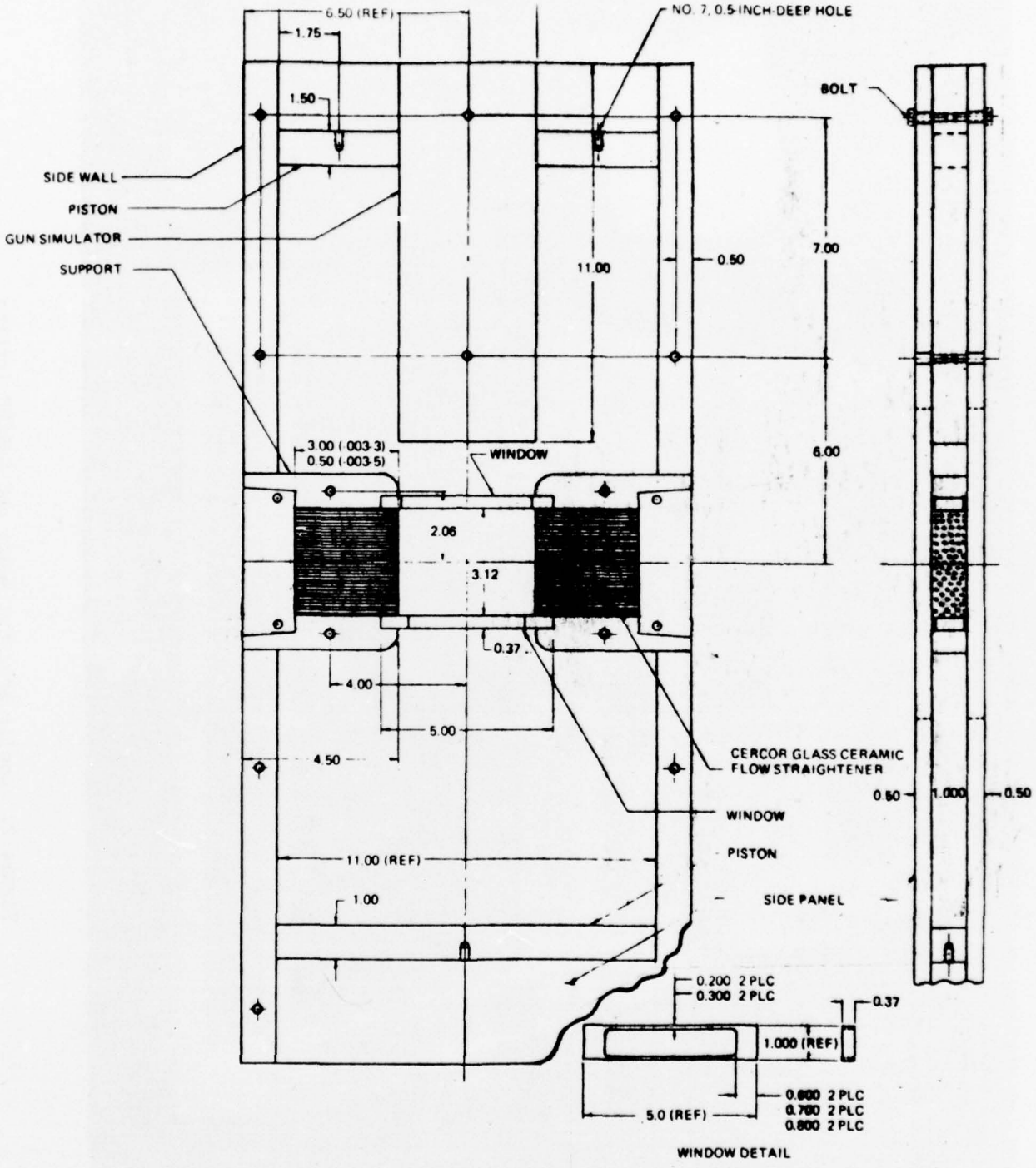

Figure 1. Lucite Acoustic Model of Typical EDL Cavity

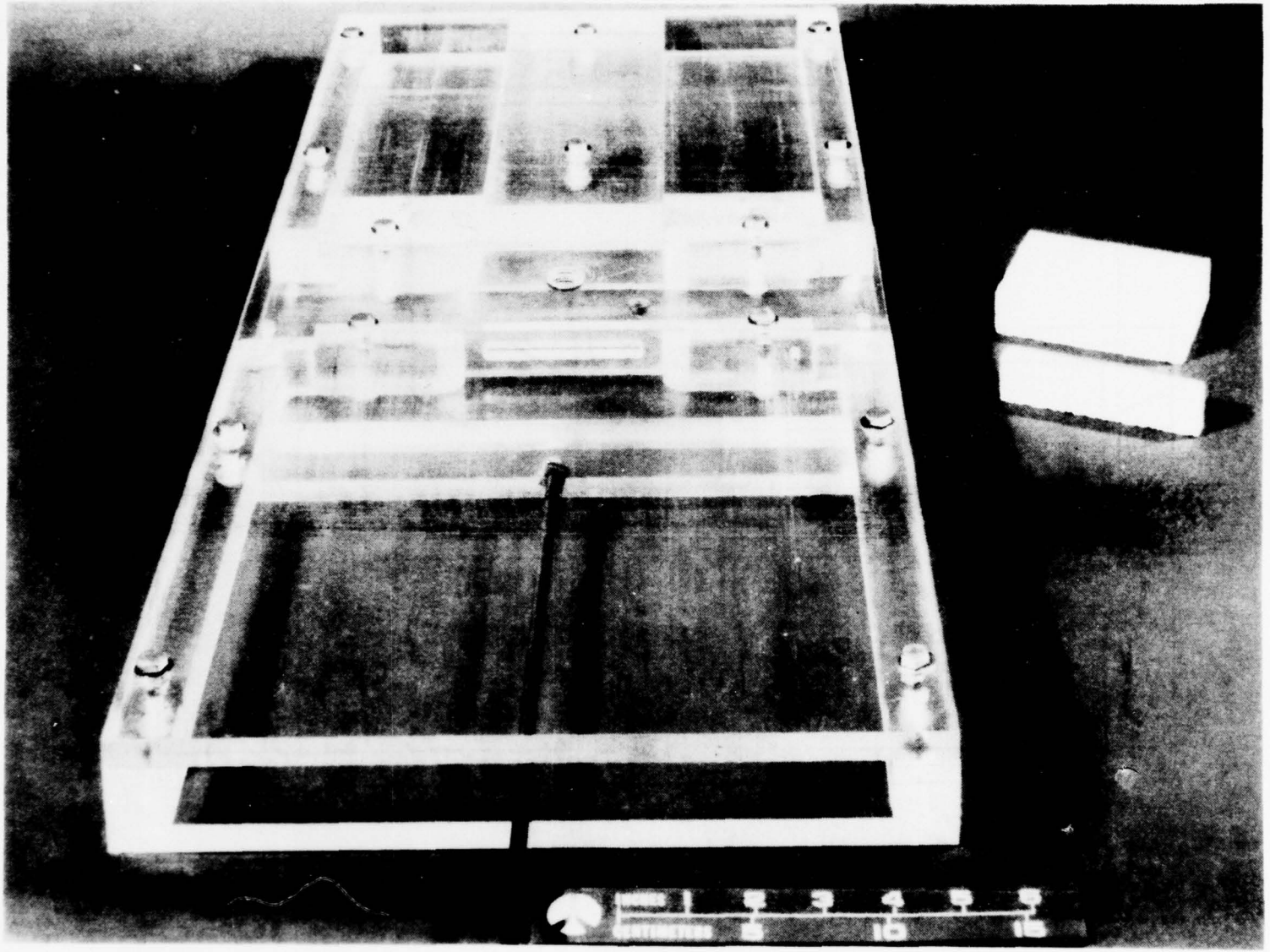

Figure 2. Lucite Acoustic Model and CERCOR Inserts

The large tapped hole located in the center of the lasing cavity (Fig. 2) was used for the insertion of the pulse initiator (explosive charge) which simulates the electrical discharge. A high-response Kistler pressure transducer (Type 603A) was located (on a diagonal) 2 inches away from the pulse initiator in the smaller tapped hole shown in the lasing cavity in Fig. 2.

A 1/8-grain lead styphnate blasting cap was employed for pulse initiation in the Lucite acoustic model. This cap, shown in Fig. 3, was initiated by 25 volts. The adequacy of this device in achieving overpressures and rise rates comparable to AFWL data is documented in Ref. 1.

TEST INSTRUMENTATION

A schematic diagram of the Lucite model test setup is shown in Fig. 4.

An oscilloscope provided an immediate record of the pressure oscillations monitored with the Kistler transducer. A circuit for simultaneous triggering of the pulse initiator and the oscilloscope was employed. A 1-inch tape recorder with 20 kHz response was used to record the test results. This provided a data storage medium that was relatively unrestrictive. A Hewlett-Packard wide-range oscillator was used to obtain a 1000-Hz oscillatory signal having a preset amplitude of 1 volt peak-to-peak. This signal was input to all tape channels for calibration purposes prior to testing.

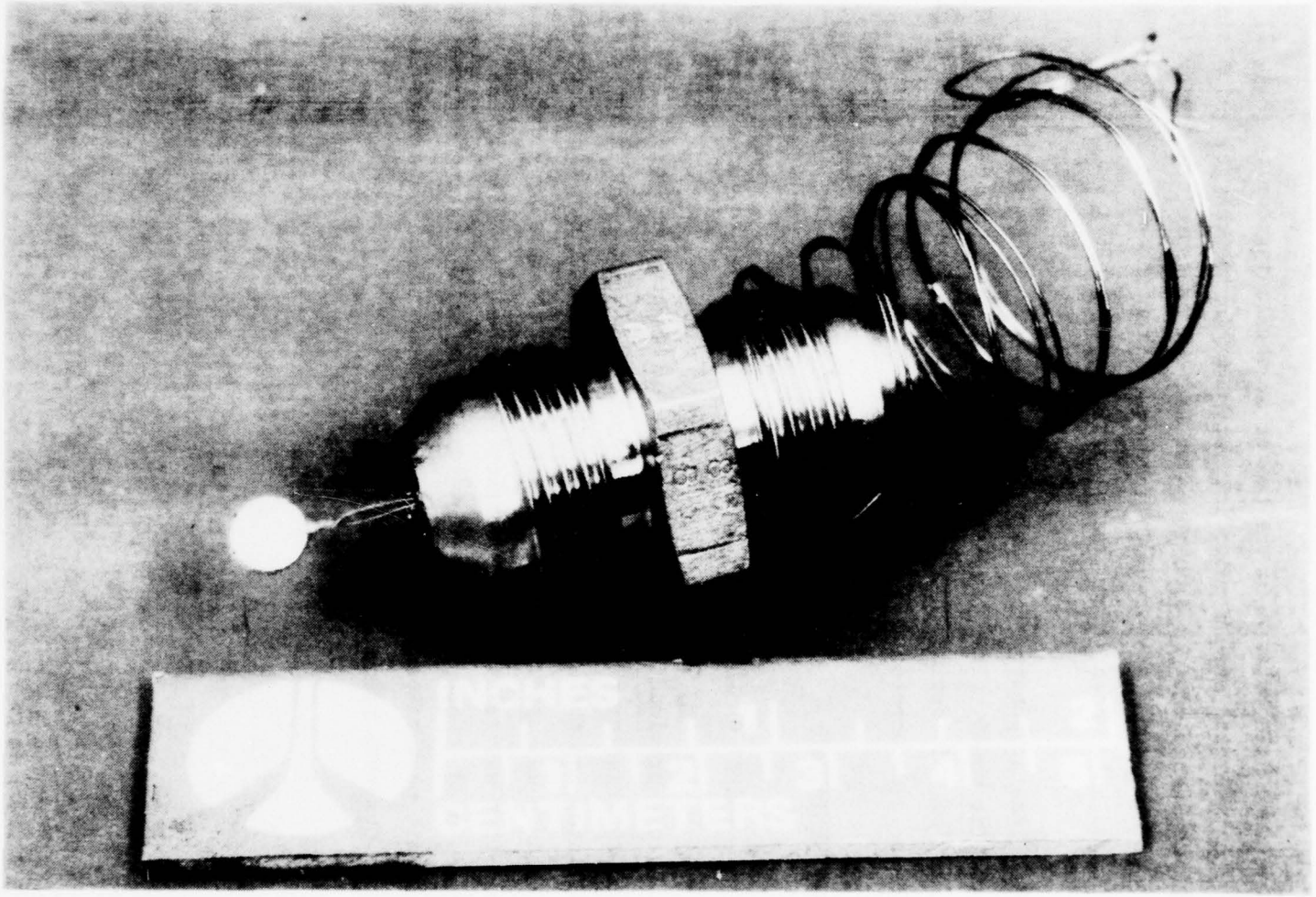

4LE37-4/4/75-S1B

Figure 3. Pulse Initiator

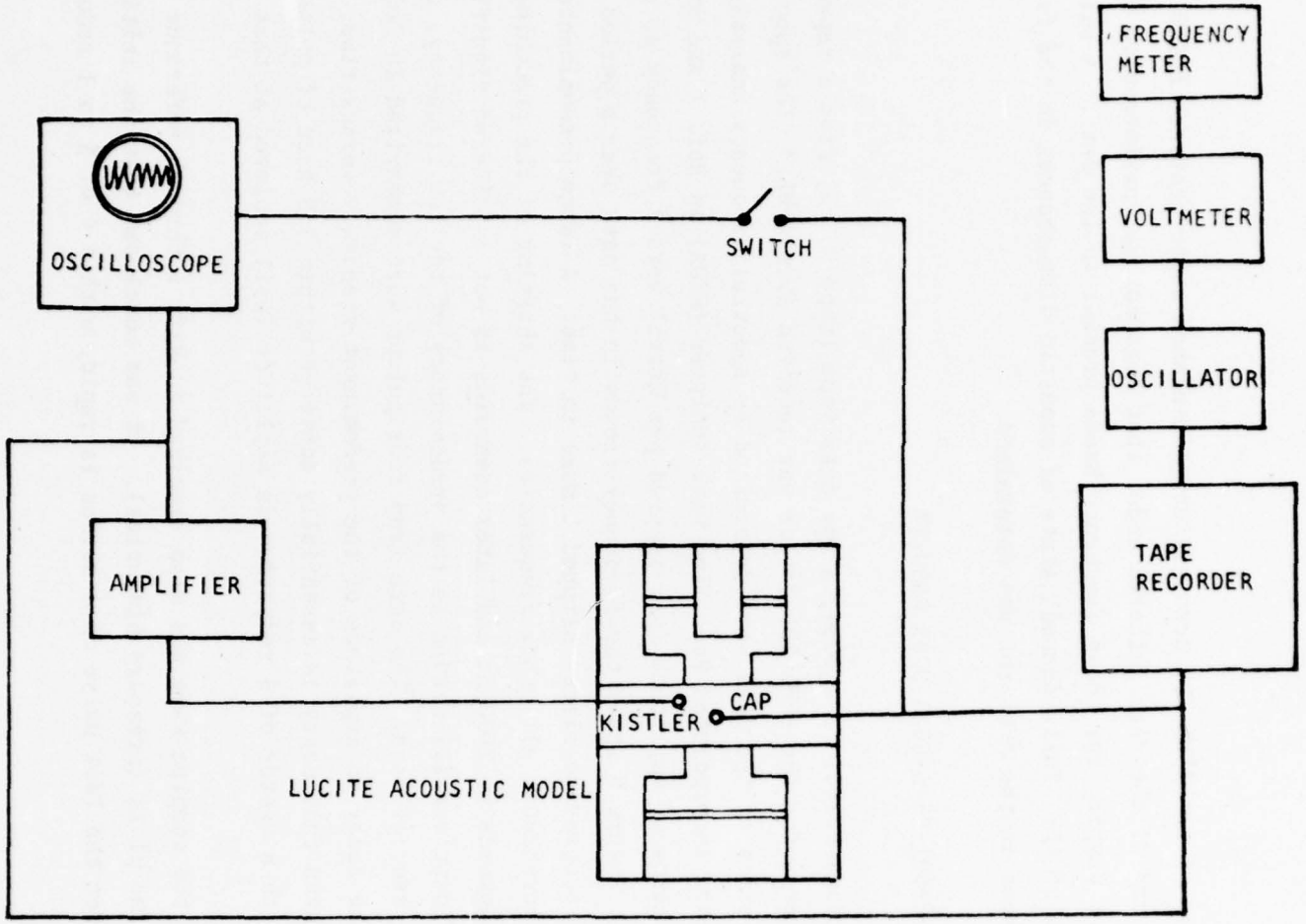

Figure 4. Test Setup for Bench-Scale Acoustic Testing

SECTION III: TASK 1 - ANALYSIS OF AFWL EDL ACOUSTIC DATA

SCOPE

An analysis of the AFWL EDL acoustic data furnished under Contract F29601-73-A-0034-0003 and of the data gathered under that contract was performed to determine the rate of damping for those frequency bands present in the data. A suitable definition of the "fully damped" state of acoustic disturbances in the frequency bands present in the AFWL EDL was determined.

CONTRACT F29601-73-A-0034-0003 RESULTS

Under Contract F29601-73-A-0034, a raw data tape (tape No. 5) from a representative discharge for the AFWL-EDL device was received from AFWL.* The spectral characteristics of the data were determined by spectral frequency analysis using the Time Data Incorporated Real Time Data Analyzer (RTDA) in Ref. 1 and are displayed in terms of amplitude (psi squared per Hertz) versus frequency as shown in Fig. 5. Figure 5 shows the frequency trends in the data over a period of 6 msec, with successive slices slipped 1 msec in time. A large predominance of $\sim$500 Hz overshadows all other frequencies. The shifting of the predominant frequency upwards to 2000 Hz and later downwards is not considered significant. The significant overall result is the predominance of the low frequency, even for only 1 msec of data. The data from four pulses were summarized in Ref. 1 by plotting the decay in amplitude of the predominant frequency versus time. These data indicated that decay is essentially achieved within 2.5 msec of pulse initiation, with a factor of 5 reduction in amplitude (psi) achieved at that time.

Damping of the complex wave was also examined in Ref. 1 through reference to pressure-time plots (pressure histories). It was concluded that the initial damping after the last pulse of a series is rapid, with a 4 or 5 to 1 reduction

*Also received were comments that associated holographic measurements indicated damping to acceptable beam quality in 4 milliseconds.

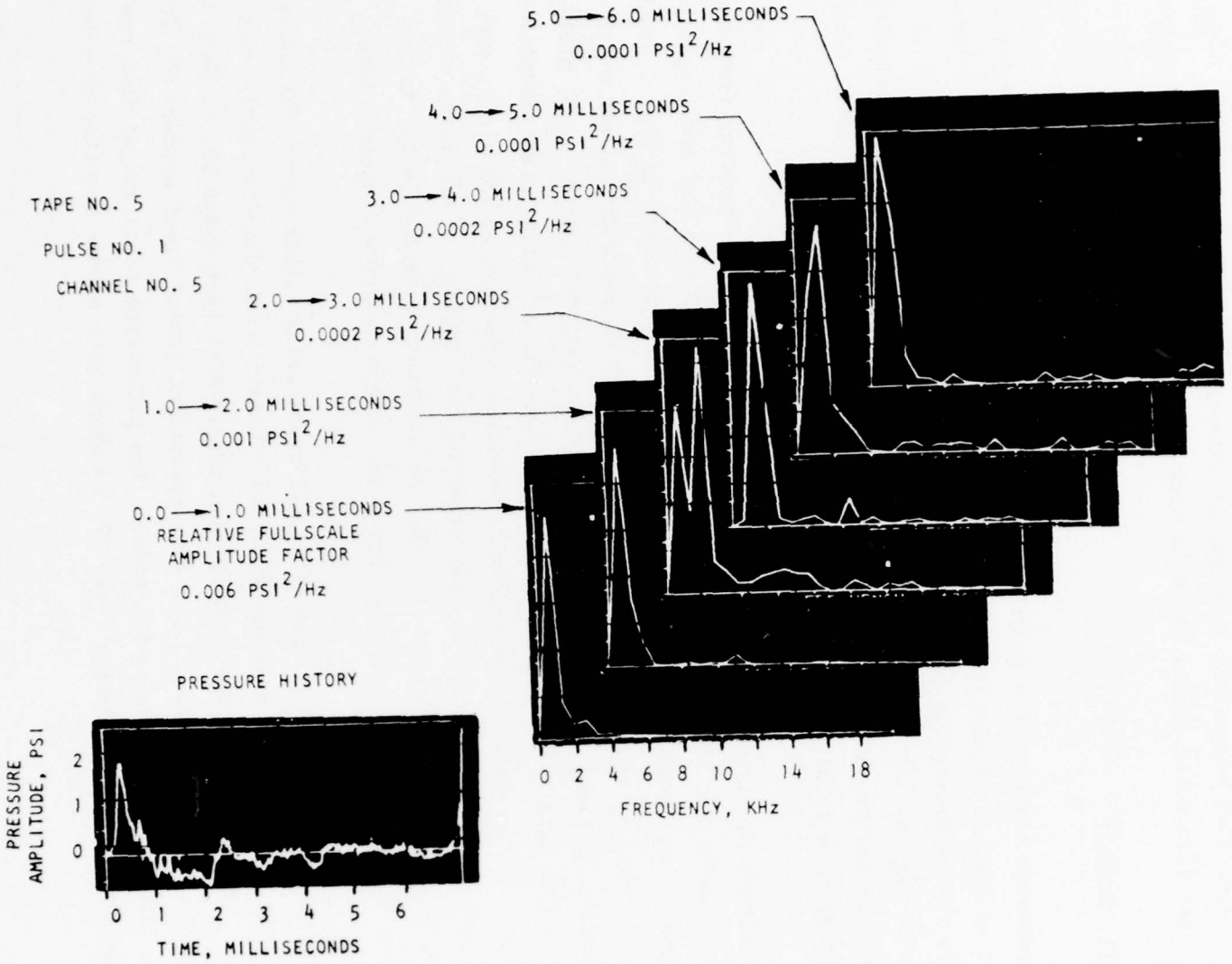

Figure 5. RTDA Spectral Analysis for Shot No. 19

in amplitude occurring in 2.5 to 4 msec. However, damping to a significantly lower level (7:1 reduction) requires an order of magnitude longer time. This trend was also noted in Ref. 1 to be true of the individual sinusoidal components.

CURRENT RESULTS

The pressure history of a representative discharge for the AFWL-EDL device is shown in Fig. 5. A similar pressure history of the detonation of an explosive charge in the Rocketdyne Lucite model of the EDL (Test No. 27 in Ref. 1) is shown in Fig. 6. In Fig. 5 and 6, it is observed that the initial overpressure appears to excite oscillations of relatively high frequency which decay rapidly, resulting in a final predominance of lower-frequency oscillations.

The spectral characteristics of the data were determined by spectral frequency analysis using the Time Data Incorporated Real Time Analyzer and are displayed in terms of amplitude (psi squared per Hertz) versus frequency in Fig. 5 and 6, also. In Fig. 5, the large preponderance of ~500 Hz overshadowed all other frequencies, a trend typical of nearly all power spectral density (PSD) plots for the AFWL data. In the Rocketdyne data (Fig. 6), a similar preponderance of about 400 Hz overshadowed the higher frequencies. Successive PSD plots, such as shown in Fig. 5 and 6, yield an indication of the damping of individual sinusoidal oscillations as a function of time. An alternative method is to examine pressure history plots of oscillations lying within a narrow frequency band.

Consequently, pressure histories of oscillations lying within narrow frequency bands were generated for a selected series of tests whose data currently existed on tape. This series of tests included a single AFWL test (Tape No. 5, Shot No. 19, Channel No. 5, last pulse) and five Rocketdyne tests* (test numbers 27, 26, 45, 61, and 71) on the Lucite EDL model. The Rocketdyne tests ranged from one that had no attenuation device (test 27) to those with either acoustic absorbers

*Reported in Ref. 1.

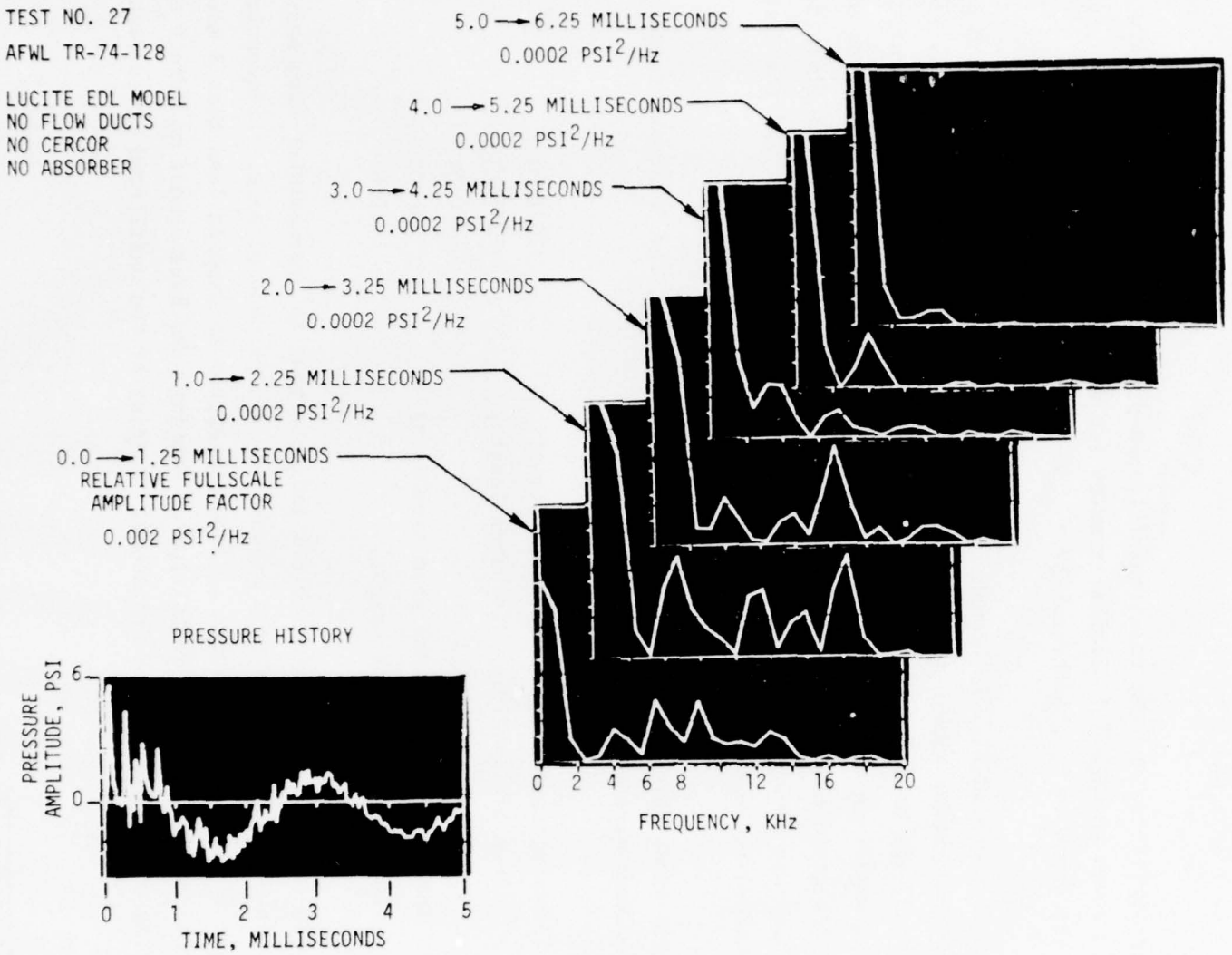

Figure 6. RTDA Spectral Analysis for Test No. 27

of a particular aperture open area or with CERCOR flow conditioners. The following frequency bands were arbitrarily selected: 100 Hz to 1 kHz, 1 to 2 kHz, 2 to 4 kHz, 4 to 5 kHz, and 5 to 10 kHz.

Both the unfiltered and the resultant filtered pressure histories for the AFWL data are shown in Fig. 7.* Similar results for Rocketdyne tests 27, 26, 45, 61, and 71 are shown in Fig. 8 through 12.*

The results shown in Fig. 7 through 12 were used to calculate damp times and predominant frequencies within the various frequency bands. Damp time, for each frequency band, was arbitrarily defined as the time required for the peak-to-peak oscillation amplitude to fall to 1/7 of the initial average† undamped overpressure for the 1/8 grain charge. The predominant frequency apparent within a given frequency band was obtained by reference to the time scale. A summary of the data thus obtained is found in Table 1.

Assuming a sound velocity of 1474 fps in the AFWL device, the following frequency estimates were made for various modes:

Lasing cavity (8-cm discharge direction)	2810 Hz
Lasing cavity (10-cm discharge length)	2245 Hz
Mirror box (22-inch length)	400 Hz
Lasing cavity (44-inch beam direction)	200 Hz
Flow channel (1-foot height)	740 Hz

The results shown in Fig. 7 and Table 1 indicate that the predominant frequency apparent in Fig. 5 is related most probably to a flow channel mode. Frequencies indicative of lasing cavity modes (> 2000 Hz) appear to damp in less than 5 msec (using the previously stated definition of damping) and have almost no effect on the damping of the predominant frequency. Damping of the unfiltered trace requires

*Filtered pressure histories appear inverted with respect to the unfiltered trace.
†Average for all charges used in the program.

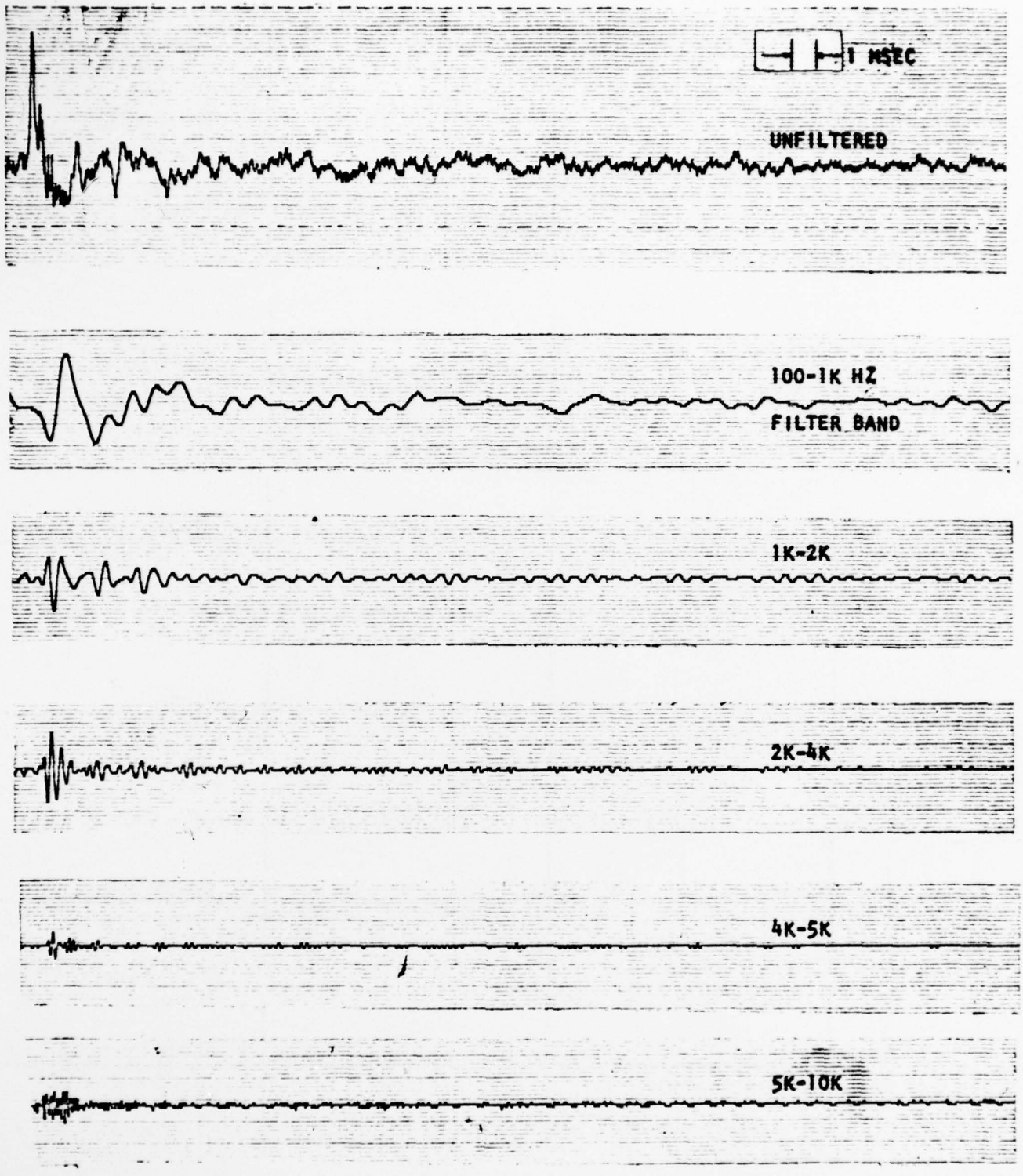

Figure 7. Pressure History for AFWL Tape No. 5, Run No. 19, Final Pulse

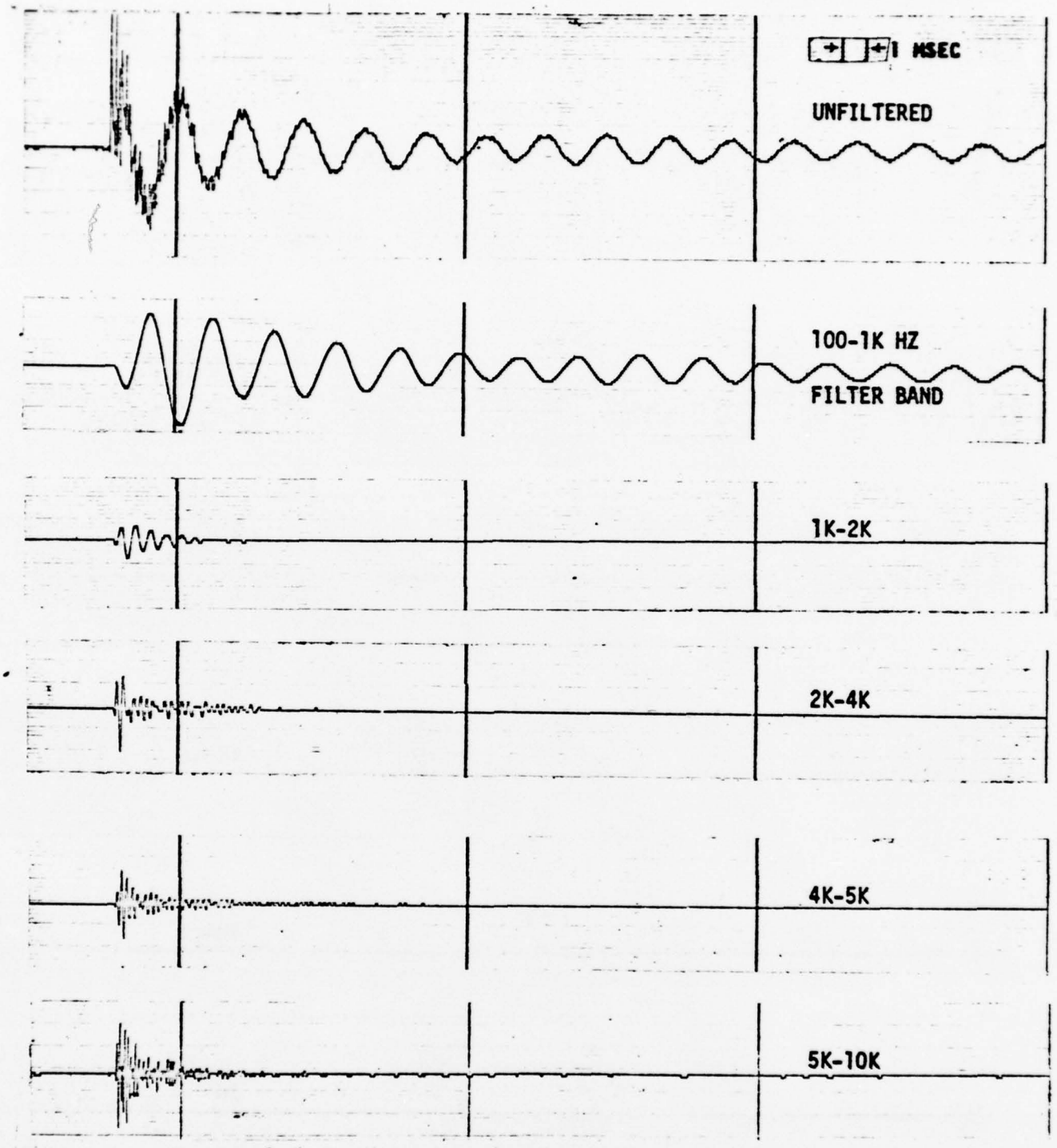

Figure 8. Pressure History for Rocketdyne Test No. 27; No CERCOR, No Acoustic Resonator

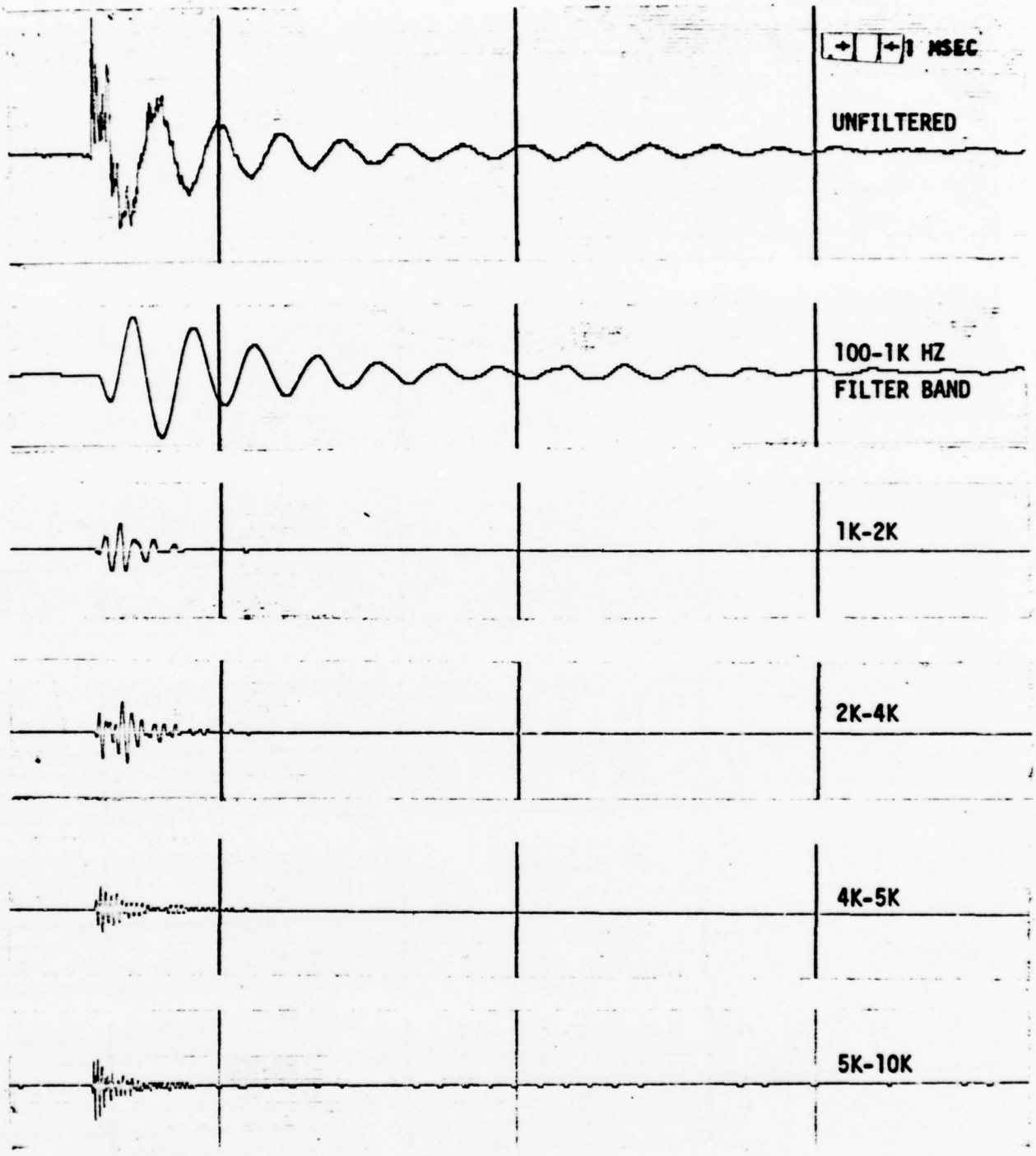

Figure 9. Pressure History for Rocketdyne Test No. 26; 0.5-Inch CERCOR, No Acoustic Absorber

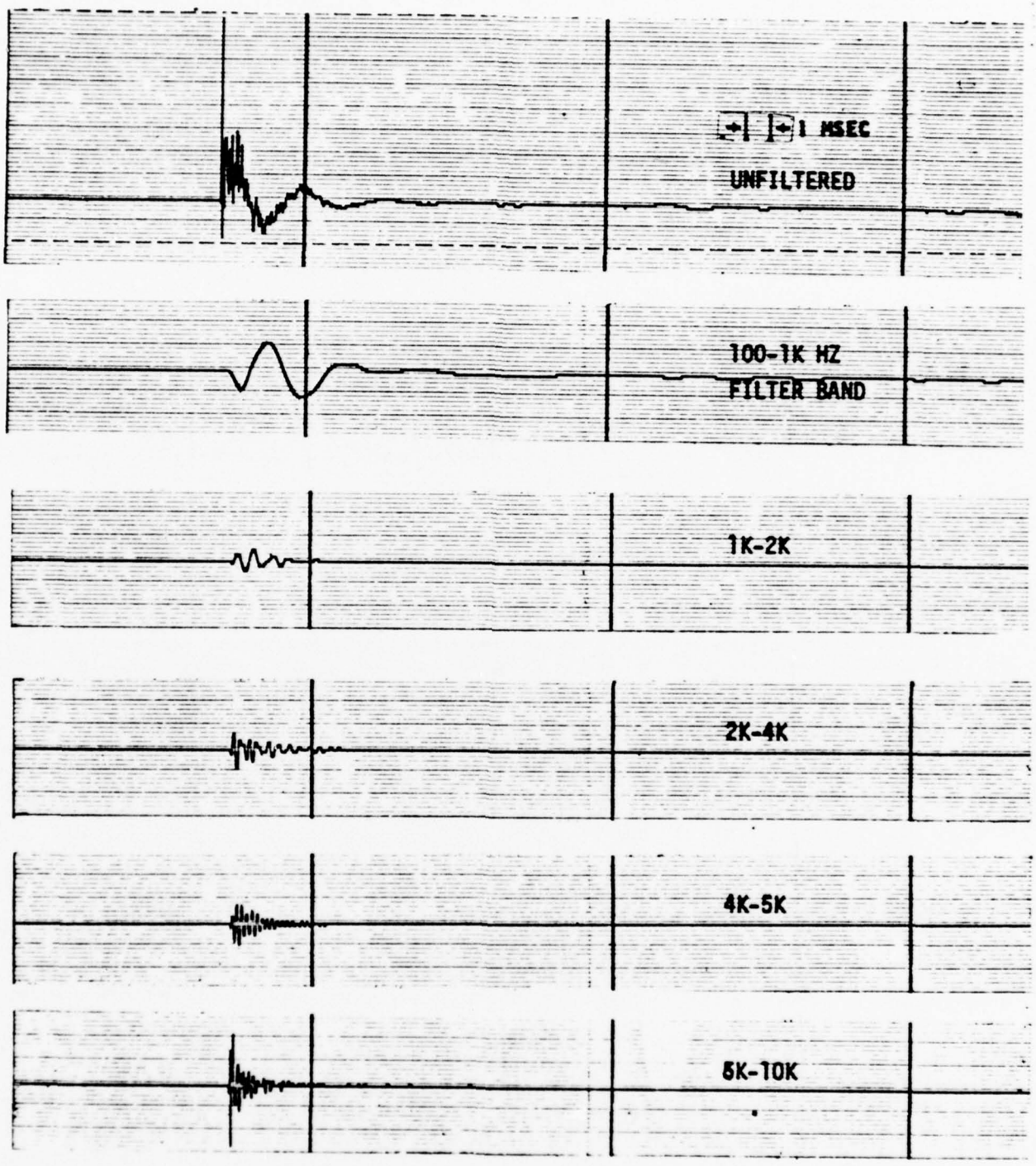

Figure 10. Pressure History for Rocketdyne Test No. 45; 3.0-Inch CERCOR, No Acoustic Resonator

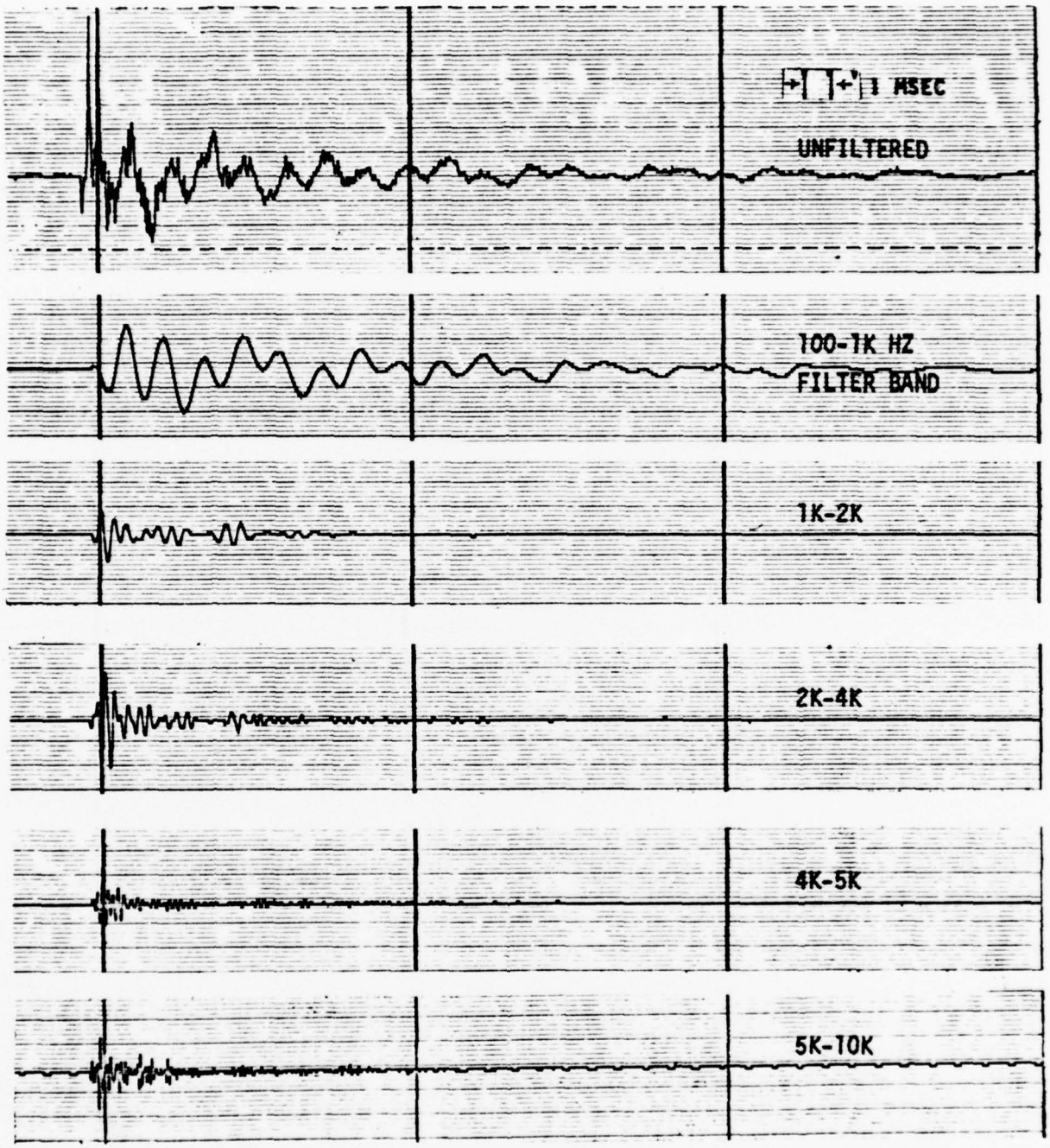

Figure 11. Pressure History for Rocketdyne Test No. 61; No CERCOR, Acoustic Resonator With 76% Open-Area and 5-Inch Piston Position

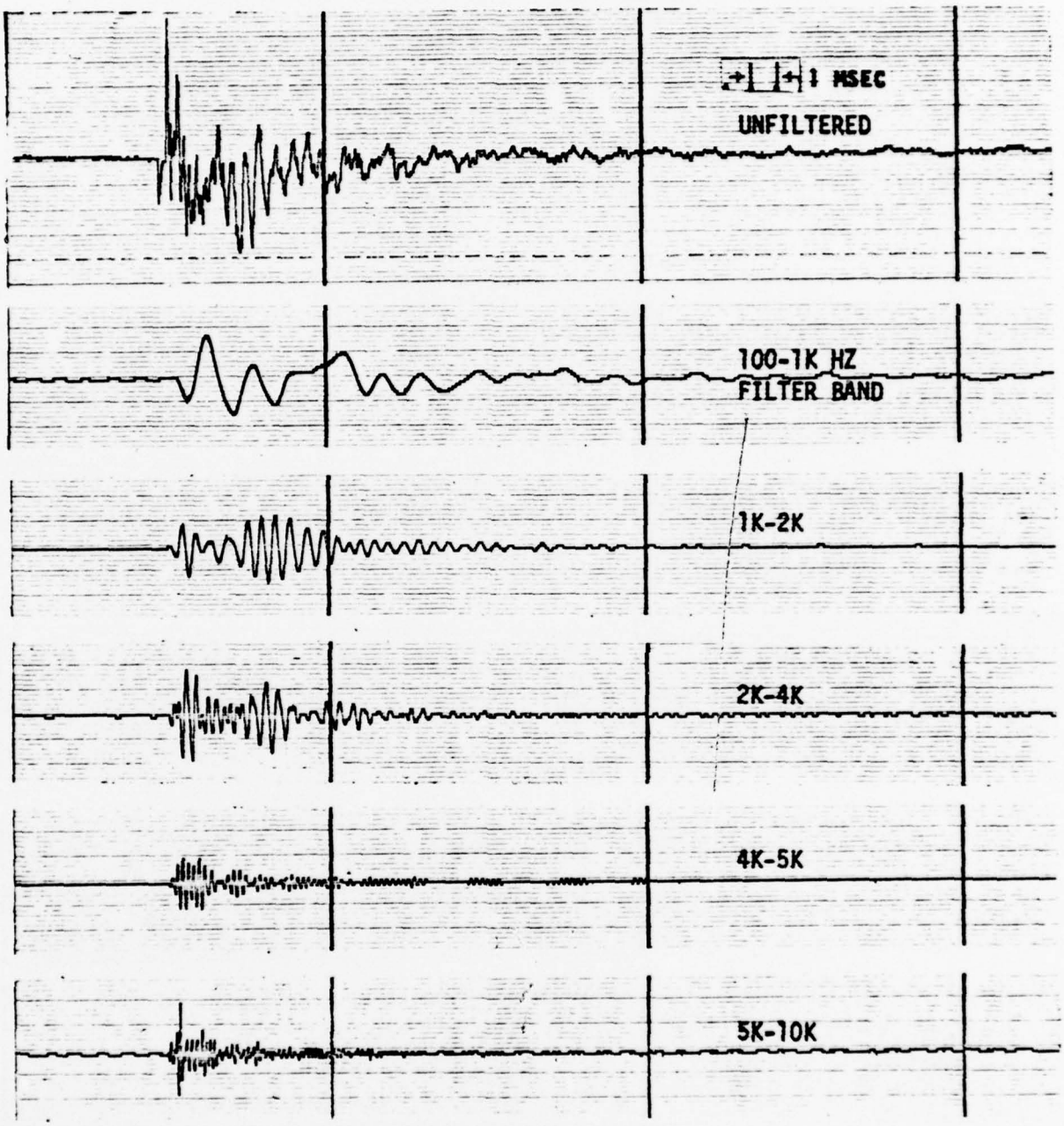

Figure 12. Pressure History for Rocketdyne Test No. 71; No CERCOR, Acoustic Resonator With 34% Open Area and 4-Inch Piston Position

TABLE 1. TASK 1 DATA SUMMARY

Test No.	CERCOR	Aperture Open Area*	Anode Piston Position	Damp Time and Predominant Frequency Within Filtered Band					
				Unfiltered	100-1K	1K-2K	2K-4K	4K-5K	5K-10K
AFWL Tape 5 Run 19	-	-	-	43 msec -	25 msec 883 Hz	6 msec 1320 Hz	5 msec 2170 Hz	1 msec 4000 Hz	2 msec 6430 Hz
27	None	76%	0	38 msec 373 Hz	38 msec 373 Hz	2.5 msec 1540 Hz	3 msec 3530 Hz	2 msec 4660 Hz	3 msec 6000 Hz
26	0.5 in.	76%	0	15 msec 388 Hz	15 msec 388 Hz	2.5 msec 1303 Hz	2 msec 2790 Hz	1.5 msec 4500 Hz	2 msec 5000 Hz
45	3.0 in.	76%	0	5 msec 313 Hz	5 msec 313 Hz	1.5 msec 1393 Hz	1 msec 2780 Hz	1.5 msec 4660 Hz	2 msec 5330 Hz
61	None	76%	5 in.	19 msec 620 Hz	19 msec 620 Hz	7 msec 2000 Hz	7 msec 2500 Hz	2 msec 4000 Hz	3 msec 5000 Hz
71	None	34%	4 in.	12 msec 1665 Hz	12 msec 550 Hz	7 msec 1755 Hz	8 msec 2000 Hz	3 msec 4290 Hz	4 msec 5450 Hz

*The aperture open area is expressed as a percentage of the total possible aperture area (4.00 in. x model thickness of 1 in.)

a somewhat greater time (about 42 msec) than does damping of the 100 Hz to 1 kHz frequency band ($\sim$25 msec). This is due to the persistance of small oscillations (within the definition of damped oscillations) in some of the other frequency bands (see Fig. 7).

Assuming a sound velocity of 1140 fps (air) in the ductless Lucite acoustic model, the following frequency estimates were made for various modes:

Lasing cavity (3.12-inch direction)	2190 Hz
Lasing cavity (4.00-inch direction)	1710 Hz

The results shown in Fig. 8 and Table 1 indicate that the predominant oscillation frequency of approximately 375 Hz corresponds to the first acoustic mode in the open-open flow direction of 13 inches in the ductless model. This was verified in Ref. 1 by probing techniques. As in the AFWL data, frequencies indicative of lasing cavity modes damp in less than 4 msec and appear to have no effect on the damping of the predominant frequency.

The effect of CERCOR may be examined by reference to Fig. 8 through 10 and Table 1. Increasing the CERCOR thickness in the flow channels immediately upstream and downstream of the lasing cavity results in a pronounced decrease in both the unfiltered damp time and the damping time of the predominant oscillation frequency (313 Hz < freq. < 388 Hz). A much less pronounced decrease in the damp time of oscillation frequencies over 1300 Hz is also evident. The CERCOR thus appears to be most effective in damping the relatively low frequency pressure oscillations which control the overall system damping.

The effect of the presence of an anode acoustic resonator on the pressure oscillation damping is observed by reference to Fig. 8, 11, 12, and Table 1. Use of an anode absorber having a 76 percent aperture open area and 5-inch piston position is observed to result in a decrease from 38 to 19 msec in the overall damp time. An equivalent decrease is noted in the damp time of the prominent lower frequency oscillation although the frequency of this oscillation is shifted from

373 to 620 Hz. Damp times of oscillation frequencies in the range 1500 to 3000 Hz appear to increase while the damp times of oscillation frequencies greater than 4 kHz remain nearly unchanged. Oscillation amplitudes of the later oscillation frequencies, however, appeared to decrease in value with the addition of the acoustic resonator.

The effect of the addition of an anode absorber with an aperture open area of 34 percent and a 4-inch piston position is observed to result in a decrease from 38 to 12 msec in the overall damp time. While an equivalent decrease in damp time is noted for the 100 Hz to 1 kHz frequency band, the unfiltered pressure trace no longer clearly shows a prominent frequency equal to that apparent in the 100 Hz to 1 kHz frequency band data. Compared to test 27 (no absorber), both the damp time and oscillation amplitude of oscillations having frequencies in the range 1500 to 2500 Hz are increased significantly. Damp time of frequencies greater than 4 kHz also indicate increases over the "no absorber" data.

It is apparent that the decrease in the unfiltered damp time occasioned by the addition of the 34 percent aperture open area absorber is due solely to the effectiveness of this absorber at relatively low ($\sim$550 Hz) frequency. The overall appearance suggests energy is removed from the 100 Hz to 1 kHz frequency band and added to the higher frequency bands.

The addition of the 76 percent aperture open area absorber, while more effective than the 34 percent open area absorber at frequencies above 1500 Hz, is not as effective at 550 Hz. The effectiveness of an absorber at this lower frequency is, however, what controls the overall damp time in this particular geometry.

It is concluded that laser cavity modes exert little influence in the attenuation of the pressure oscillation. Flow channel geometry is believed to be the most important factor. The present method of determining damp time, i.e., measuring the time required for the peak-to-peak pressure oscillation to fall to a specified fraction (1/7) of its average initial value is believed satisfactory for use in further test effort. The importance of the flow channel geometry suggests that

pressure oscillations in any EDL system may commonly contain a relatively low predominant frequency (as compared to the frequencies associated with lasing cavity modes). Low oscillation frequencies may be attenuated rapidly through the use of such honeycomb material as CERCOR in the flow channel and/or moderate aperture open-area acoustic resonators. The designer of attenuation devices, however, must exercise caution lest more rapid damping of the predominant lower frequency oscillations (characteristic of flow channel modes) be achieved at too great expense of higher frequency oscillations (possibly characteristic of lasing cavity modes).

SECTION III: FLOW EXPERIMENTS

SCOPE

Nitrogen gas (GN_2) was used to simulate air flow at a Mach number of 0.1 through the cavity section of the Lucite acoustic model. Pressure measurements were made, and damp time determined, for flow and no-flow tests using: no CERCOR flow conditioner, 0.5-inch CERCOR, and 3.0-inch CERCOR in the flow channels immediately upstream and downstream of the lasting cavity. By comparison of the results of flow and no-flow tests, the effect of cavity throughflow on damping was determined.

TEST SETUP

As a means of obtaining a constant high Mach number flow in the model, a large volume high-pressure gas source was sought whose pressure is unaffected by the volumetric flow through the model and whose flowrate can be precisely controlled. The 2000-psig GN_2 system used for propellant tank pressurization at Rocketdyne was selected for this use. The properties of nitrogen are almost identical to air near ambient temperature and pressure conditions (see Table 2) and thus provide adequate simulation in the model.

TABLE 2. GAS PROPERTIES

Gas	T, F	ρ, lb/ft^3	$\mu \times 10^5$, lb/ft-sec	a, ft/sec
Air	0	0.086	1.110	1053
Air	100	0.071	1.285	1166
N_2	0	0.084	1.055	1070
N_2	100	0.069	1.222	1180

A schematic of the GN_2 flow system is shown in Fig. 13. A sonic orifice having a diameter of 0.100 inch was placed in the 1-inch line upstream of the Lucite model in order to provide a mass flowrate of GN_2 dependent only upon the pressure upstream of the sonic orifice (independent of downstream ΔP).

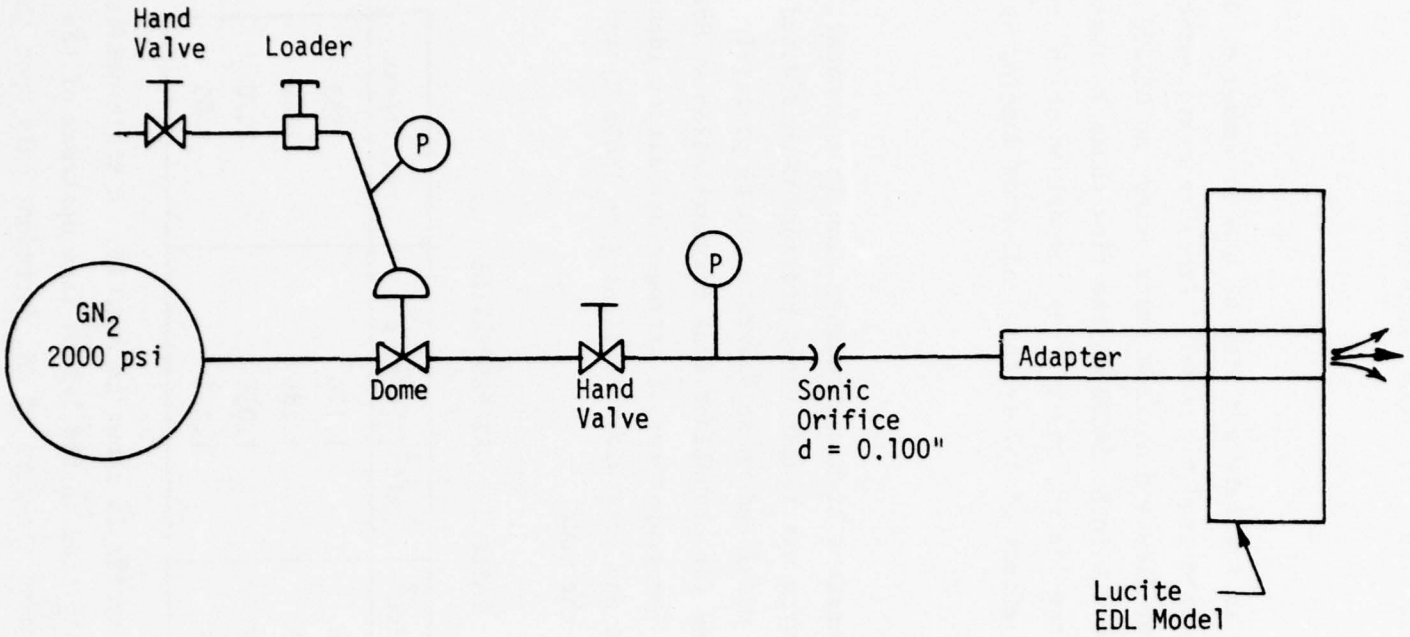

Figure 13. Nitrogen Gas Flow System

An aluminum adapter section shown in Fig. 14 and 15 was fabricated to allow for orderly transition from a velocity of about 535 fps in the 1-inch line immediately downstream of the sonic orifice to a value of 114 fps (Mach No. = 0.100) in the Lucite EDL model. To further ensure a uniform gas flowfield in the model, a series of fine-mesh screen was placed near the exit end of the adapter. The velocity through the cavity section was measured and confirmed to be 114 fps or a Mach No. of 0.1.

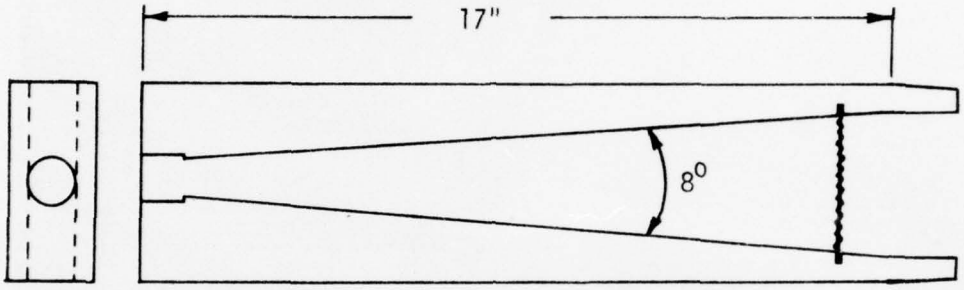

Figure 14. Aluminum Adapter

RESULTS

A series of GN_2 flow tests was then performed at a constant velocity of 114 fps (Mach No. = 0.10) through the model. A 20% aperture open-area window was employed in the anode absorber while a 0% open-area (solid) window was employed in the cathode absorber.

Tests were made in the open-ended model* with and without CERCOR inserts in the flow channel over a range of piston positions (acoustic resonator volumes). A test summary is found in Table 3. Resulting pressure histories are shown in Fig. 16 to 18. Damp time comparisons are shown in Fig. 19.

*The aluminum adapter, of course, was attached to the one end of the model.

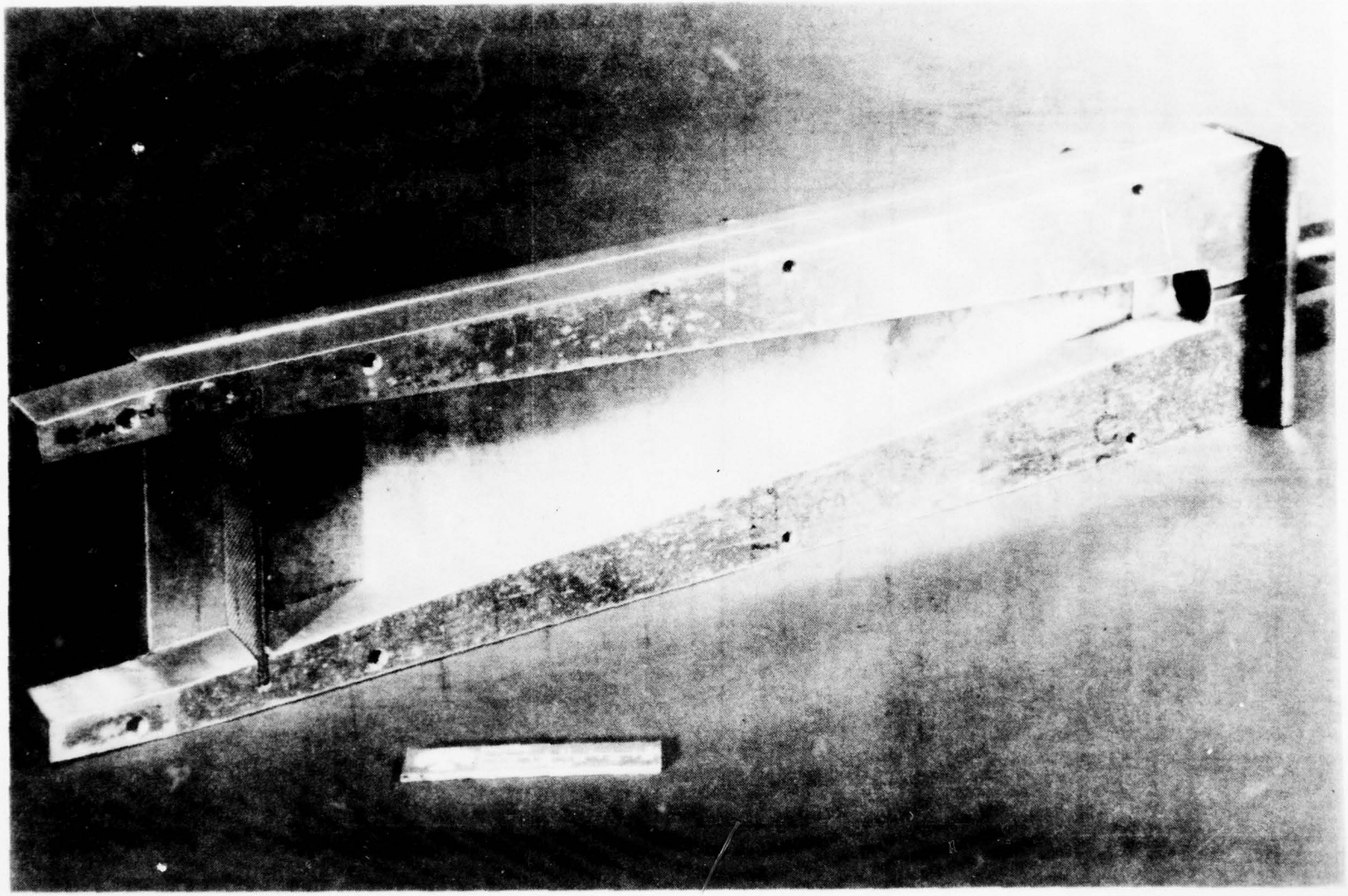

4LE37-4/4/75-S1F

Figure 15. Adapter for Flow Tests

TABLE 3. TASK 2 TEST SUMMARY

Test No.	Anode Window Open Area, percent	CERCOR	Anode Piston Position, inch	M = 0.1 Flow	Damp Time, msec
1	20	None	0	no	3.5
2			0	yes	4.5
3			2	no	5.0
4			2	yes	6.0
5			4	no	4.0
6			4	yes	5.5
7		0.5 in.	0	no	4.0
8			0	yes	3.5
9			1	no	3.0
10			1	yes	2.5
11			2	no	4.0
12			2	yes	3.0
13			4	no	3.0
14			4	yes	3.5
15		3.0 in.	0	no	2.0
16			0	yes	1.5
17			1	no	2.0
18			1	yes	2.0
19			2	no	2.0
20			2	yes	2.0
21			4	no	2.5
22			4	yes	2.0

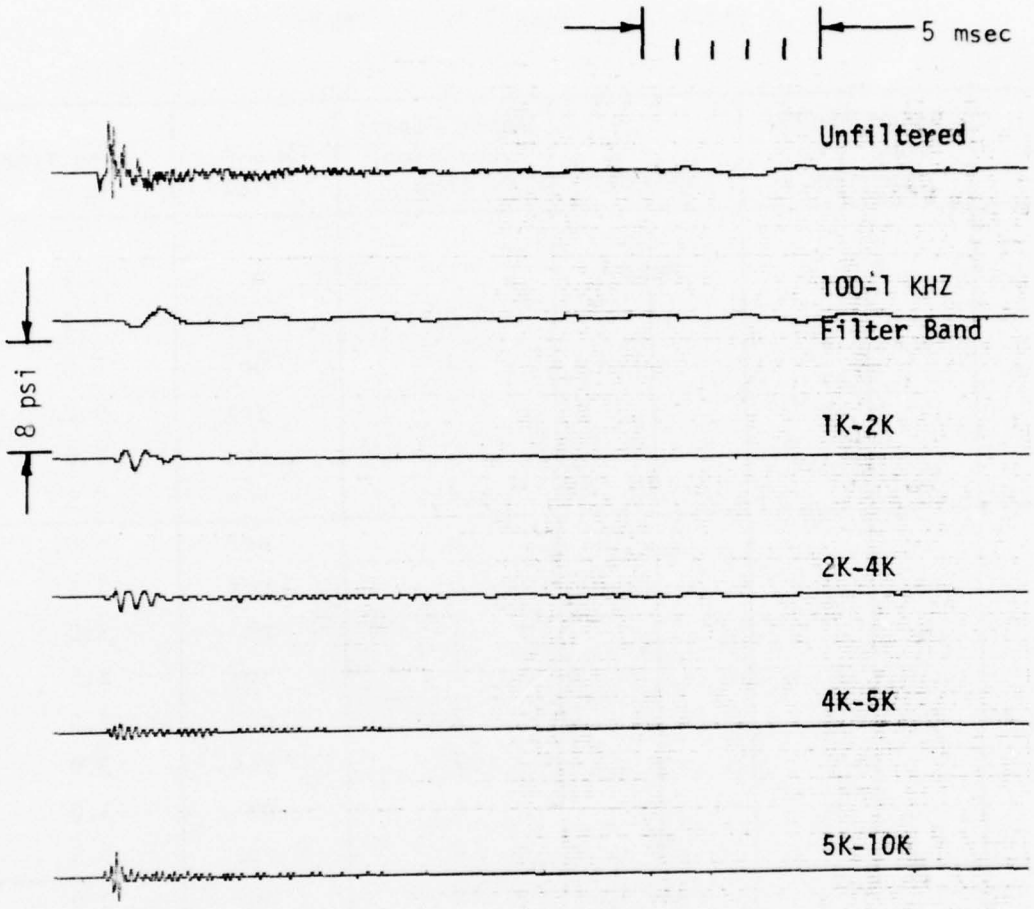

Figure 16. Pressure History for 20% Aperture Open-Area, no CERCOR, no Cavity Throughflow

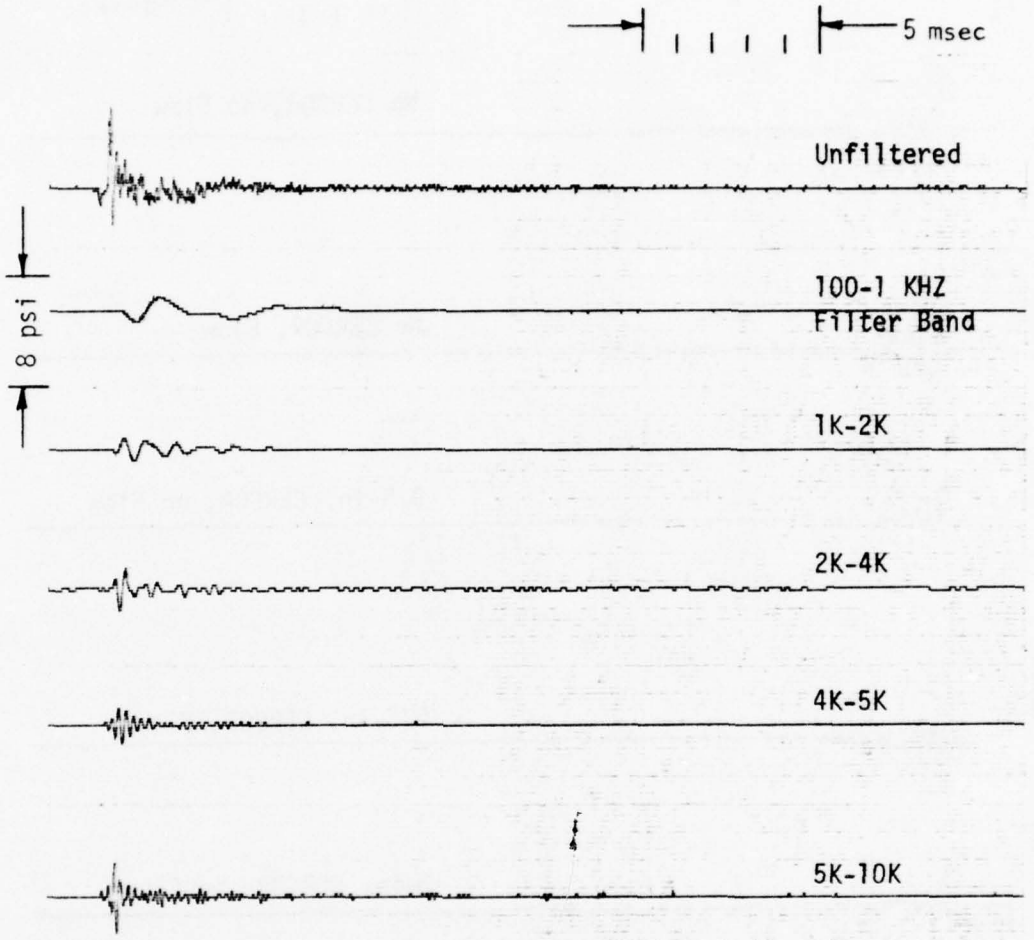

Figure 17. Pressure History for 20% Aperture Open-Area, no CERCOR, Mach 0.1 Cavity Throughflow

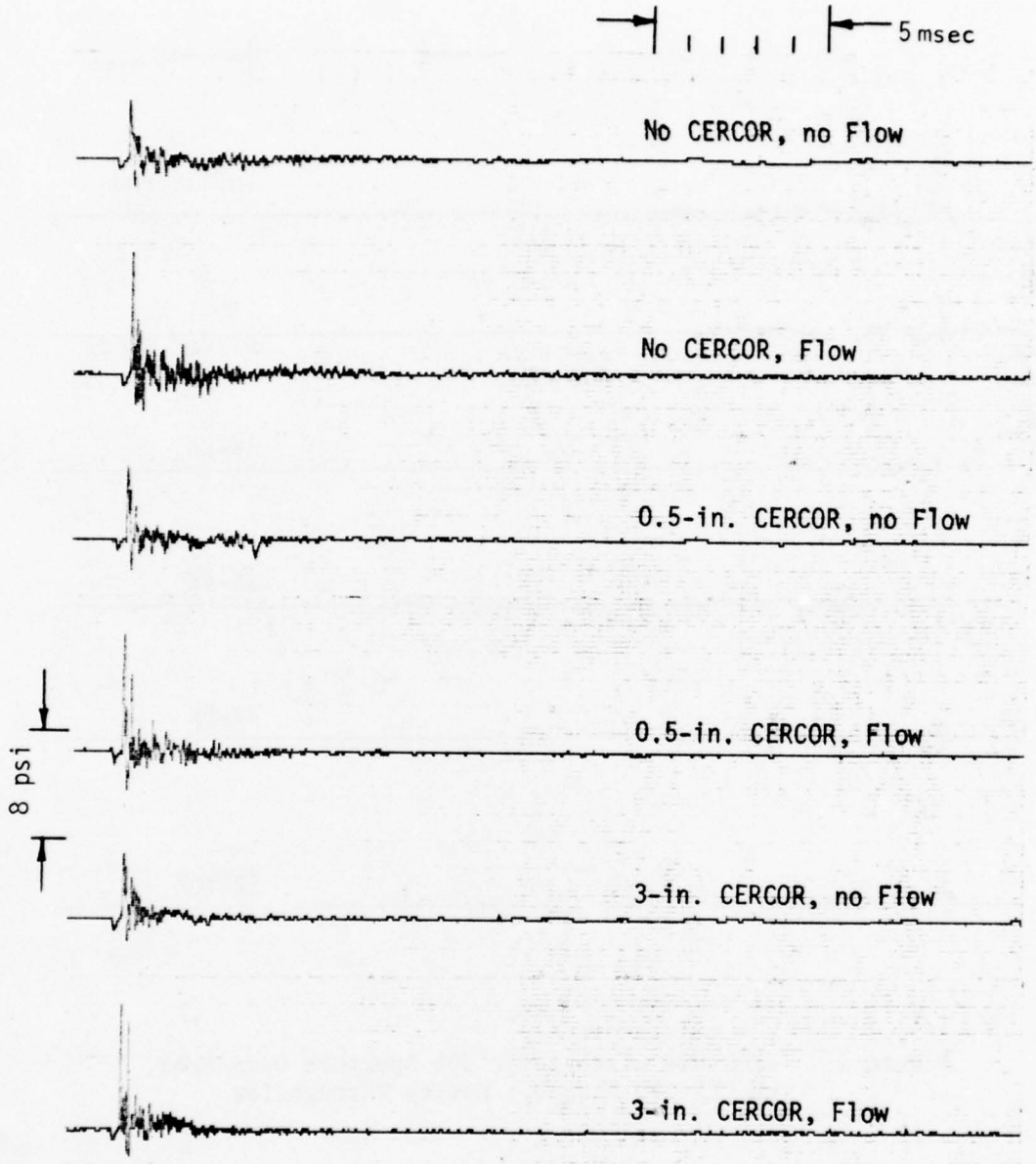

Figure 18. Effect of Cavity Throughflow and CERCOR on Pressure History; 2-inch Piston Position

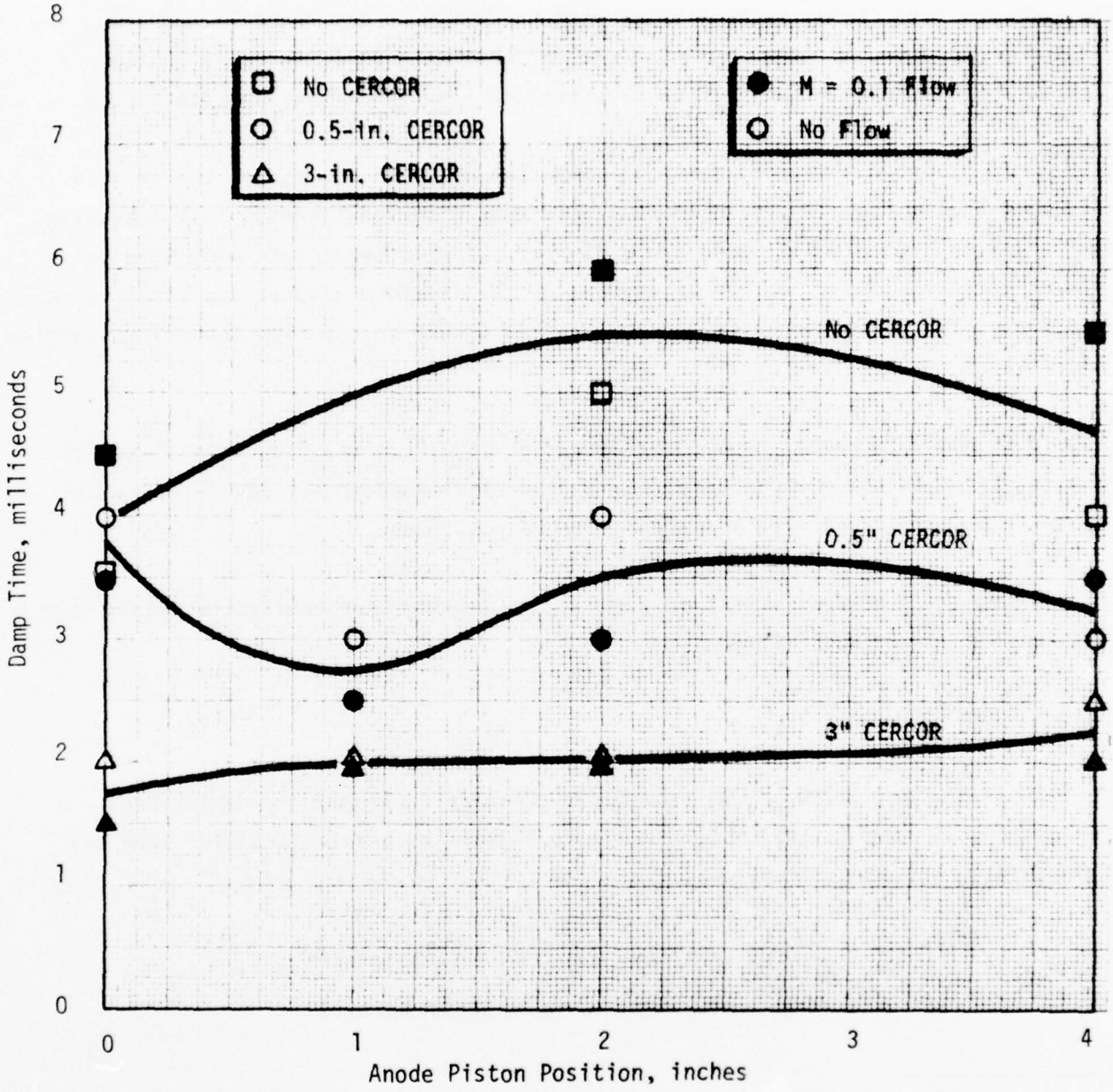

Figure 19. Task 2 Results - Effect of Flow on Damping Characteristics

Figures 16 and 17 show both the unfiltered and filtered pressure histories for no-flow and flow tests, respectively, with no CERCOR in the channels and zero piston position. The nearly exact agreement between each filter band in Fig. 16 and 17 substantiate the negligible effect of flow on damping charcteristics.

It should be noted, however, that the damp time observed in Fig. 16 and 17, i.e., 3.5 to 4.5 msec, is significantly less than that observed later in Task 3 testing under corresponding conditions, i.e., 23 msec. The difference in damp time is almost certainly due to an effect exerted by the aluminum adapter and its screens. The screens themselves probably act similar to CERCOR in the flow channel in rapidly attenuating the pressure oscillation.

Figure 18 shows the small beneficial effect of CERCOR in the flow channel at the 2-inch piston position under both flow and no-flow conditions. Figure 19 illustrates the same effect over a range of piston positions.

It was concluded that no effect of flow on the damping characteristics exists over the range $0 <$ Mach No. < 0.100.

CERCOR PRESSURE DROP

An expression for CERCOR ΔP is provided by Corning.* Assuming a cavity Mach Number of 0.10, the following CERCOR pressure drops were calculated for room air flow through the acoustic model:

ΔP = 0.350 psi with two 0.5-inch CERCOR inserts

ΔP = 2.10 psi with two 3.0-inch CERCOR inserts

---

*$\Delta P = \frac{4f}{144} \frac{L\rho V^2}{d\ 2g}$

where ΔP = psi; $f = 13.3/Re$ for $Re < 1250$; L = in.; ρ = lb/ft^3; V = fps; $g = 32.2$ ft/sec^2; d = 0.020 in. for T20-38 CERCOR; CERCOR open area = 67%; $Re = \frac{dV\rho}{12\mu}$; μ = lb/ft sec

The Reynolds Number (Re) at this Mach Number was 1778. This value of Re may be outside the limit of applicability of the friction factor expression in the Corning literature and consequently may result in still higher CERCOR ΔP.

Upon completion of the flow tests, the pulse initiator was removed from the Lucite model and a pressure gauge substituted in its place. Pressure readings were then recorded for various GN_2 velocities in the lasing cavity for both 0.5-inch and 3.0-inch CERCOR thicknesses. The resulting data indicated a nearly linear relationship between ΔP and velocity (for both CERCOR thicknesses) over a range of 54 fps to 108 fps ($920 < Re < 1850$ for 40 F GN_2).

As expected, the ΔP for the 3.0-inch CERCOR was nearly six times (5.4 to 5.8) that for the 0.5-inch CERCOR. Unexpectedly, however, the measured ΔP's were from 1.7 to 2.4 times the ΔP's calculated using the Corning expression. One possible explanation for the higher than expected CERCOR ΔP's is that the petrolatum grease used to seal the Lucite model may have plugged a (small) percentage of the CERCOR channels.

SECTION IV: TASK 3 - ACOUSTIC RESONATOR OPTIMIZATION

SCOPE

Experimental optimization of the acoustic resonator in the ductless lucite EDL model was accomplished in terms of aperture area and resonator volume. The effect of honeycomb flow conditioners in both the flow channels and in the acoustic resonator aperture itself was also determined.

EXPERIMENTAL SETUP

All tests in this task were performed using the ductless EDL acoustic model shown in Fig. 20 (see Fig. 1 and 2). The model is 13 inches in total length and is open-ended. No gaseous cavity throughflow was employed. Instead, the model contained quiescent room temperature air. No cathode absorber was employed on any test in the entire program. The cathode pistons were held at zero inch and a zero-percent aperture (i.e., solid) cathode window was inserted in the model (see Fig. 20).

APERTURE VARIATION

Testing of various aperture open area absorbers was conducted in the ductless acoustic model (see Fig. 20). No CERCOR flow channel inserts were used. The cathode window was solid while the anode window or anode aperture, contained a slot of given area. Aperture open-areas (expressed as percentages of the 4- by 1-inch laser cavity area) of 54, 34, 20, 10, and 0 percent were tested. A photograph of the anode windows having aperture open-areas of 10, 20, 34, 54, and 76 percent (left to right) is shown in Fig. 21.

A summary of the tests made in this portion of Task 3 (tests 1-34) is included in Table 4.

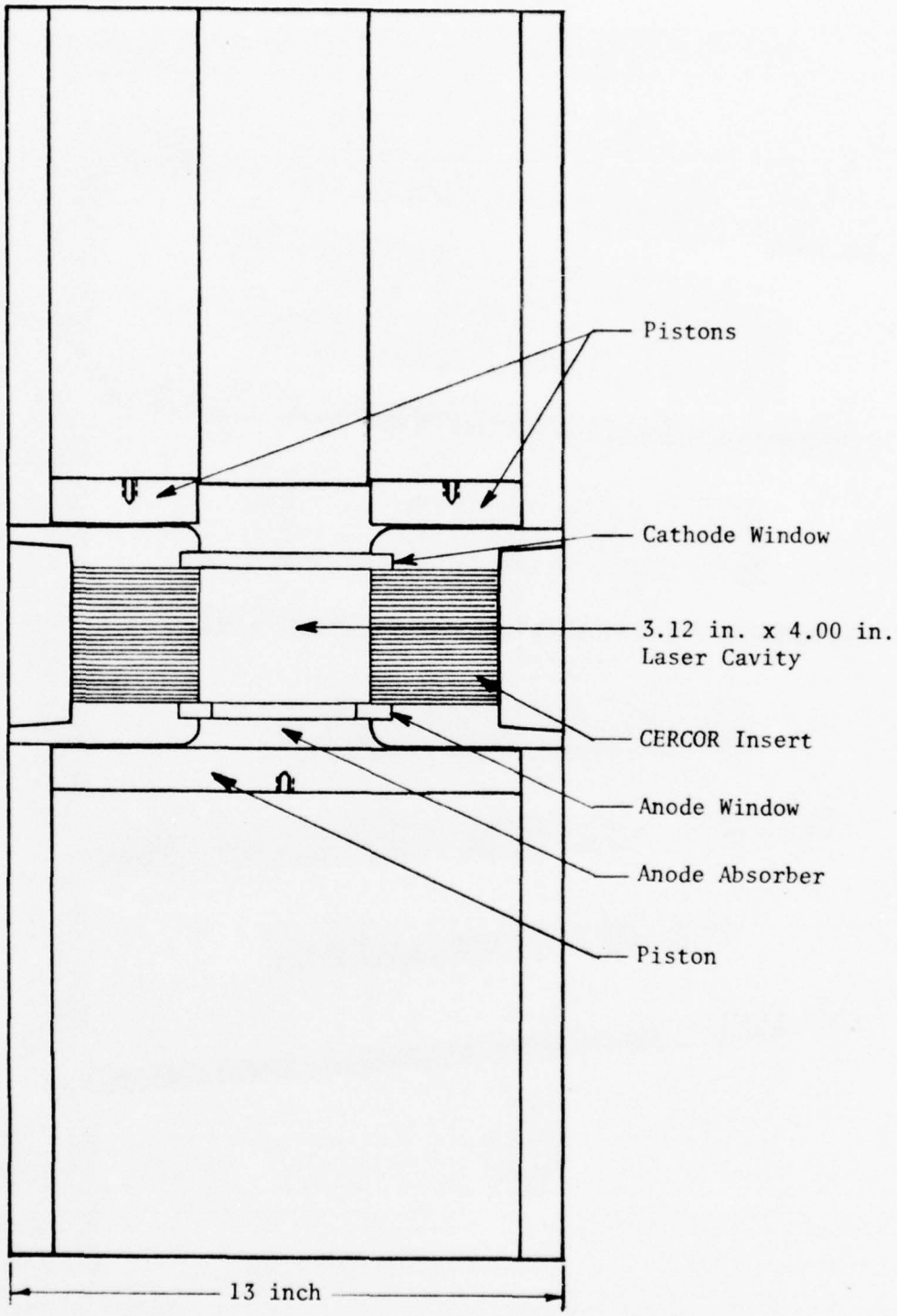

Figure 20. Ductless EDL Acoustic Model

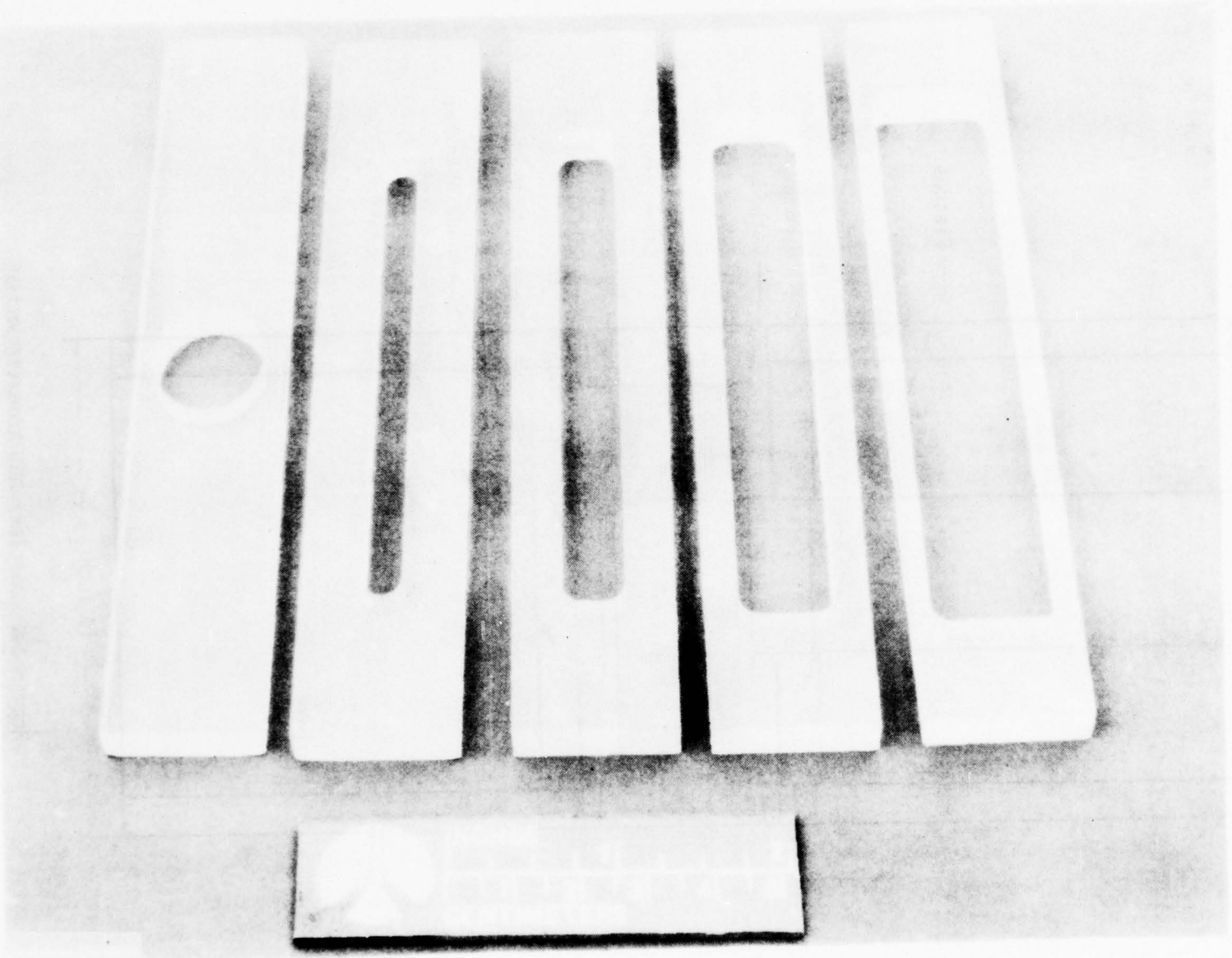

Figure 21. Anode Windows Having Various Aperture Open-Areas

TABLE 4. TASK 3 TEST SUMMARY

Test No.	Anode Window Open Area, percent	CERCOR in Channel	Anode Piston Position, inch	CERCOR in Resonator	Damp Time, msec
1	54	None	0	None	21.5
2	↓	↓	1	↓	15.5
3	↓	↓	2	↓	14.5
4	↓	↓	3	↓	9.0
5	↓	↓	4	↓	12.0
6	↓	↓	5	↓	12.0
7	↓	↓	5	↓	14.5
8	↓	↓	6	↓	14.0
9	↓	↓	8	↓	10.0
10	34	None	0	None	23.0
11	↓	↓	1	↓	15.0
12	↓	↓	2	↓	14.0
13	↓	↓	3	↓	16.0
14	↓	↓	4	↓	14.5
15	↓	↓	5	↓	15.5
16	↓	↓	6	↓	15.5
17	↓	↓	8	↓	27.5
18	20	None	0	None	23.0
19	↓	↓	1	↓	6.0
20	↓	↓	2	↓	4.0
21	↓	↓	3	↓	5.0
22	↓	↓	4	↓	6.5
23	↓	↓	5	↓	6.5
24	↓	↓	6	↓	6.5
25	↓	↓	8	↓	9.5
26	10	None	0	None	22.0
27	↓	↓	1	↓	5.5
28	↓	↓	2	↓	7.0
29	↓	↓	3	↓	7.5
30	↓	↓	4	↓	7.5
31	↓	↓	5	↓	8.5

TABLE 4. (Continued)

Test No.	Anode Window Open Area, percent	CERCOR in Channel	Anode Piston Position, inch	CERCOR in Resonator	Damp Time, msec
32	10	None	6	None	10.5
33	↓	↓	8	↓	12.5
34	0	None	0	None	33.0
35	34	0.5 in.	0	None	18.0
36	↓	↓	1	↓	10.0
37	↓	↓	2	↓	7.0
38	↓	↓	3	↓	7.5
39	↓	↓	4	↓	9.5
40	↓	↓	5	↓	9.0
41	↓	↓	6	↓	11.5
42	20	0.5 in.	0	None	12.5
43	↓	↓	1	↓	7.0
44	↓	↓	2	↓	4.5
45	↓	↓	3	↓	5.5
46	↓	↓	4	↓	5.5
47	↓	↓	5	↓	6.0
48	↓	↓	6	↓	10.0
49	34	3.0 in.	0	None	6.0
50	↓	↓	1	↓	6.0
51	↓	↓	2	↓	6.0
52	↓	↓	3	↓	7.0
53	↓	↓	4	↓	7.5
54	↓	↓	5	↓	7.0
55	↓	↓	6	↓	7.0
56	20	3.0 in.	0	None	6.0
57	↓	↓	1	↓	5.0
58	↓	↓	2	↓	5.5
59	↓	↓	3	↓	5.0
60	↓	↓	4	↓	5.0
61	↓	↓	5	↓	6.0
62	↓	↓	6	↓	6.0

TABLE 4. (Continued)

Test No.	Anode Window Open Area, percent	CERCOR in Channel	Anode Piston Position, inch	CERCOR in Resonator	Damp Time, msec
63	20	None	0	0.5 in.	18.0
64	↓	↓	1	↓	5.0
65			2		7.0
66			3		8.0
67			4		7.5
68			5		10.0
69			6		11.0
70	20	0.5 in.	0	0.5 in.	16.0
71	↓	↓	1	↓	6.0
72			2		6.5
73			3		7.0
74			4		8.5
75			5		9.5
76			6		8.5
77	20	3.0 in.	0	0.5 in.	7.0
78	↓	↓	1	↓	3.5
79			2		4.5
80			3		4.5
81			4		5.0
82			5		5.5
83			6		4.5
84	20	None	2.5	3.0 in.	15.0
85	↓	↓	3	↓	10.5
86			4		11.5
87			5		9.5
88			6		11.5
89	20	0.5 in.	2.5	3.0 in.	11.0
90	↓	↓	3	↓	10.5
91			4		10.0
92			5		10.5
93			6		12.0

TABLE 4. (Concluded)

Test No.	Anode Window Open Area, percent	CERCOR in Channel	Anode Piston Position, inch	CERCOR in Resonator	Damp Time, msec
94	20	3.0 in.	2.5	3.0 in.	4.5
95	↓	↓	3	↓	6.5
96			4		6.5
97			5		5.0
98			6		5.0

The pressure response for each test was recorded on magnetic tape. Permanent records of the response were then obtained by tape playback. Pressure histories of oscillations lying within frequency bands of 100 to 1000 Hz, 1 to 2 kHz, 2 to 4 kHz, 4 to 5 kHz, and 5 to 10 kHz were also obtained as was done in Task 1.

Pressure histories for the various aperture open-areas are shown in Fig. 22 to 25 as a function of anode piston position (absorber volume). An anode piston position of zero inches corresponds to the piston position shown in Fig. 20. In actuality, therefore, a small resonator volume exists with any aperture open-area other than zero percent. A comparison of the damp times* for the individual apertures is shown in Fig. 26. The difference between the damp time of 33 msec for 0-percent aperture area, 0-inch position and the damp time of 21.5 to 23 msec for all other aperture areas and 0-inch piston position is believed due to the small resonator volume existing between the anode window and the anode piston at 0 inch.

At 0-piston position, the predominant frequency of the pressure oscillation varied from 484 Hz for 0-percent aperture area to about 454 Hz for the other aperture areas. This corresponds to the first acoustic mode in the open-open flow direction of 13-inches with an end correction of 0.55 inch at each end. The effect of lasing cavity modes (1600 to 2200 Hz) on the damp time of the unfiltered oscillation was unobservable with the exception of the 34-percent aperture open-area case. In this instance, oscillations of about 1650 Hz appeared to couple with the lower frequency oscillations predominant in the other cases and control the damp time of the unfiltered oscillation as shown in Fig. 23. Similar results were obtained in Task 1. While the damp time of the filtered 1 to 2 kHz trace was nearly equivalent to the damp time of the unfiltered trace for the 34-percent aperture case, in no other case was the damp time of the 1 to 2 kHz filtered trace greater than about 3 msec.

*Damp time is defined as the time required for the peak-to-peak pressure oscillation amplitude to fall to 1/7 of the initial average overpressure. The initial average overpressure for all tests performed under this contract was 5.7 psi. The vast majority of tests ranged within 1 psi of this value although initial disturbance amplitudes as low as 2.0 psi and as high as 12.6 psi were recorded for the "identical" explosive charges used for pulse initiation.

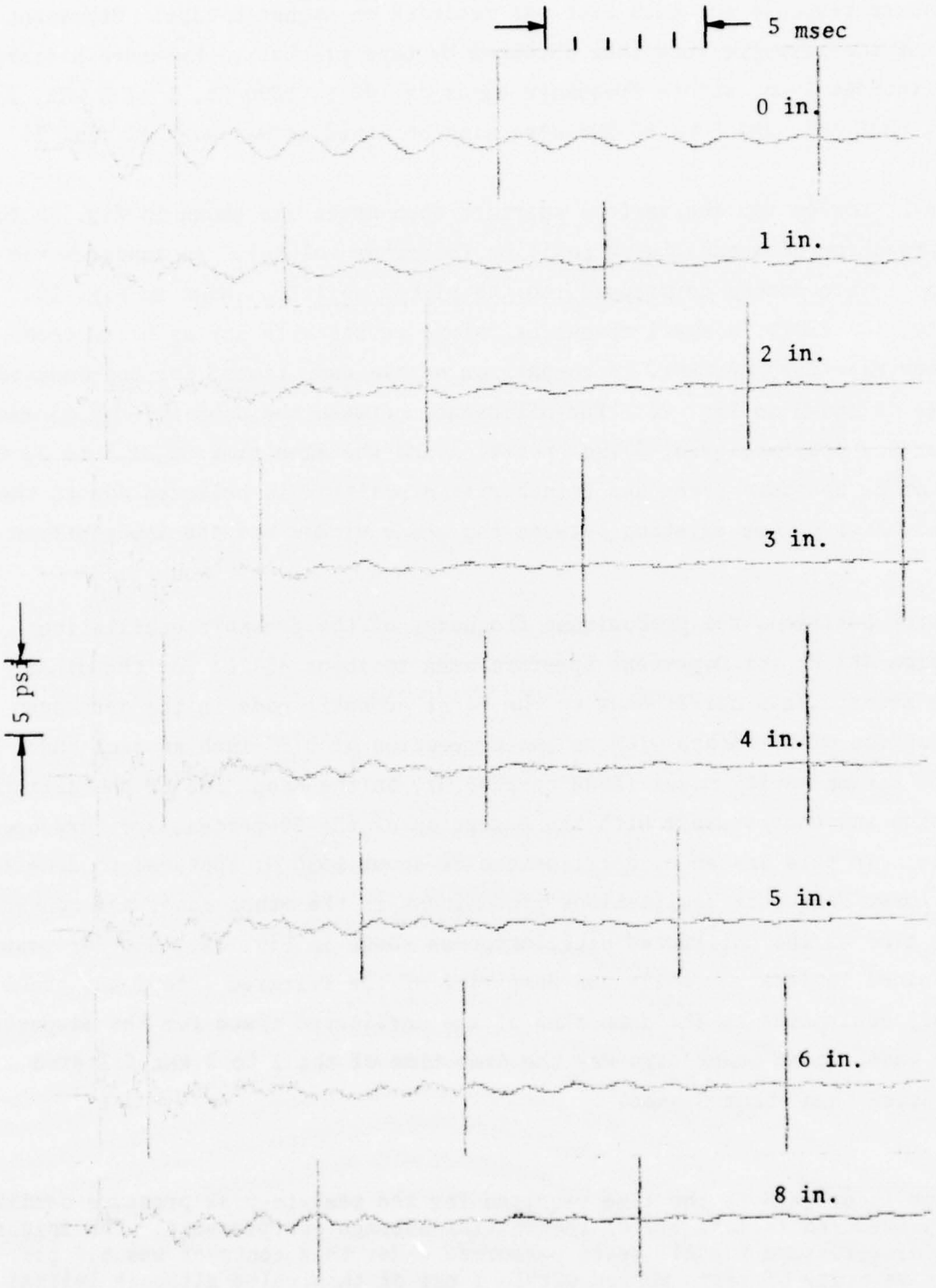

Figure 22. Effect of Piston Position on Pressure History; 54% Aperture Area, No CERCOR

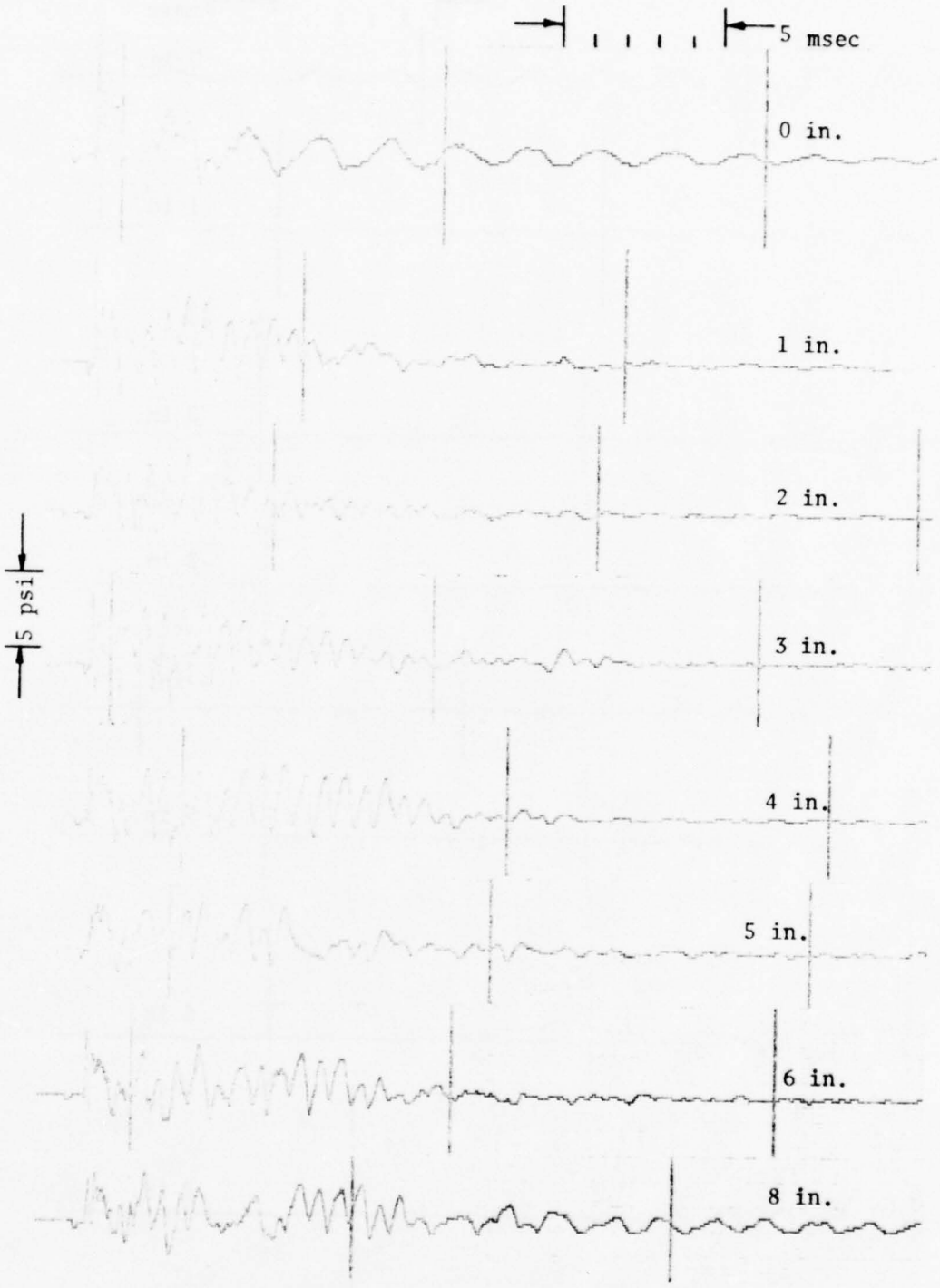

Figure 23. Effect of Piston Position on Pressure History; 34% Aperture Area, No CERCOR

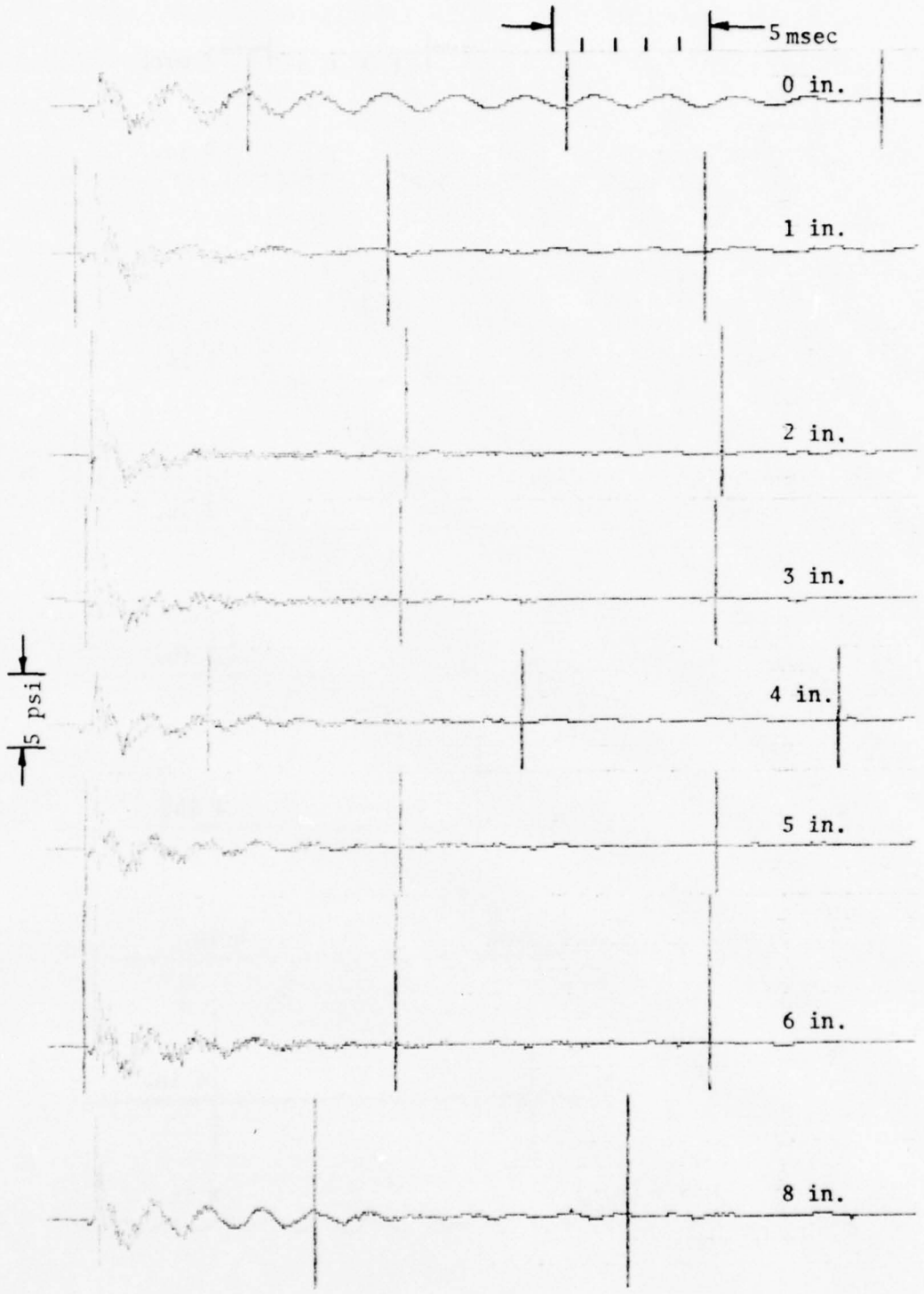

Figure 24. Effect of Piston Position on Pressure History; 20% Aperture Area, No CERCOR

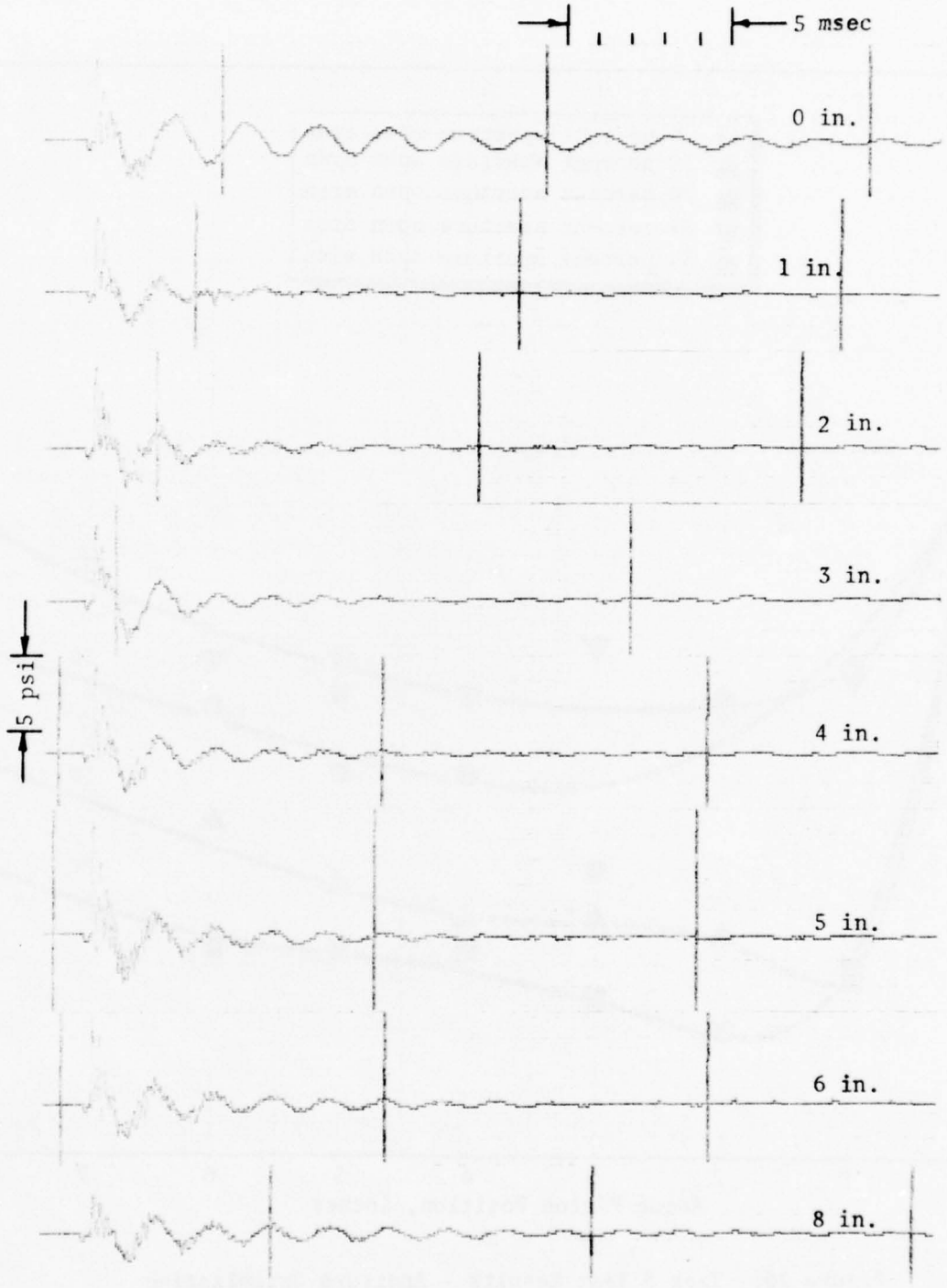

Figure 25. Effect of Piston Position on Pressure History; 10% Aperture Area, No CERCOR

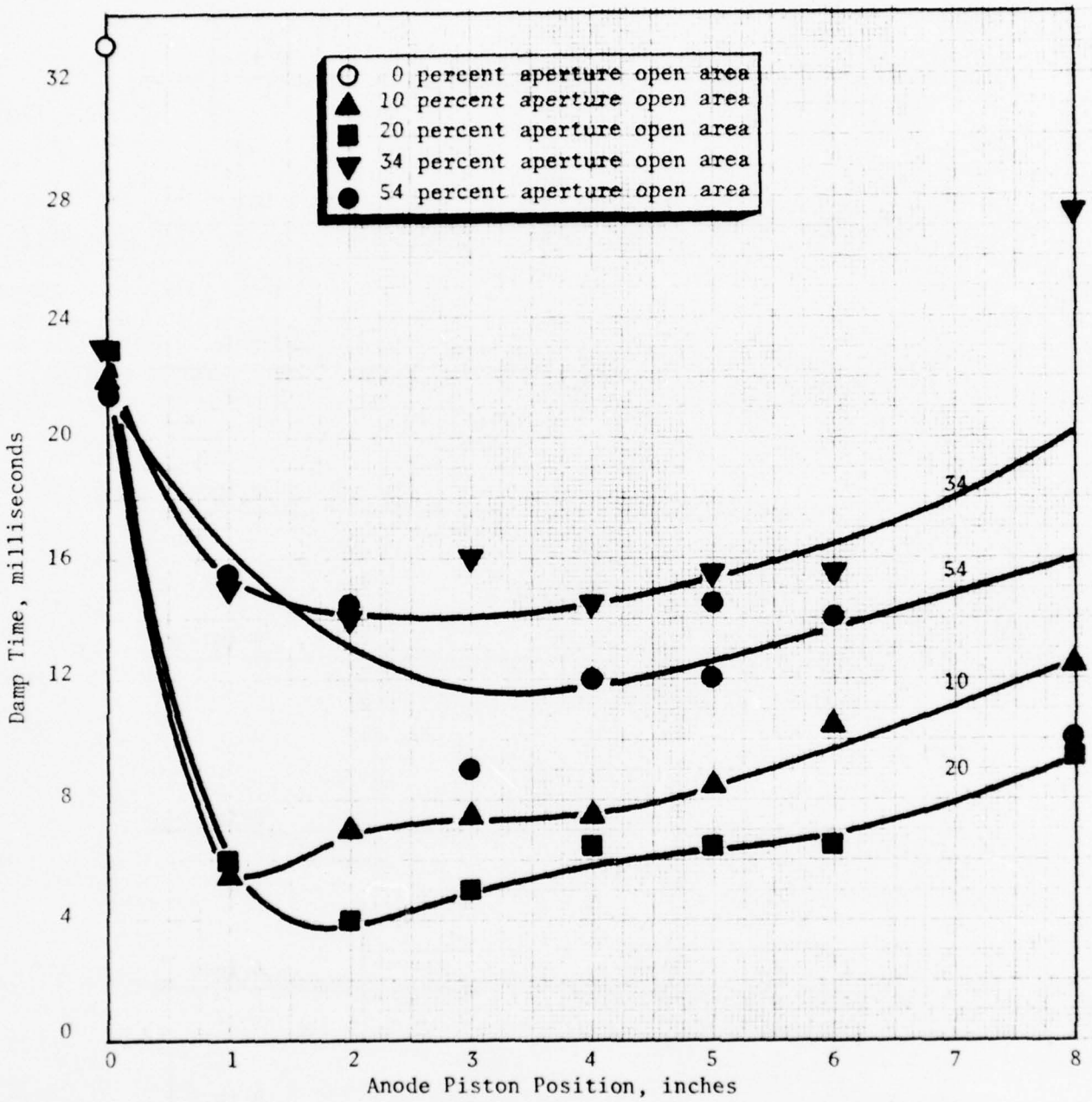

Figure 26. Task 3 Test Results - Aperture Optimization

Based upon the results shown in Fig. 22 to 26, it was concluded that the performance of the 20-percent aperture area absorber was optimum. This aperture open area which permits damping within 4 to 5 msec at a piston position of 2-inches was thus selected for predominant use in the latter part of Task 3 and in Task 4.

CERCOR INSERTS IN THE FLOW CHANNEL

The open-ended acoustic model (Fig. 20) was used to determine the effect of CERCOR in the flow channel (upstream and downstream of the EDL cavity) over a range of absorber volumes using both 20 and 34% aperture open areas. These tests (tests 35 to 62) are summarized in Table 4. Pressure histories are shown in Fig. 27 to 30. A comparison of the damp times for the various aperture/CERCOR combinations is shown in Fig. 31.

In the case of the 34% aperture open area, the addition of 0.5-inch CERCOR reduces the damp time from about 14 msec (see Fig. 26) to about 7 msec. The addition of 3.0-inch CERCOR reduces the damp time a bit further to about 6 msec.

In the case of the 20% aperture open area, the addition of 0.5-inch CERCOR results in a damp time of about 4.5 msec compared to a value of about 4 msec recorded previously (see Fig. 26) with no CERCOR. The addition of 3-inch CERCOR results in a damp time of about 5 msec.

Thus, it is apparent that no advantage is derived from the addition of CERCOR in the flow channels with the 20% aperture open area absorber. The addition of CERCOR does improve the damp time of the 34% aperture open-area absorber but not to a point where it outperforms the 20% absorber.

CERCOR INSERTS IN THE RESONATOR

The effect of inserting CERCOR directly behind the anode window in the resonator volume was also investigated using the open-ended Lucite model. A 20% aperture open area was employed and tests were made both with and without CERCOR in the flow channels. The physical appearance of the model with CERCOR in the resonator

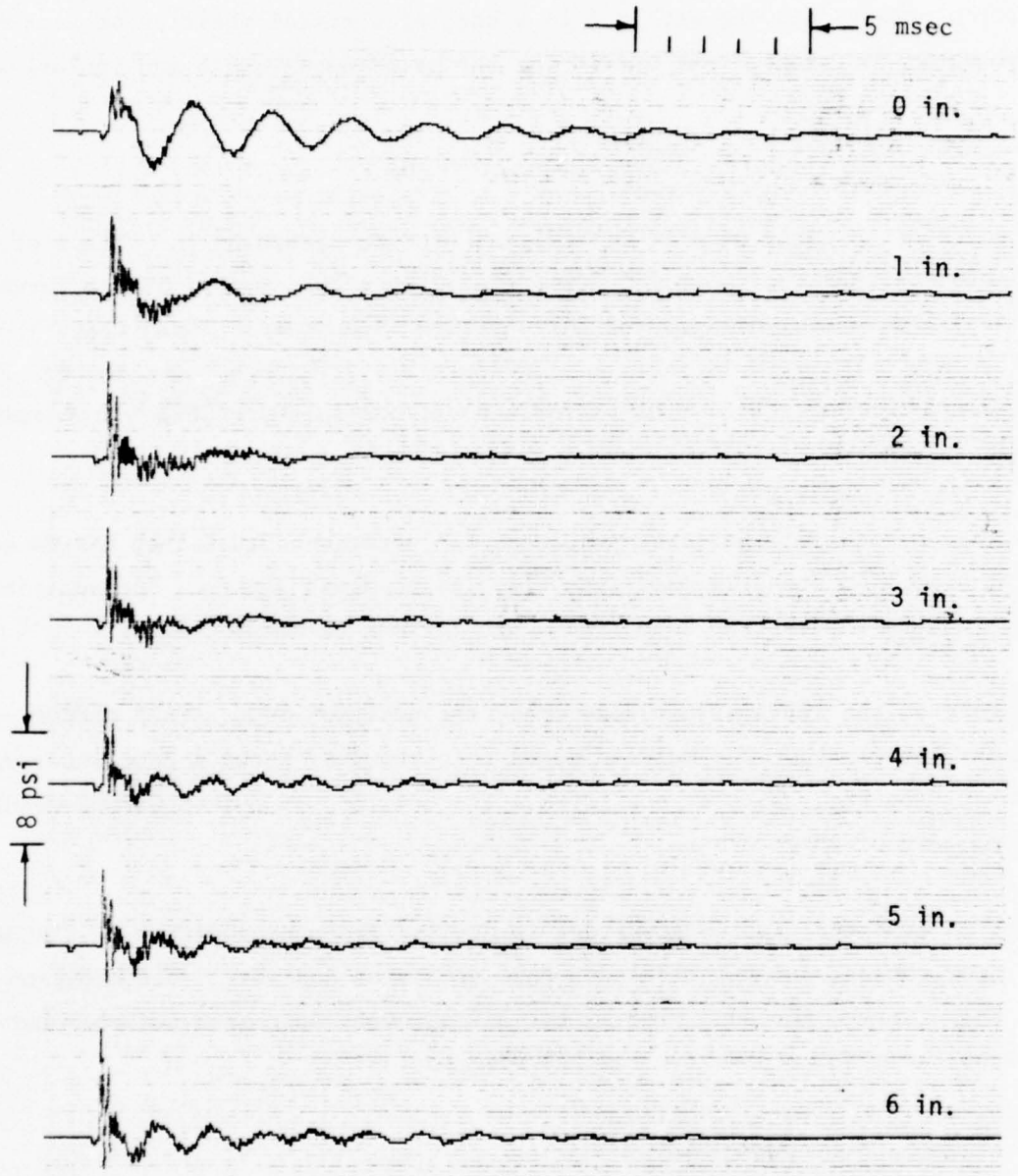

Figure 27. Effect of Piston Position on Pressure History; 34% Aperture Open Area, 0.5-inch CERCOR

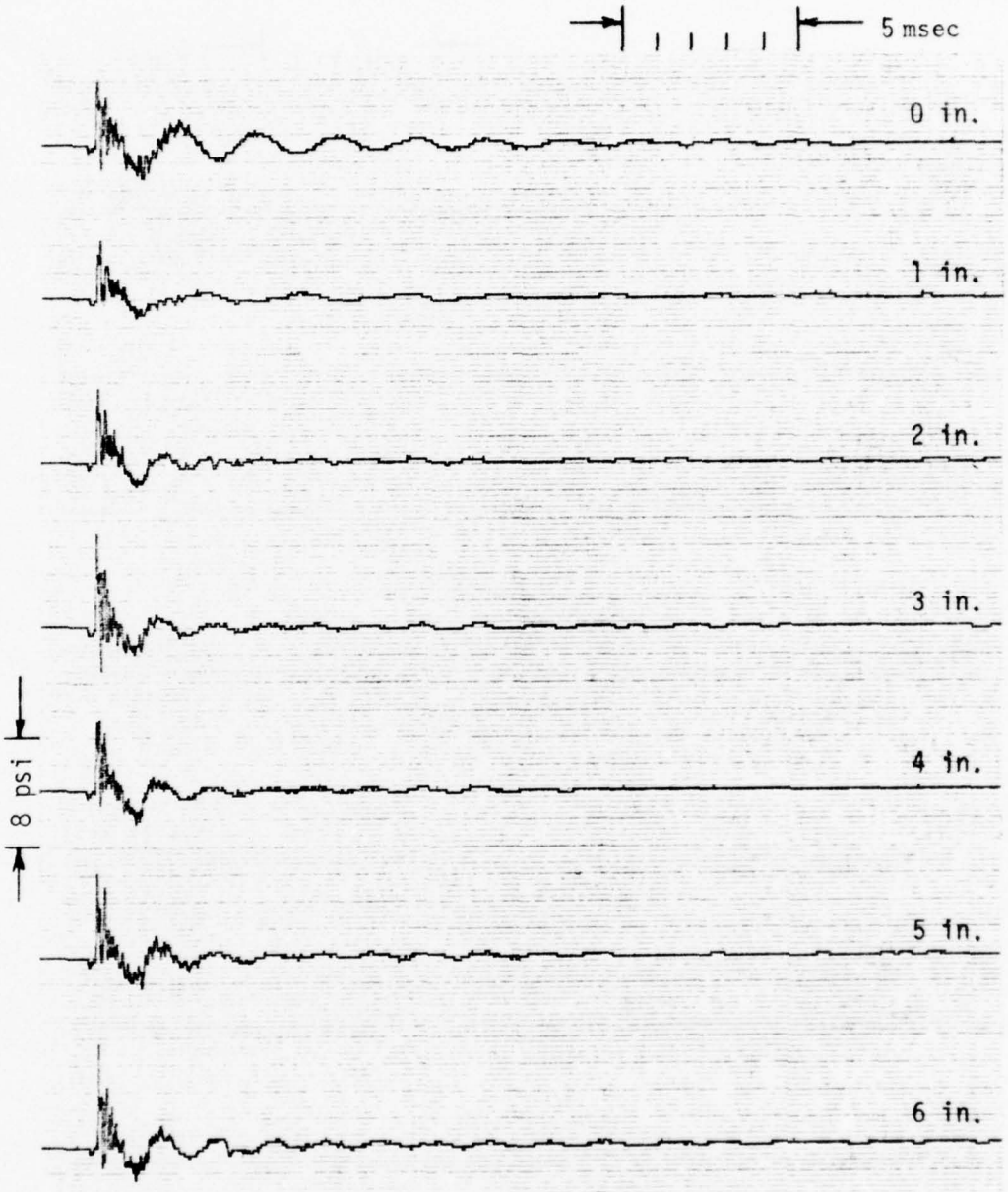

Figure 28. Effect of Piston Position on Pressure History; 20% Aperture Open Area, 0.5-inch CERCOR

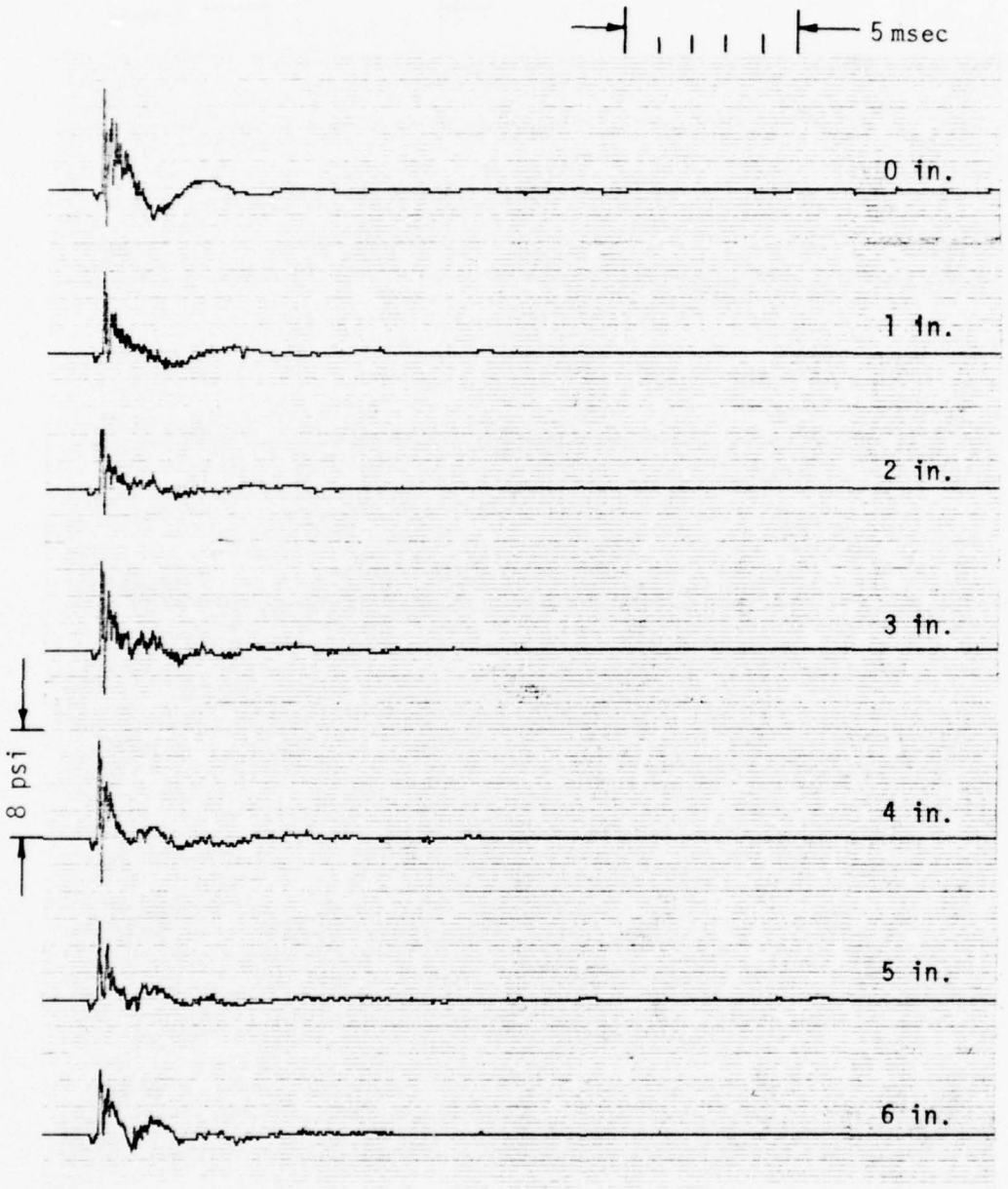

Figure 29. Effect of Piston Position on Pressure History; 34% Aperture Open Area, 3-inch CERCOR

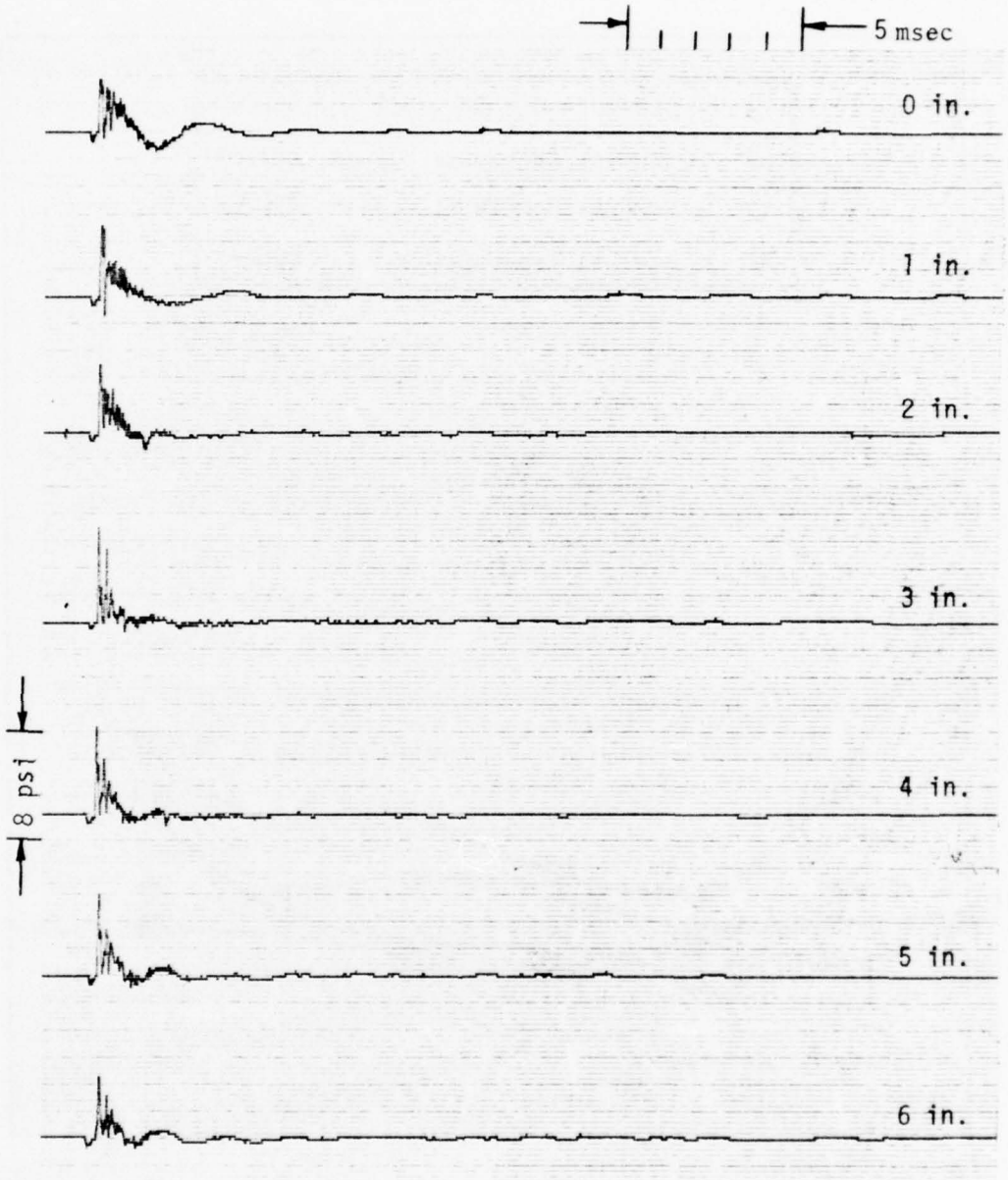

Figure 30. Effect of Piston Position on Pressure History; 20% Aperture Open Area, 3-inch CERCOR

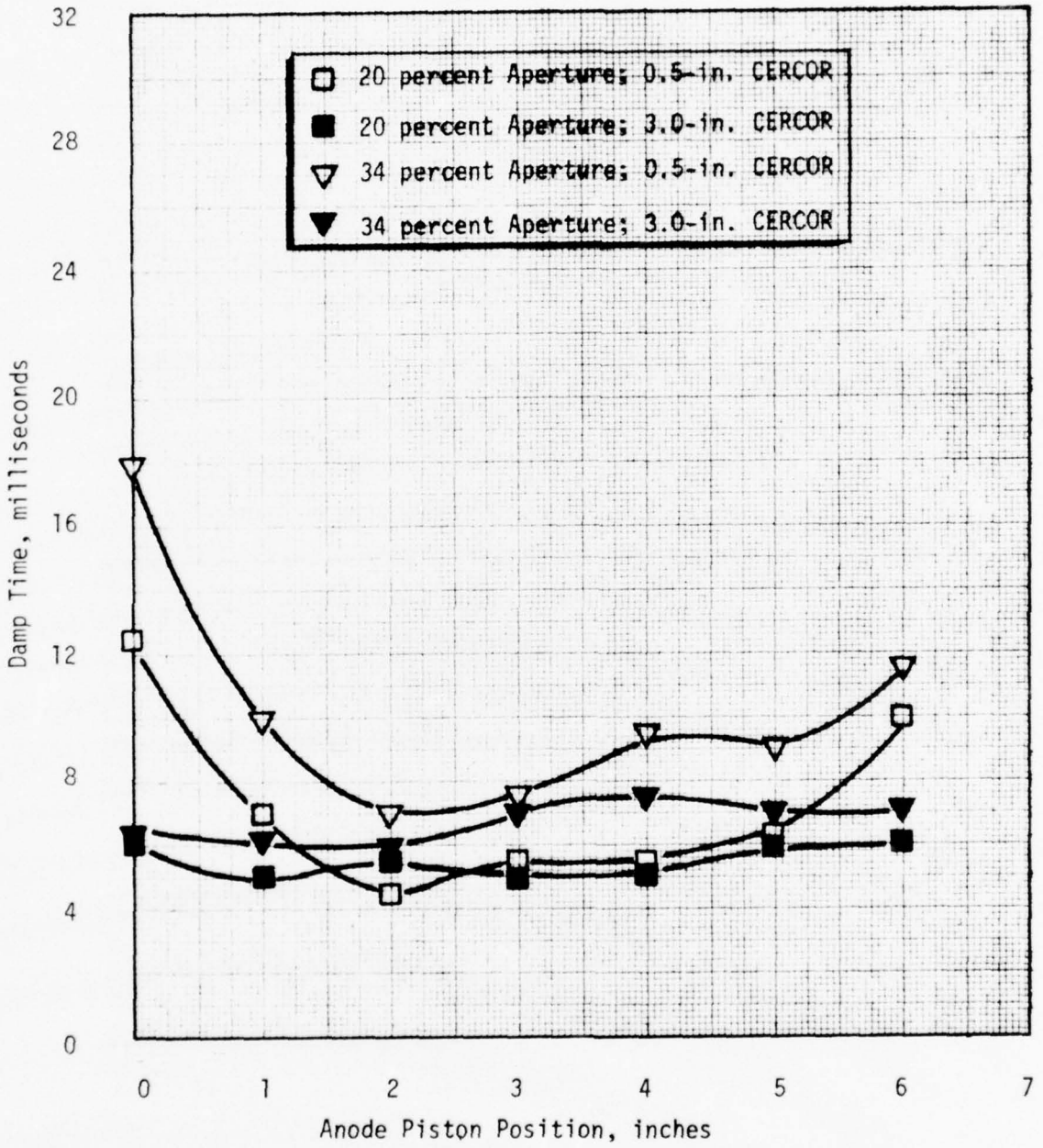

Figure 31. Task 3 Test Results - Effect of CERCOR in Flow Channel

volume is shown in Fig. 32. When the 3-inch CERCOR was placed in the resonator volume, the piston was restricted to positions $\geq$ 2.5 inches with a void space existing at the sides of the CERCOR. Results for these tests (tests 63 to 98) are summarized in Table 4. Pressure histories are shown in Fig. 33 to 38. A comparison of the damp times for the two CERCOR thicknesses (0.5 and 3.0 inches) is shown in Fig. 39 and 40.

As mentioned earlier (no CERCOR in resonator), damp times of approximately 4, 4.5, and 5 msec were recorded for the 20% absorber with no CERCOR, 0.5-inch CERCOR, and 3-inch CERCOR, respectively, in the flow channels (Fig. 26 and 31). With the addition of 0.5-inch CERCOR in the resonator volume, damp times of approximately 5, 6, and 3.5 msec were observed for the same three cases (Fig. 39). Similarly, with the addition of 3.0-inch CERCOR in the resonator volume, damp times of approximately 10, 10 and 5 msec were observed for the same three cases (Fig. 40).

Consequently, it is concluded that the addition of CERCOR in the resonator volume does not appear at all attractive in the case of the 20% aperture open-area absorber.

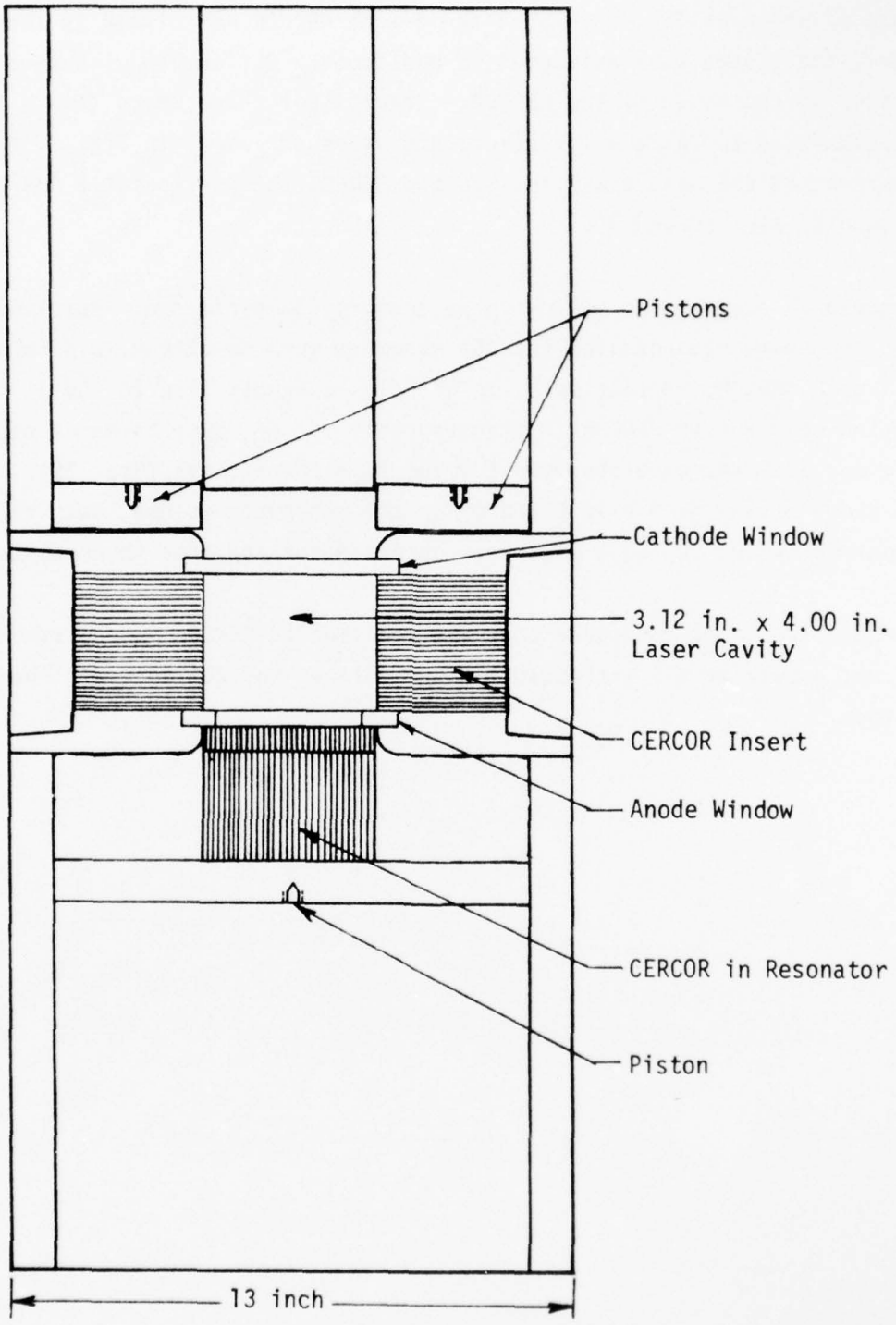

Figure 32. Ductless EDL Acoustic Model with CERCOR in Resonator Volume

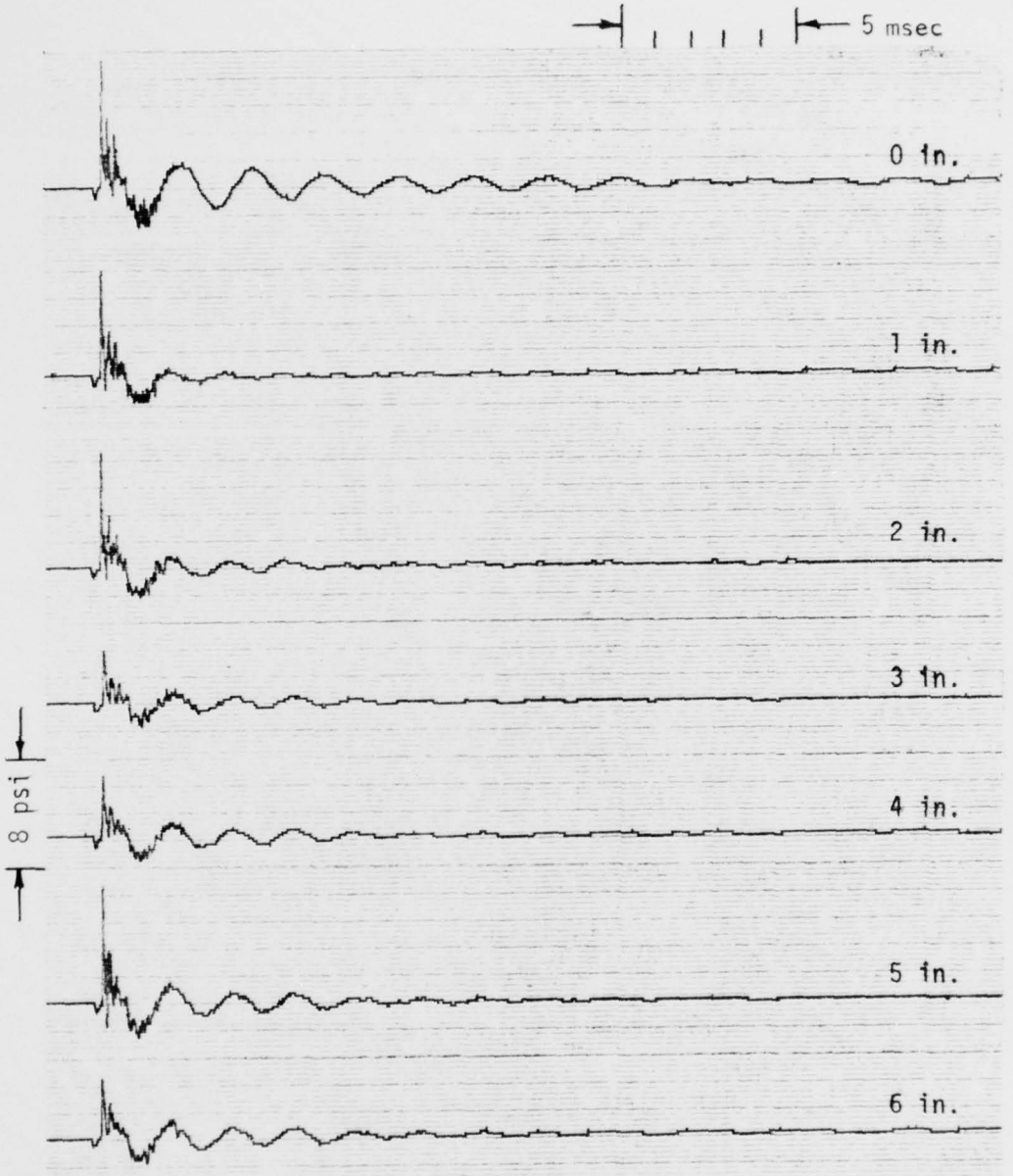

Figure 33. Effect of Piston Position on Pressure History; 20% Aperture Open Area, ½-inch CERCOR in Resonator, no CERCOR in Channel

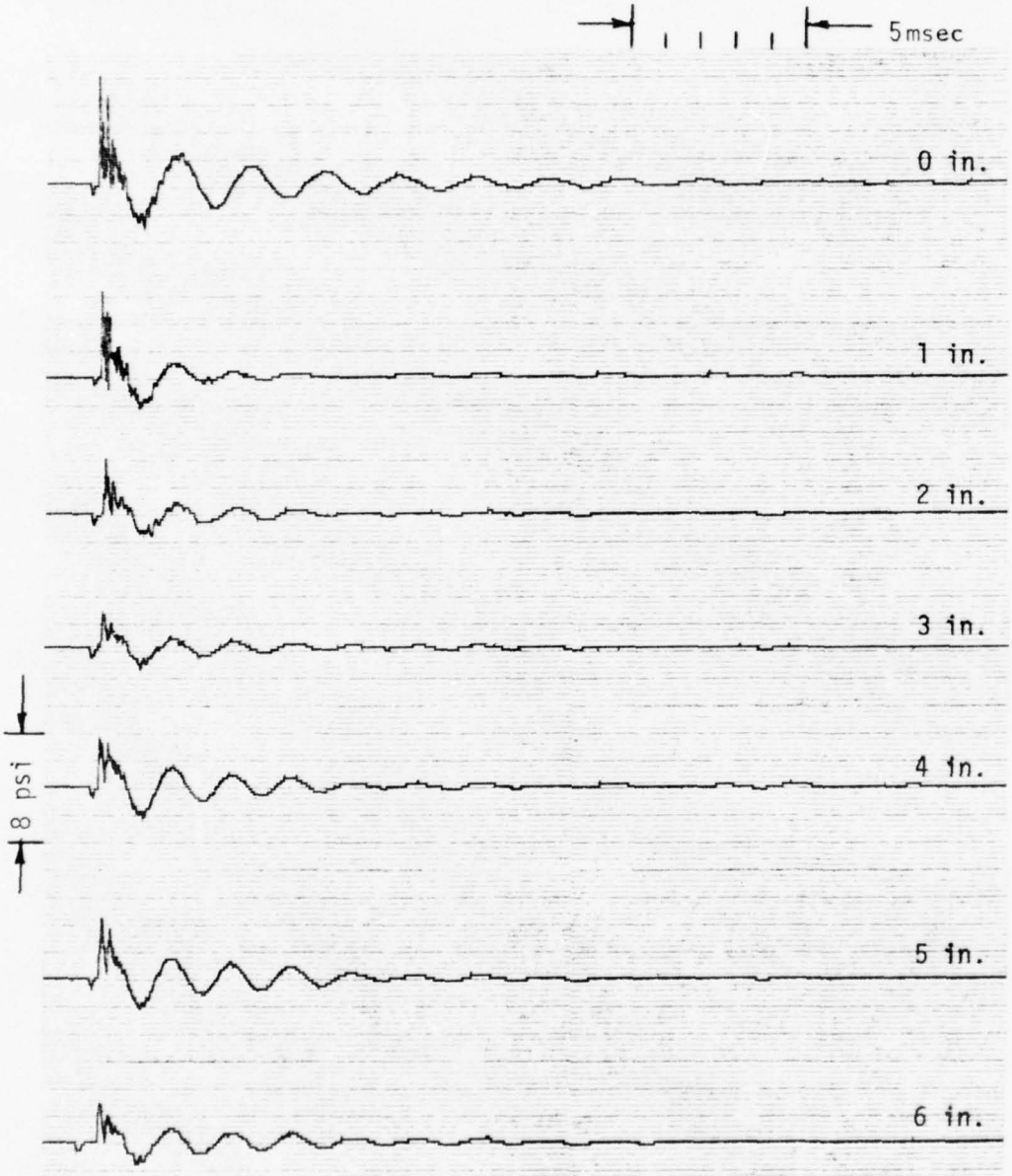

Figure 34. Effect of Piston Position on Pressure History; 20% Aperture Open Area, ½-inch CERCOR in Resonator, ½-inch CERCOR in Channel

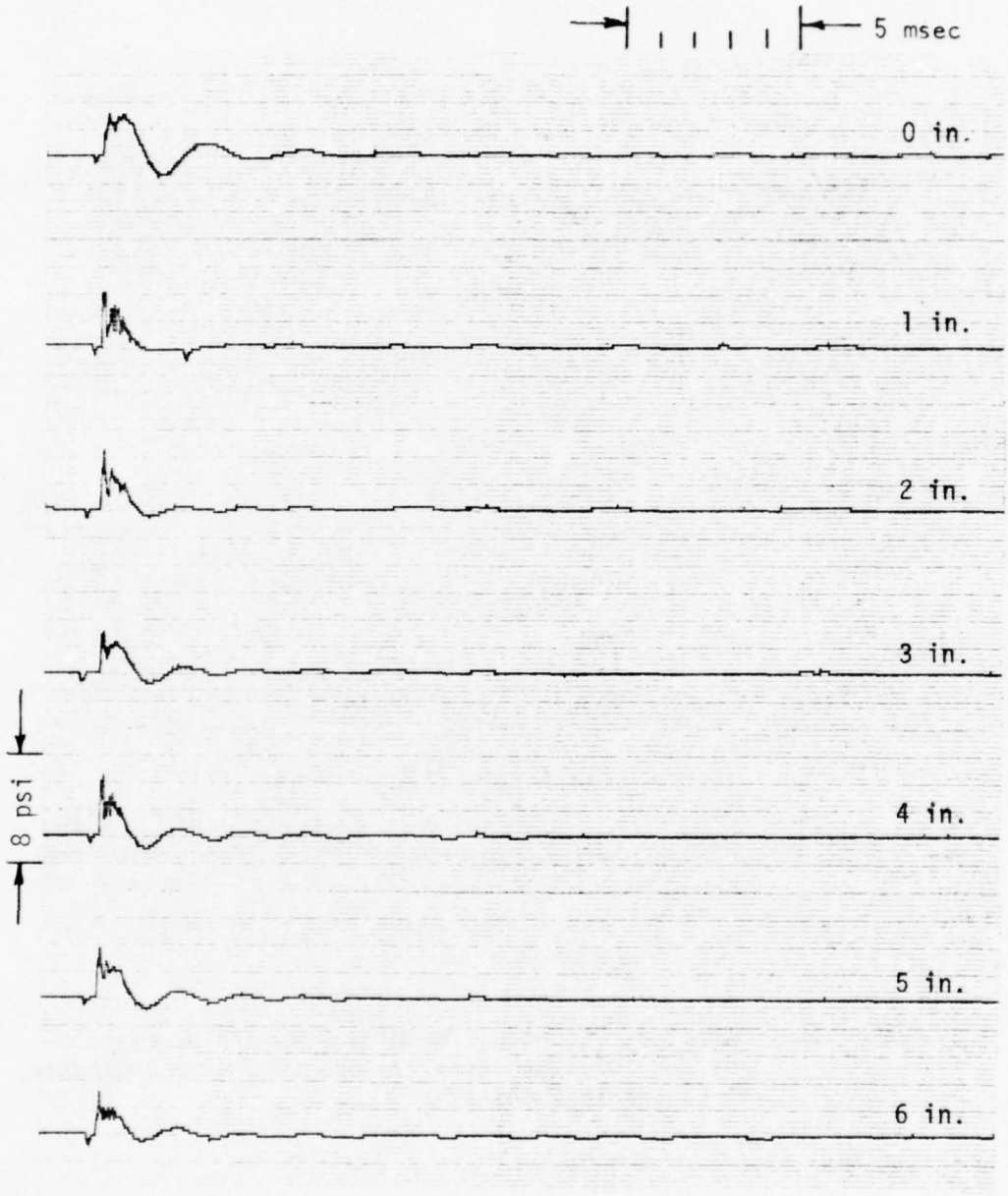

Figure 35. Effect of Piston Position on Pressure History; 20% Aperture Open Area, ½-inch CERCOR in Resonator, 3-inch CERCOR in Channel

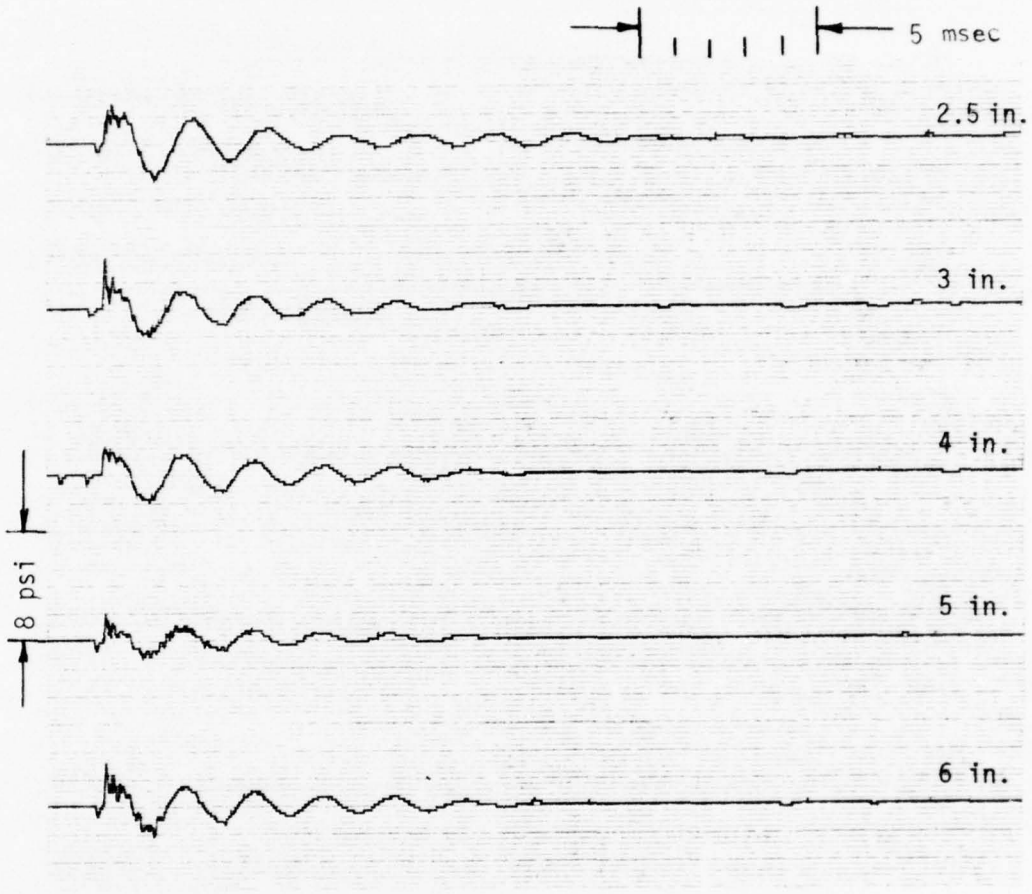

Figure 36. Effect of Piston Position on Pressure History; 20% Aperture Open Area, 3-inch CERCOR in Resonator, no CERCOR in Channel

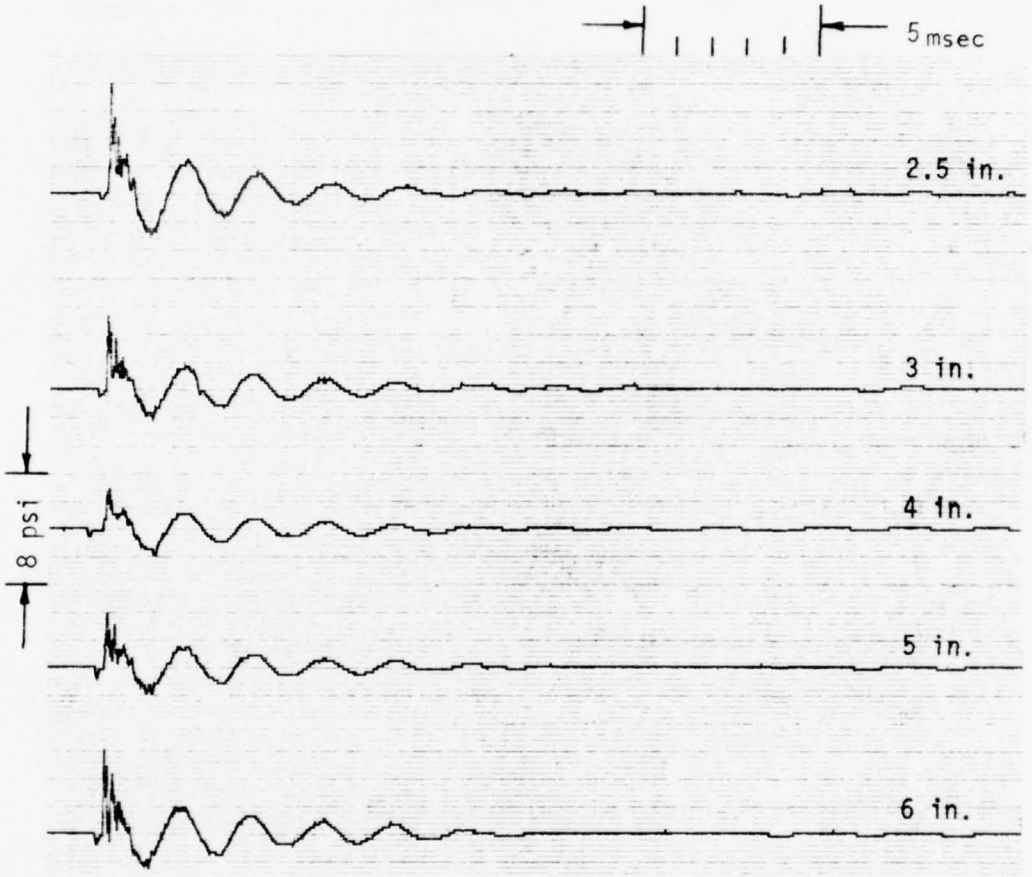

Figure 37. Effect of Piston Position on Pressure History; 20% Aperture Open Area, 3-inch CERCOR in Resonator, ½-inch CERCOR in Channel

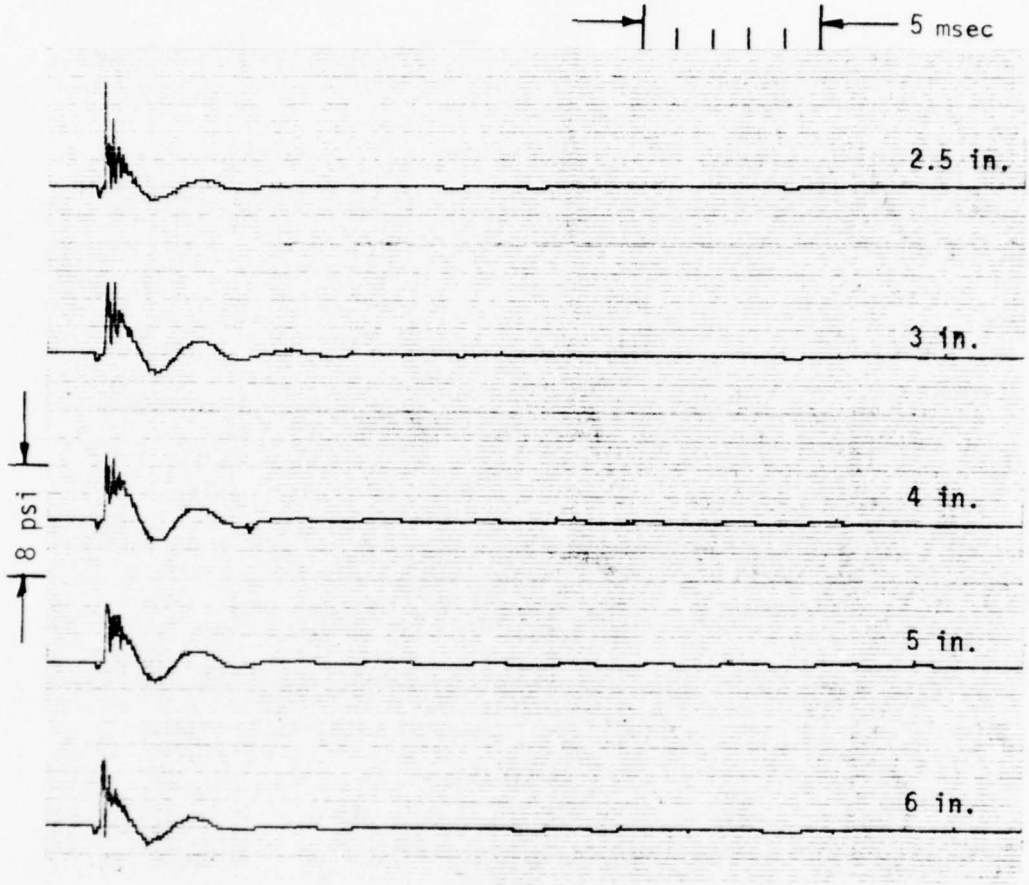

Figure 38. Effect of Piston Position on Pressure History; 20% Aperture Open Area, 3-inch CERCOR in Resonator, 3-inch CERCOR in Channel

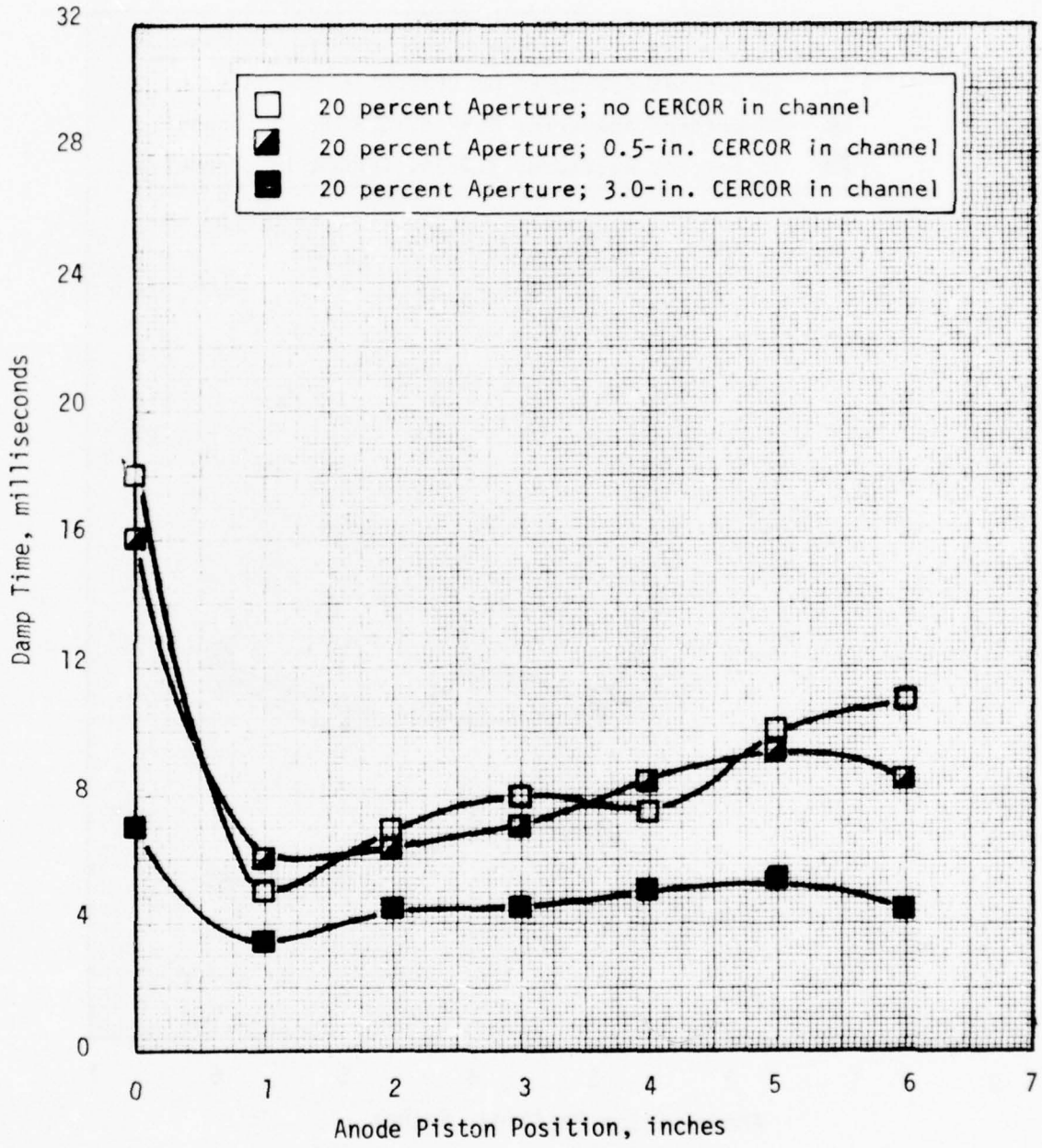

Figure 39. Task 3 Test Results - Effect of 0.5-inch CERCOR in Resonator

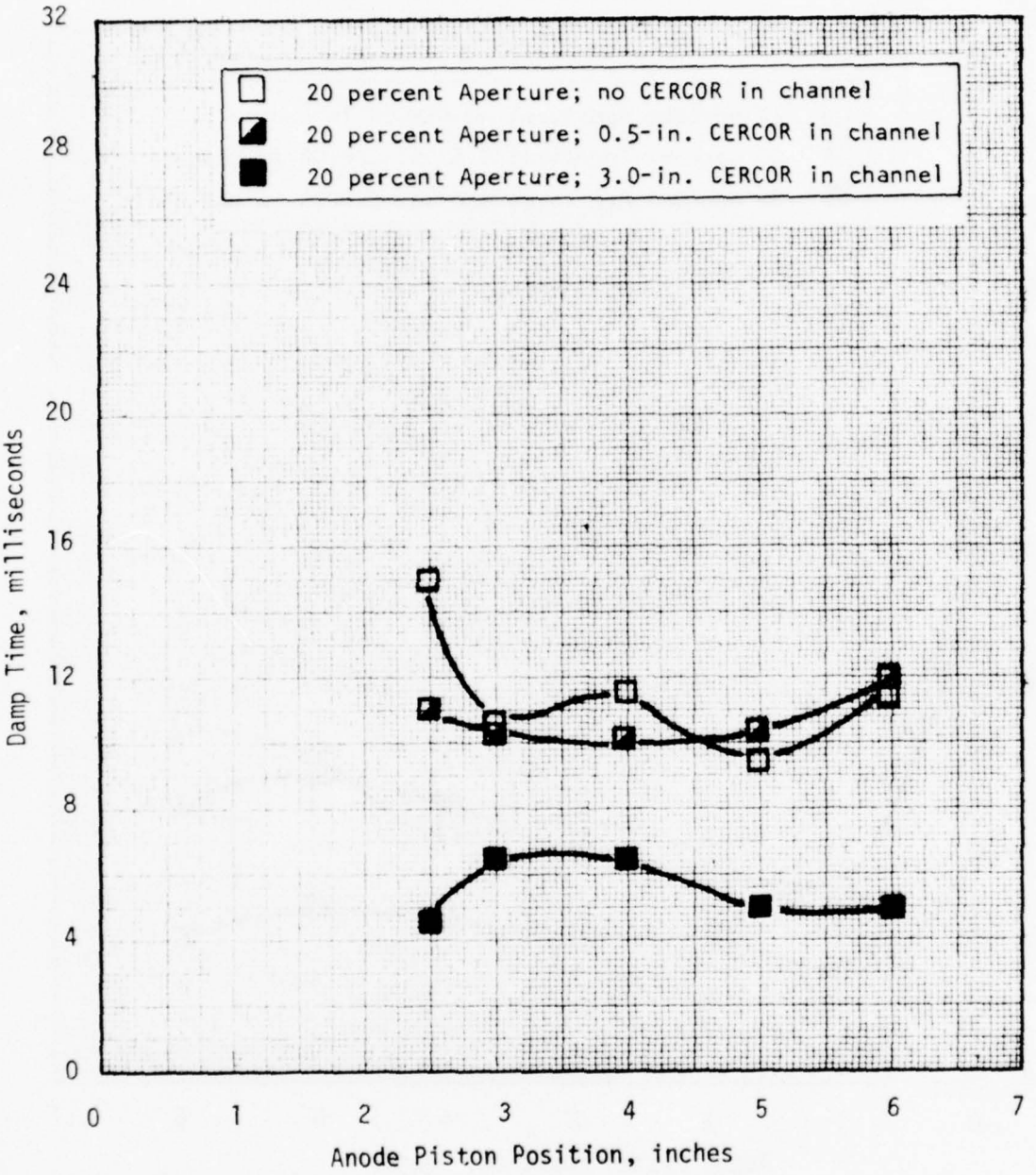

Figure 40. Task 3 Test Results - Effect of 3-inch CERCOR in Resonator

SECTION V: TASK 4 - DUCT TERMINATION STUDIES

SCOPE

The open-ended Lucite EDL acoustic model shown in Fig. 2 was modified to include three types of flow duct terminations:

1. Simple closed-duct termination wherein the cavity exhaust flows into a simple straight section which is blocked to induce longitudinal pressure wave modes similar to those observed in the AFWL EDL acoustic data.
2. Complex duct termination wherein the cavity exhaust is ducted into a flow channel which is partially blocked to simulate a heat exchanger.
3. Plenum duct termination wherein a large plenum volume will be incorporated adjacent to the cavity inlet and exit regions.

Tests were performed to optimize the acoustic resonator and investigate the effect of CERCOR in the flow channels for each type of duct termination.

TASK 4A - SIMPLE CLOSED-DUCT TERMINATION

The simple closed-duct termination consisted simply of an insert for each end of the 13-inch-long open-ended acoustic model which closes each end so that the end-to-end channel length of the model is 13-inches. A sketch of this insert is shown in Fig. 41 and a photograph of the insert is shown in Fig. 42. The insert serves to effectively double the frequency of the first acoustic mode in the model (see Fig. 43), raising it from 484 Hz to 1044 Hz. This brings the predominant frequency closer to the 883 Hz measured in the AFWL data in Task 1.

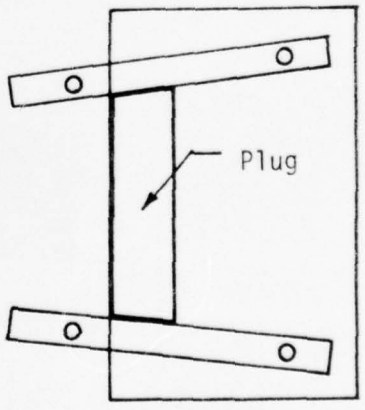

Figure 41. Design of Simple Closed-Duct Termination

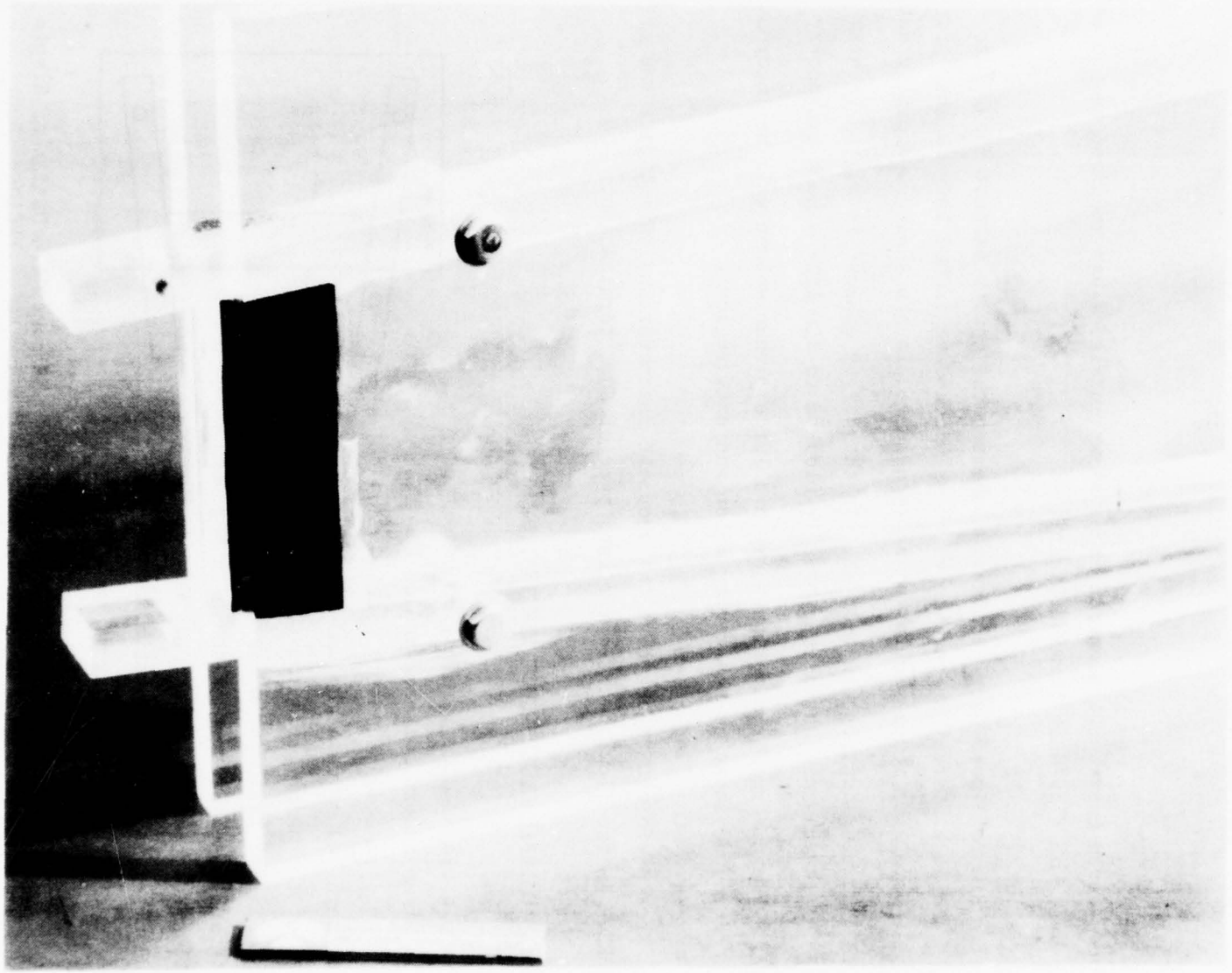

Figure 42. Simple Closed-Duct Termination

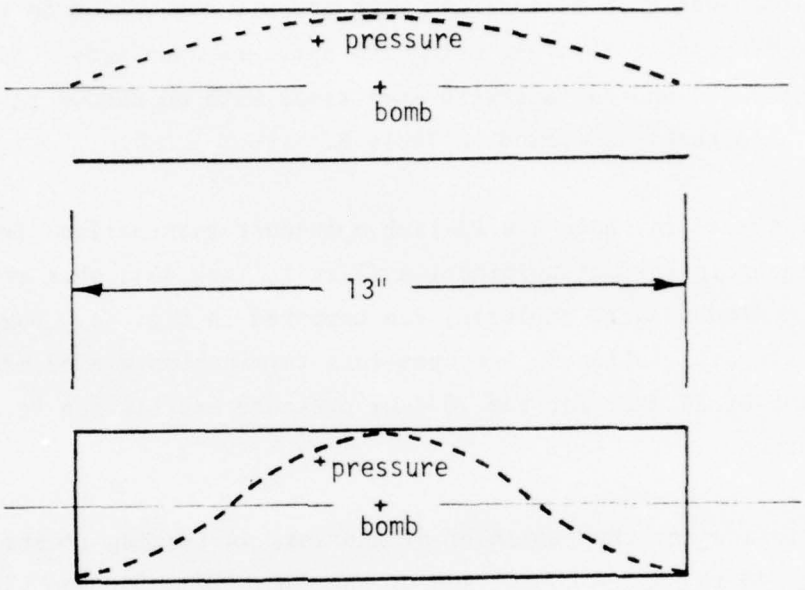

Figure 43. Comparison of Pressure Wave in Open-Ended and Closed-Ended Acoustic Models

As in Task 3, all tests in Task 4 were made with no cathode absorber.

The simple closed-duct termination was initially tested with zero anode aperture area to establish a base value of oscillation frequency and damp time. The closed-duct termination was then tested both with and without CERCOR in the flow channels over a range of resonator volume using 20% aperture open area. Additional tests were made using 10% and 34% aperture open areas with no CERCOR in the flow channels. Results of these tests are found in Table 5.

Oscilloscope traces for both the 13-inch open-duct termination (Test 34, Task 3) and the 13-inch closed-duct termination (Test 1, Task 4A), when both anode and cathode solid windows were employed, are compared in Fig. 44. Damp time for the 484-Hz pressure oscillation in the open-duct termination was 33 msec compared to a damp time of 27 msec for the 1044-Hz pressure oscillation in the closed-duct termination.

Pressure histories for the remainder of the Task 4A testing (tests 2 to 31) are shown in Fig. 45 to 50. A comparison of the damp times for the various aperture open-area/CERCOR combinations is shown in Fig. 51.

Figure 45 shows both unfiltered and filtered pressure histories for 20% aperture open-area, no CERCOR, and a 5-inch piston position. The predominance of the 1050-Hz mode is evident. In addition, the importance of higher frequencies representative of possible cavity modes are also much in evidence.

Damp times of approximately 12, 6, and 2 msec were recorded for 20% aperture open-area tests with no CERCOR, 0.5-inch CERCOR, and 3.0-inch CERCOR, respectivel-. These can be compared with the damp times of approximately 4, 4.5, and 5 msec recorded for similar tests in the open-ended model. Thus, it appears that the 20% aperture open area absorber is not as effective at the higher frequency characteristic of the closed-duct termination as it is at the lower frequency characteristic of the open-ended model. The presence of CERCOR has a much greater effect at the higher frequency, however.

TABLE 5 . TASK 4A TEST SUMMARY

Test No.	Anode Window Open Area, percent	CERCOR in Channel	Anode Piston Position, inch	Damp Time, msec
1	0	None	0	27.0
2	20	None	0	12.0
3			1	13.0
4			2	16.0
5			3	23.0
6			4	17.0
7			5	16.5
8			6	14.5
9	20	0.5 in.	0	6.0
10			1	7.0
11			2	7.0
12			3	8.0
13			4	8.0
14			6	9.0
15	20	3.0 in.	0	2.0
16			1	1.5
17			2	2.5
18			2	3.0
19			3	2.0
20			4	2.0
21			6	2.5
22	34	None	0	19.0
23			1	13.0
24			2	16.0
25			3	19.0
26			4	21.0
27	10	None	0	12.5
28			1	18.0
29			2	19.0
30			3	20.0
31			4	21.0

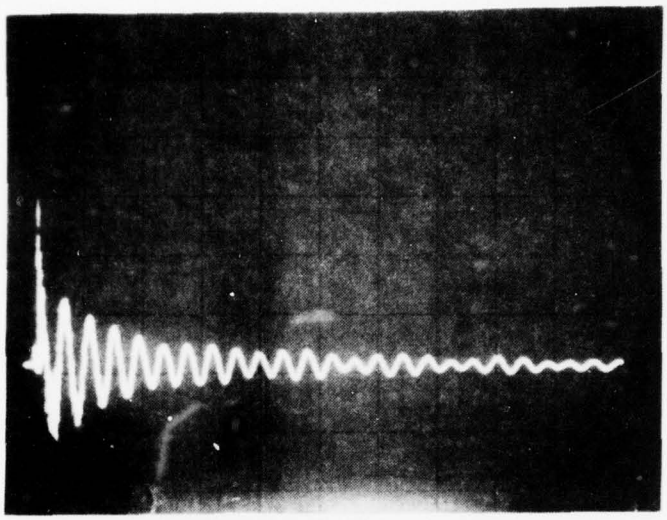

2 $\frac{psi}{cm}$

5 msec/cm

Open-Duct Termination (484 Hz)

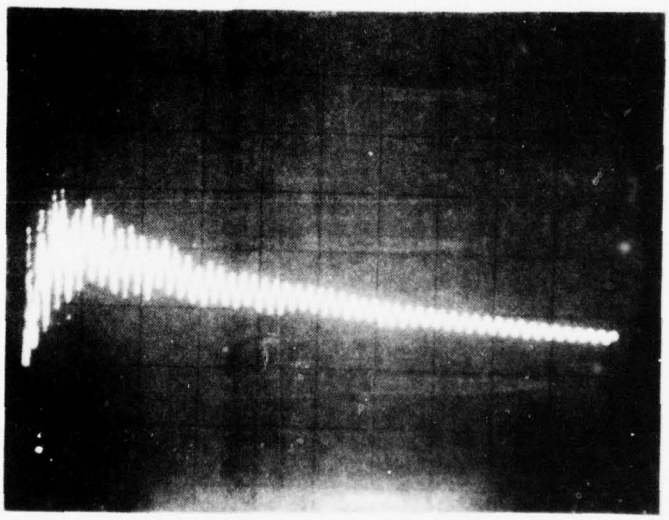

2 $\frac{psi}{cm}$

5 msec/cm

Simple Closed-Duct Termination (1044 Hz)

Figure 44. Comparison of Pressure Histories for Open- and Closed-Duct Termination

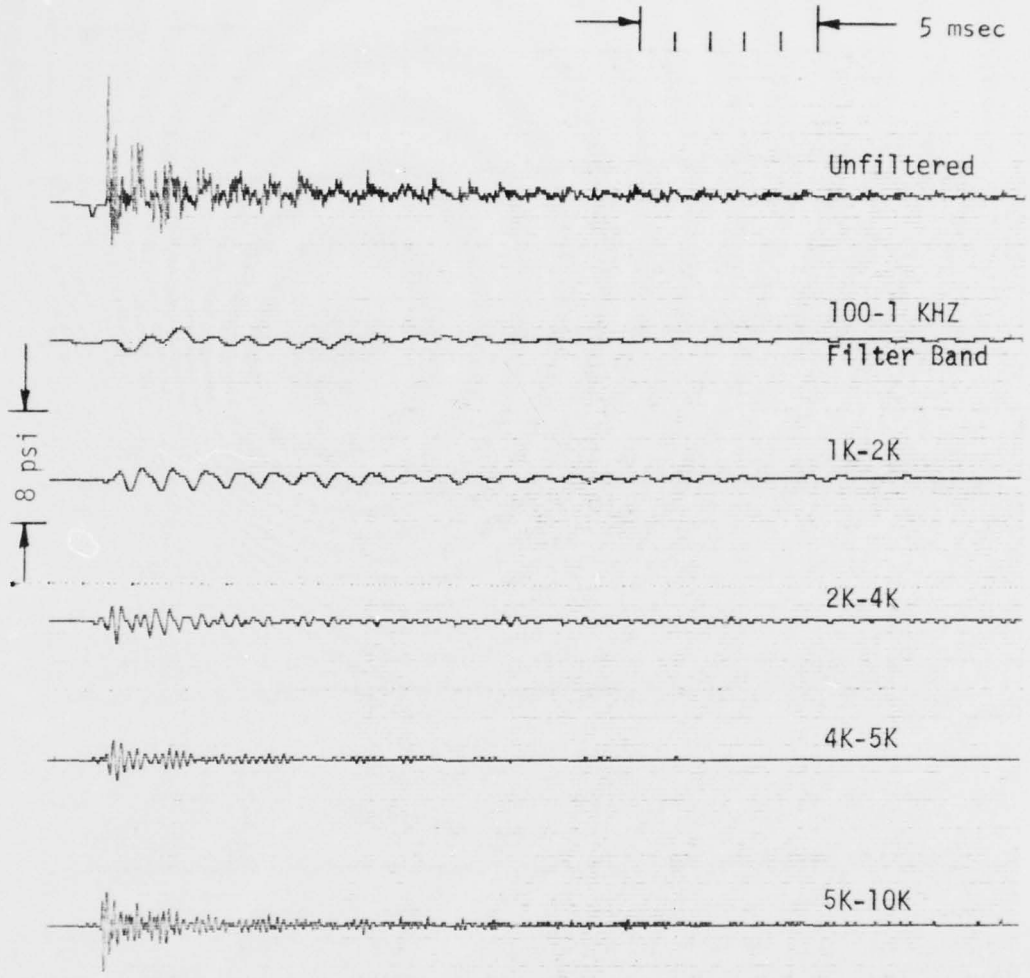

Figure 45. Pressure History for Closed-Duct Termination; 20% Aperture Open Area, no CERCOR, 5-inch Piston Position

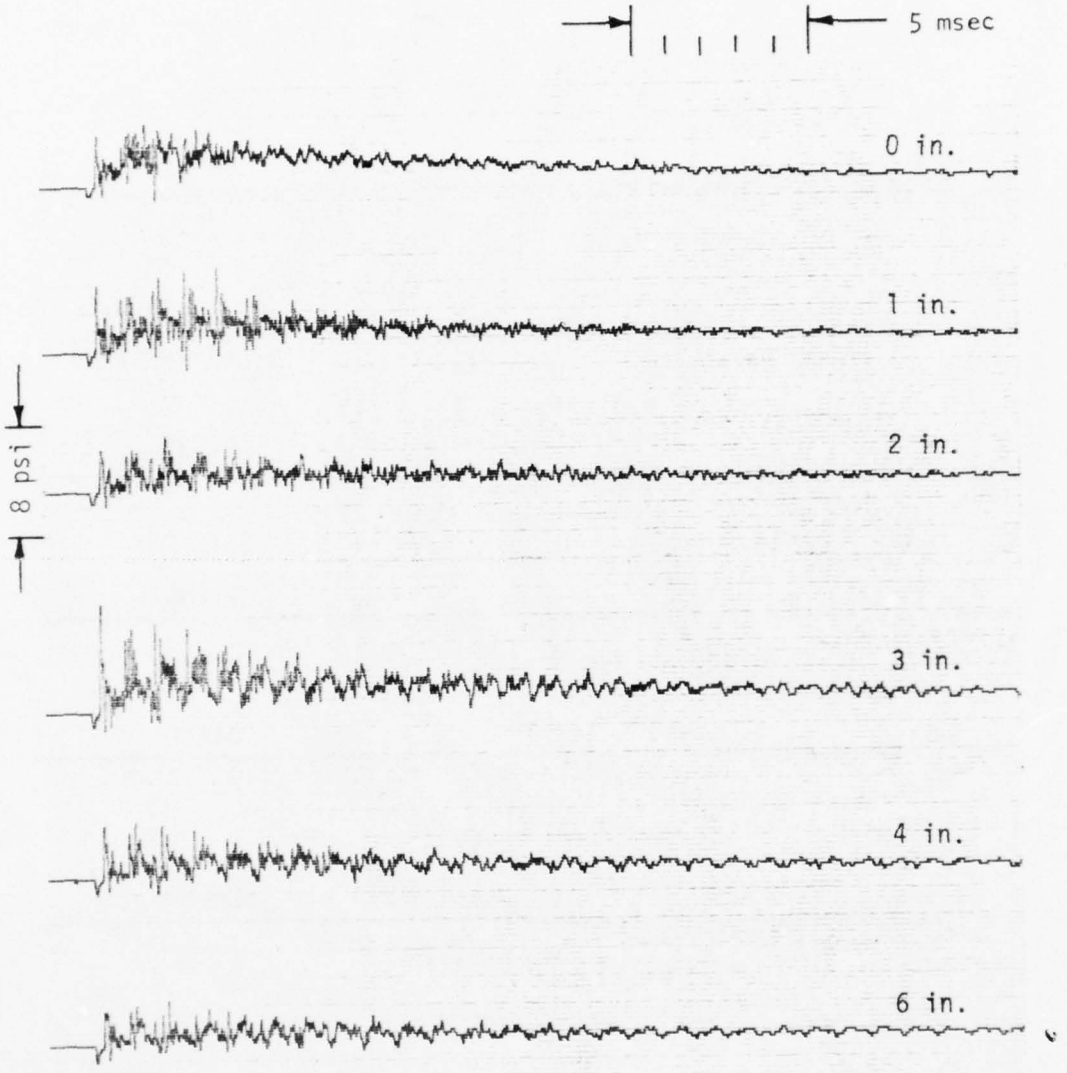

Figure 46. Effect of Piston Position on Pressure History for Closed-Duct Termination; 20% Aperture Open Area, no CERCOR

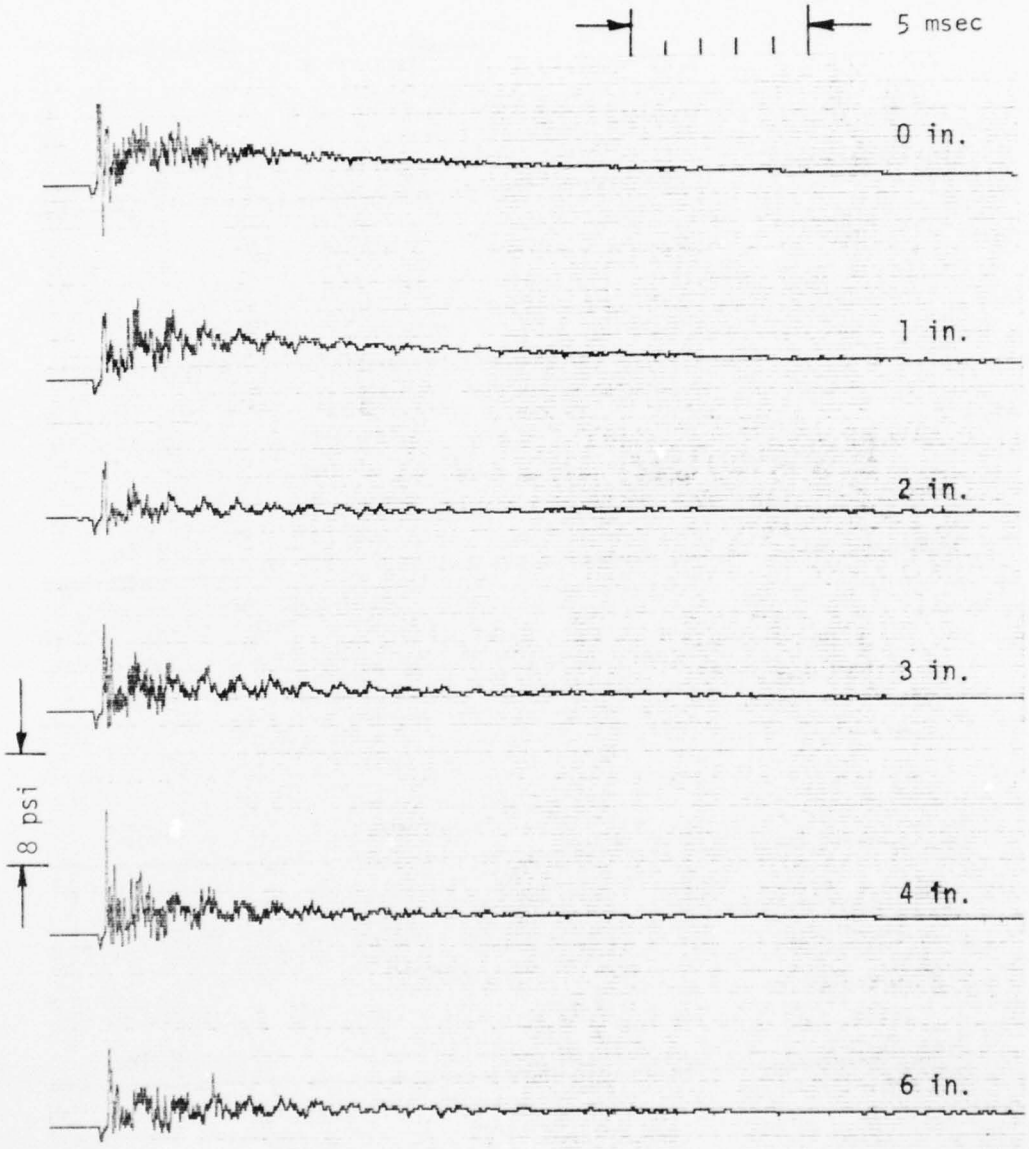

Figure 47. Effect of Piston on Pressure History for Closed-Duct Termination; 20% Aperture Open Area, ½-inch CERCOR

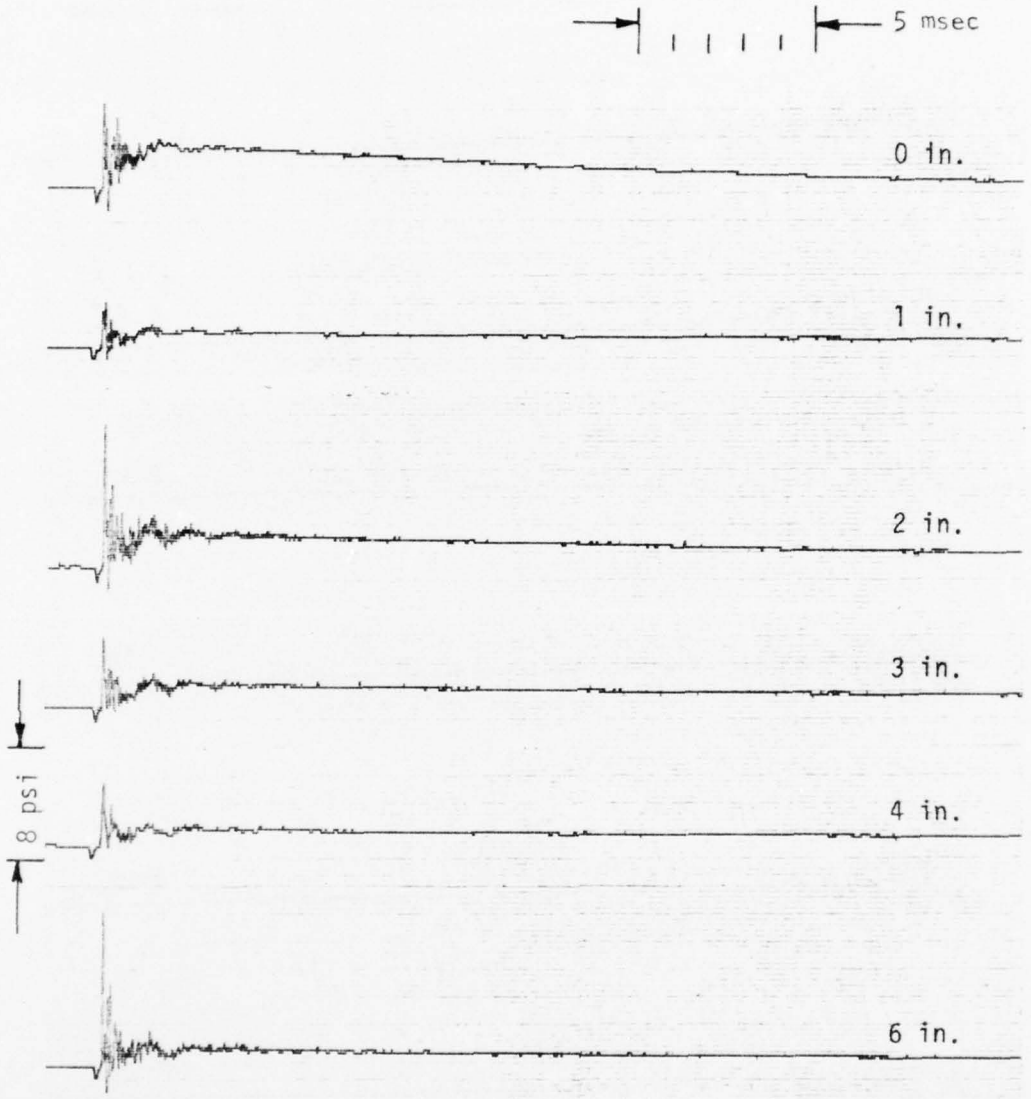

Figure 48. Effect of Piston Position on Pressure History for Closed-Duct Termination; 20% Aperture Open Area, 3-inch CERCOR

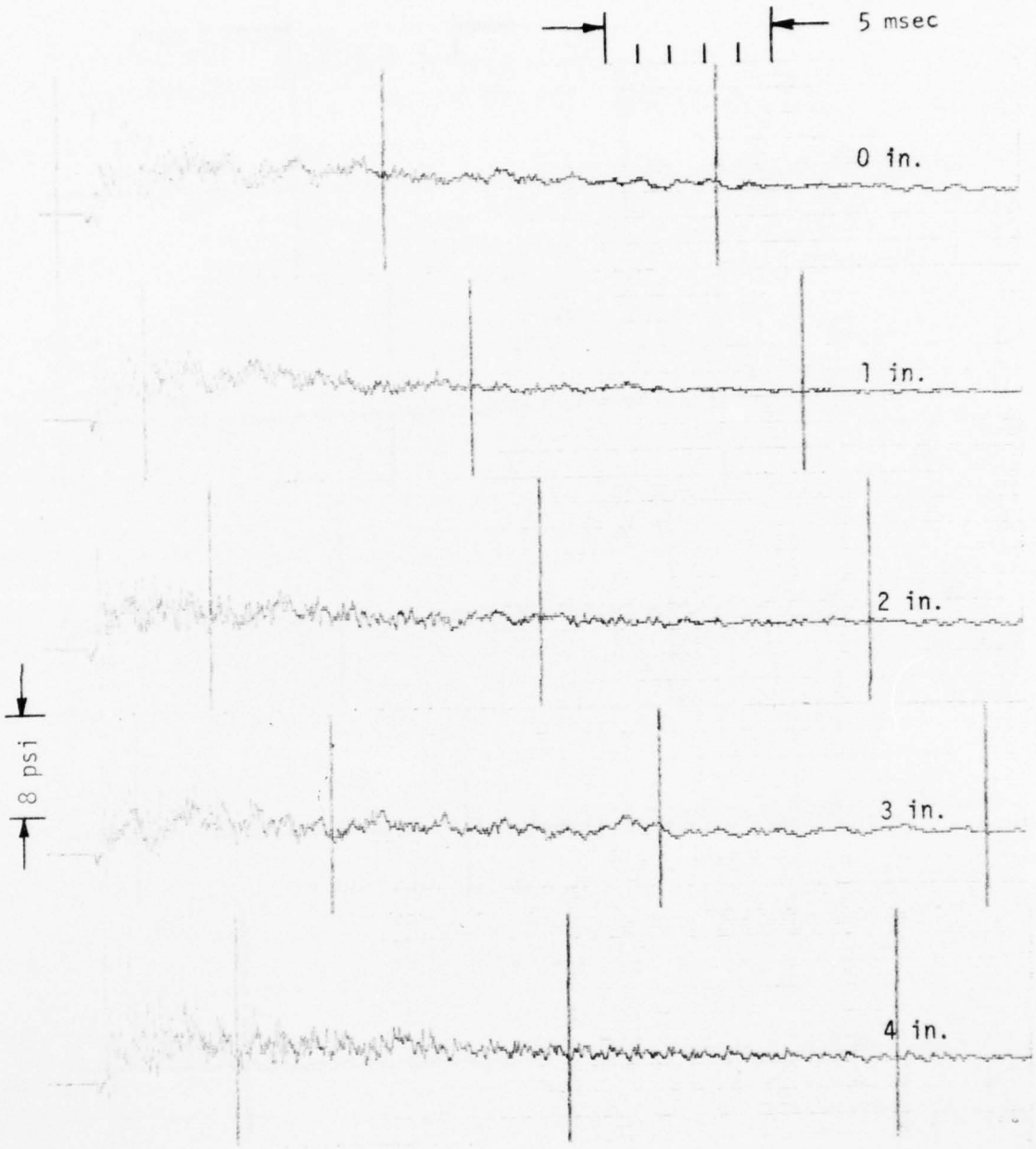

Figure 49. Effect of Piston Position on Pressure History for Closed-Duct Termination; 34% Aperture Open Area, no CERCOR

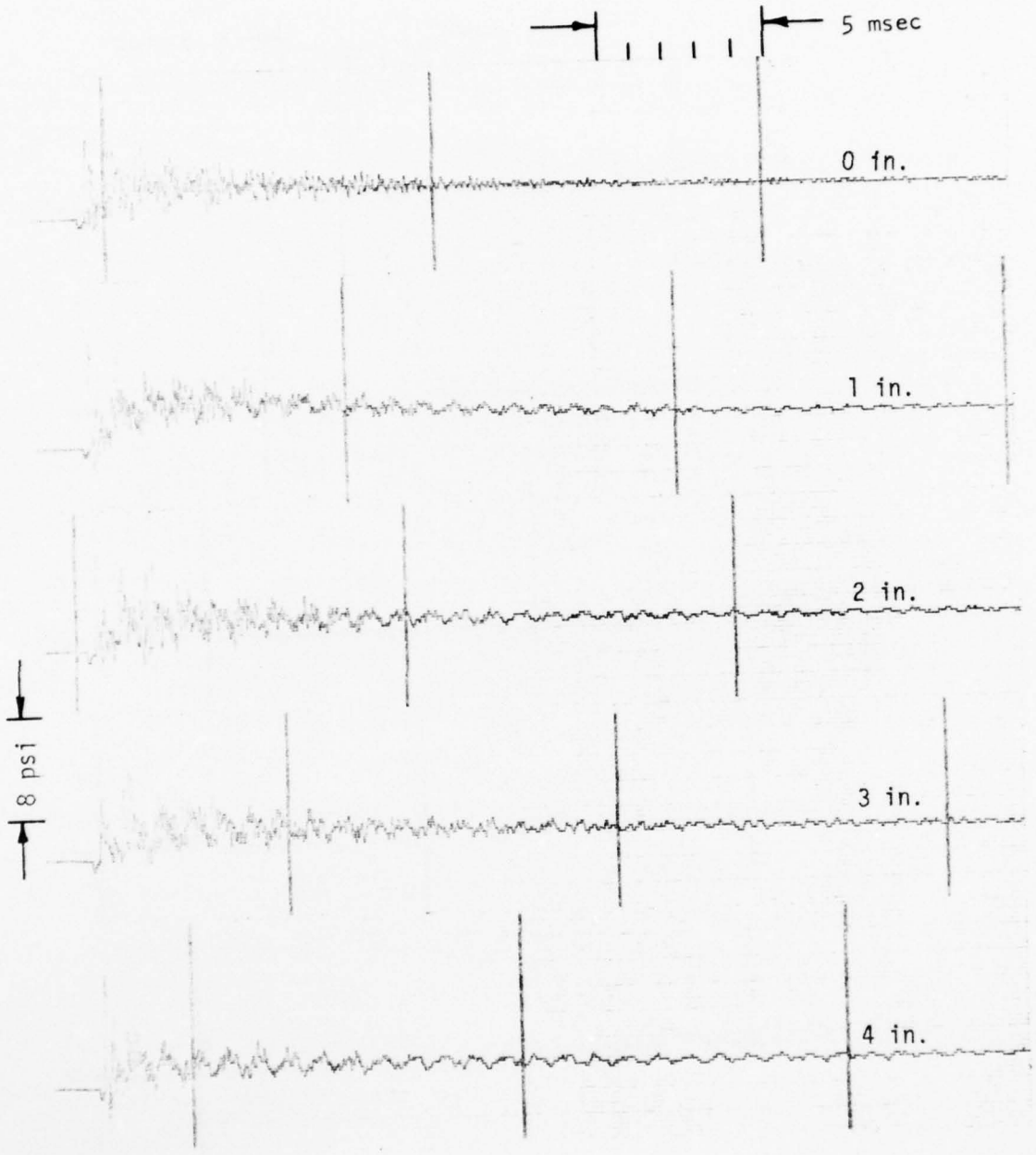

Figure 50. Effect of Piston Position on Pressure History for Closed-Duct Termination; 10% Aperture Open Area, no CERCOR

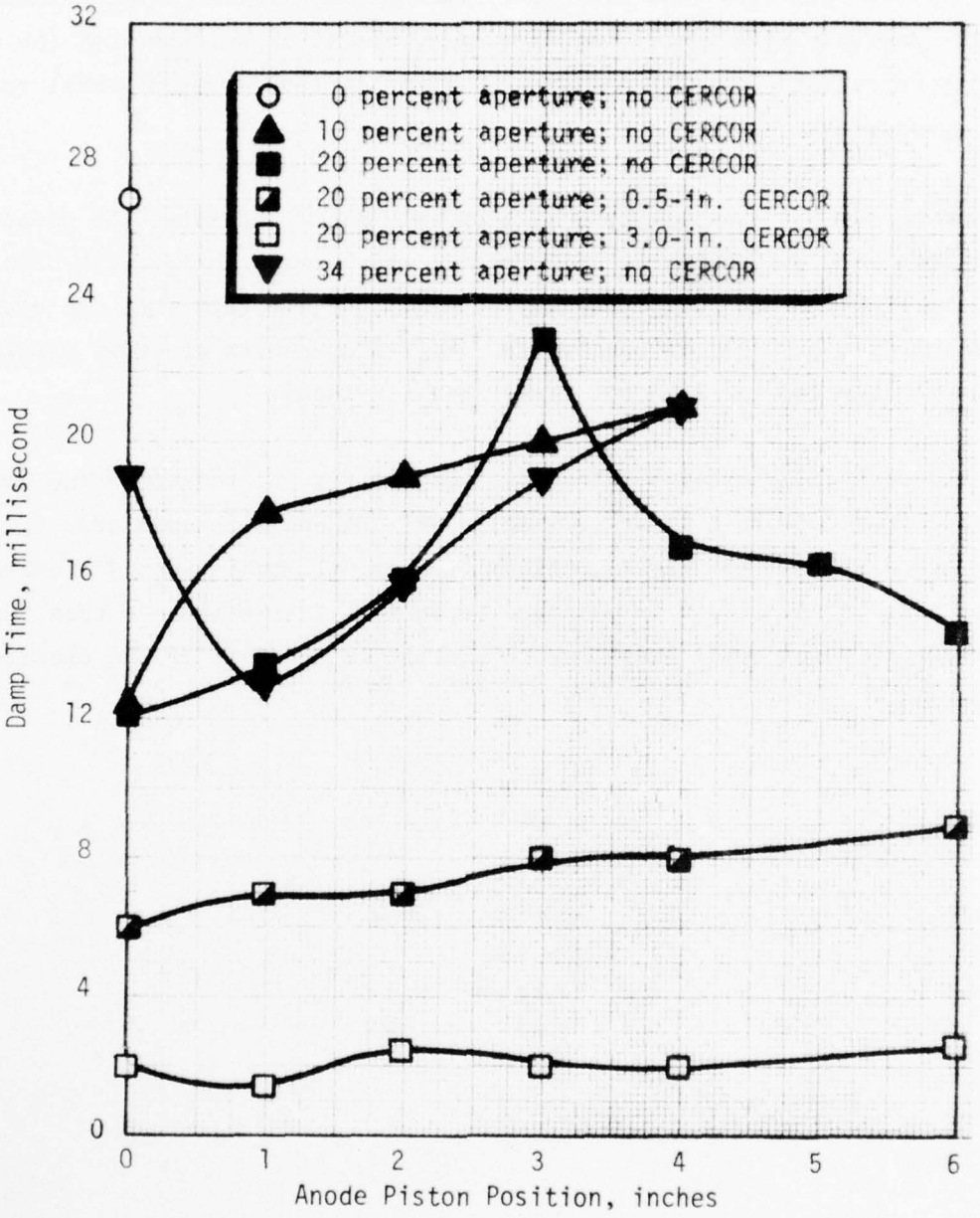

Figure 51. Task 4A Test Results - Effect of Closed-Duct Termination

The strange curve shown for 20% aperture open area and CERCOR in Fig. 51 is due, no doubt, to the presence of the small volume which exists behind the aperture even at zero piston position (see Fig. 20). The optimum piston position should theoretically decrease with increasing frequency, and it is evident that the data indicate optimum tuning occurs at a distance within the ever-present small volume behind the aperture.

Filtered traces for 34% aperture open area and no CERCOR indicated the presence of a 570-Hz mode in addition to the 1050-Hz mode which predominated with both 20% and 10% aperture open area. This probably accounts for the fact that the optimum piston position (see Fig. 51) is greater for the 34% open-area absorber (i.e., 1 inch) than for the 20% and 10% open areas (i.e., 0-inch).

The use of an acoustic absorber by itself is seen in Fig. 51 to reduce the damp time by a factor of 2.3 (from 27 to 12 msec). The 20% aperture open area found optimum in Task 3 appears to also be optimum or near optimum in Task 4A. However, the acoustic absorber by itself is observed to be much less effective than the 3.0-inch CERCOR in damping the pressure oscillation in the case of the closed-duct termination.

TASK 4B - COMPLEX CLOSED-DUCT TERMINATION

The complex closed-duct termination consisted simply of an insert for each end of the 13-inch-long, open-ended acoustic model which, while still open at the ends, contains a flow area partially blocked by rods (which attempts to simulate the flow of gas through a bank of heat exchanger tubes). Details of the arbitrarily selected rod configuration, which contained 50 0.10-inch-diameter rods spaced 0.1875 inch apart and positioned perpendicular to the flow axis, are shown in Fig. 52. A photograph of the inserts is shown in Fig. 53.

The complex closed-duct termination was initially tested with zero anode aperture area (solid window) to establish a base value of oscillation frequency and damp time. An oscilloscope trace of this test (test 1, Task 4B) is shown in Fig. 54. The oscillation frequency of 304 Hz corresponds to the first open-open acoustic mode in the 20.5-inch-long (end to end) model (with an end correction of 1.0 inch at each end). A very short damp time of about 9.5 msec was noted.

The complex closed-duct termination was then tested both with and without CERCOR in the flow channels over a range of resonator volume using 20 percent aperture open area. Results of all Task 4B tests are found in Table 6.

Pressure histories for tests 2 to 19 are shown in Fig. 55 to 57. A comparison of the damp times for the tests with and without CERCOR is shown in Fig. 58. Figures 55 and 56 reveal the presence of a 1700 Hz oscillation frequency in addition to the 300 Hz mode. This frequency may indicate interaction with cavity modes. The optimum damp time, however, is about 6 msec for this duct determination for the acoustic absorber alone (see Fig. 58). The use of CERCOR does not appreciably improve damp time. The fact that neither optimization of the acoustic absorber nor use of the CERCOR flow conditioner improves damp time by any more than 4 or 5 msec implies that the solid rods in the duct inserts (heat exchanger tube simulants) provide a very significant amount of damping by themselves.

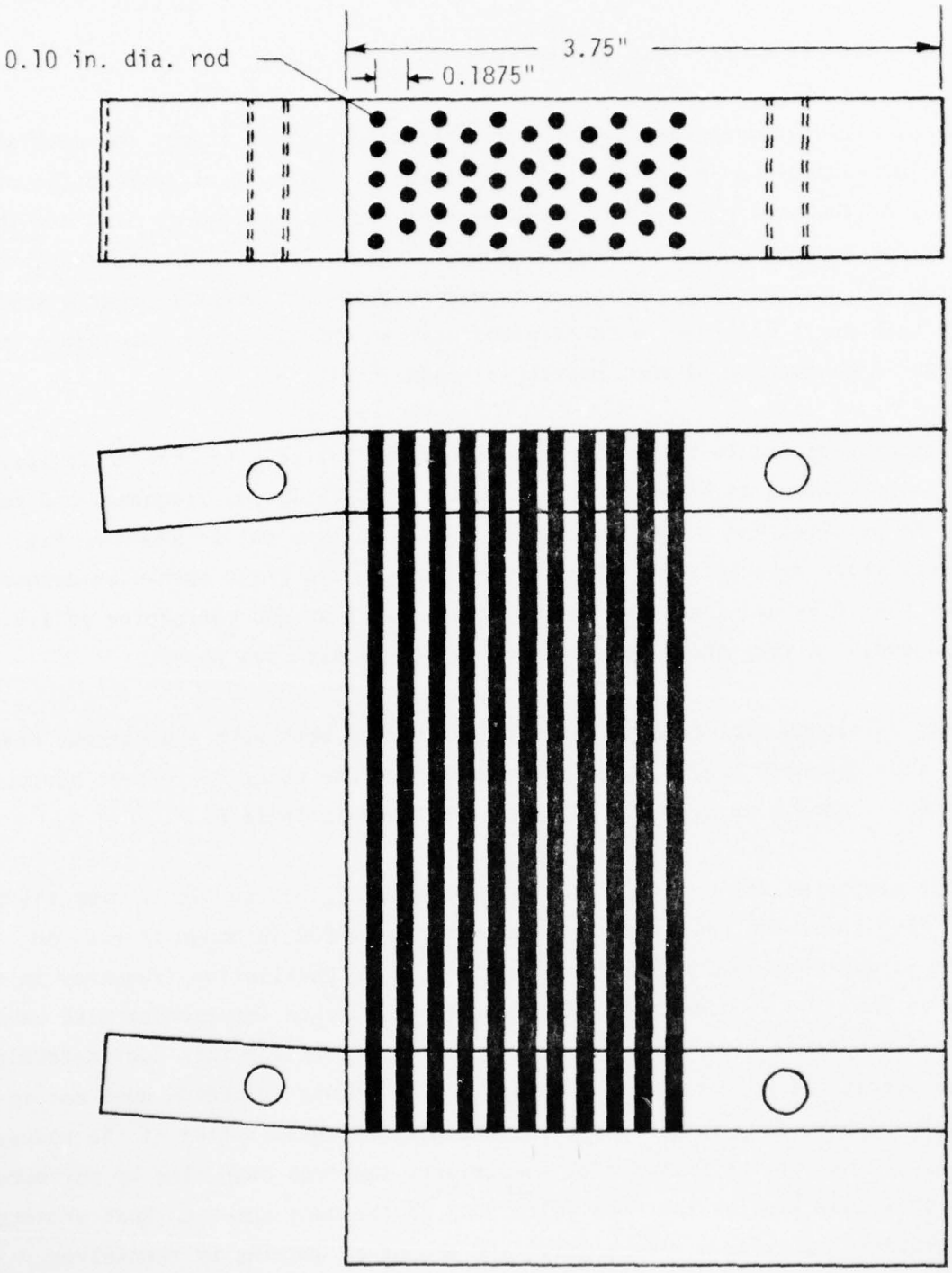

Figure 52. Complex Closed-Duct Termination Design

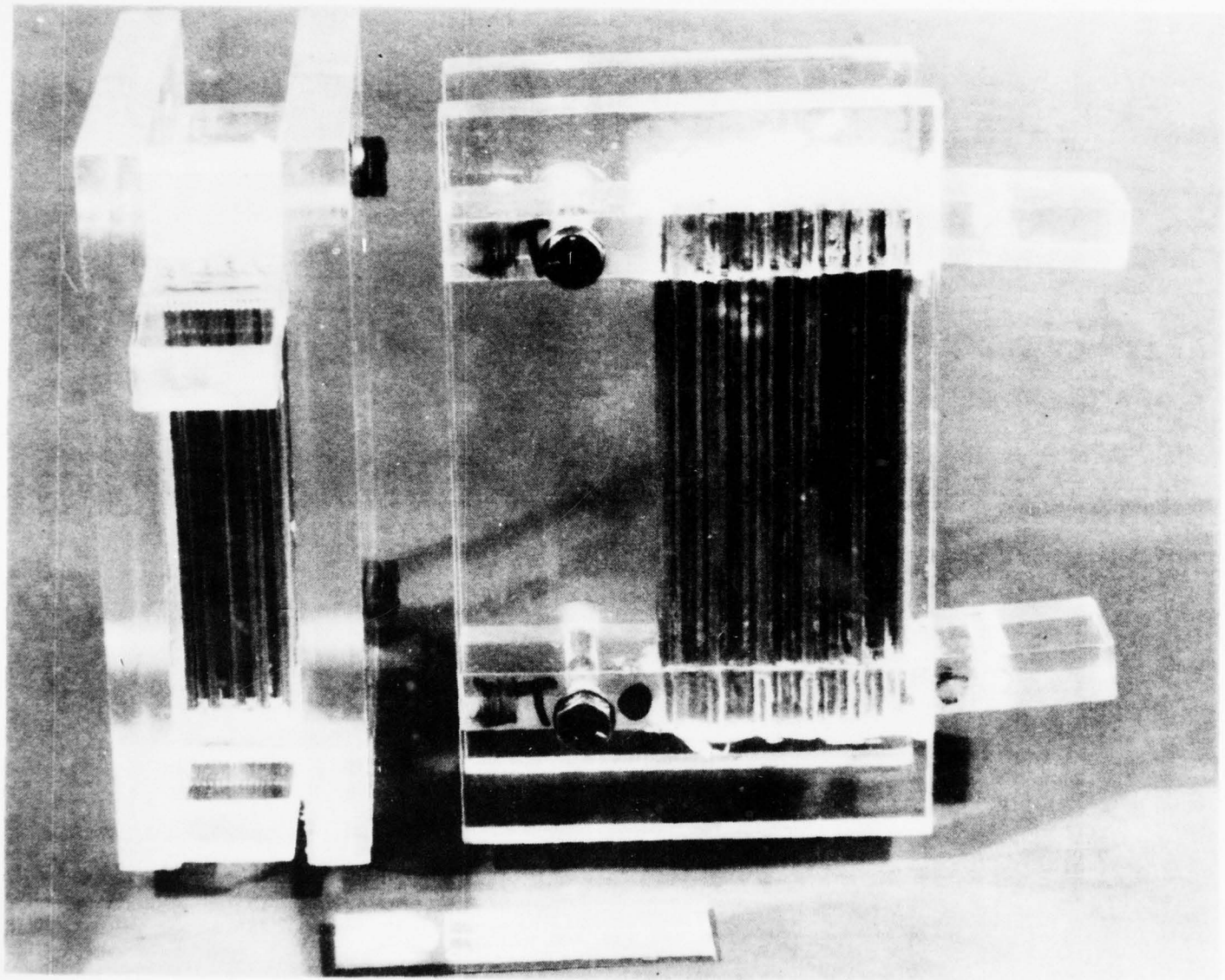

Figure 53. Complex Closed-Duct Termination

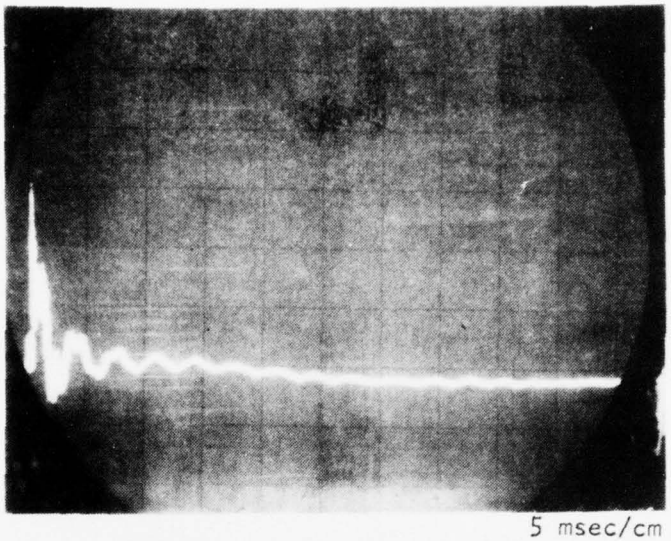

Complex Closed-Duct Termination (304 Hz)

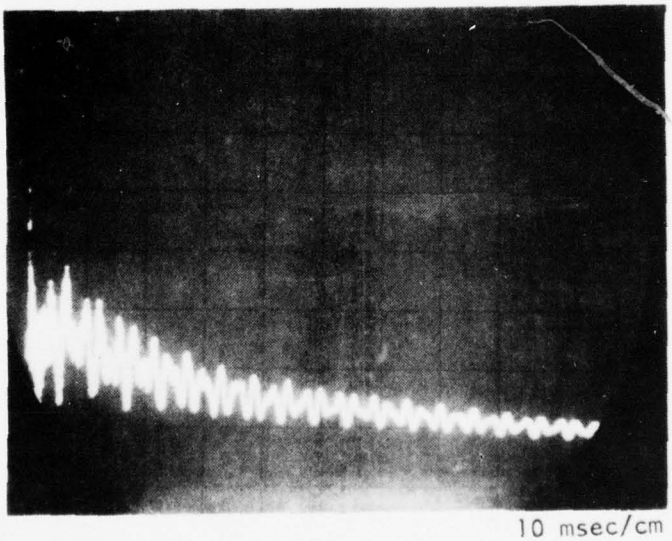

Plenum Duct Termination (694 Hz)

Figure 54. Comparison of Pressure Histories for Complex Closed and Plenum Duct Terminations

TABLE 6. TASK 4B TEST SUMMARY

Test No.	Anode Window Open Area, percent	CERCOR in Channel	Anode Piston Position, inch	Damp Time, msec
1	0	None	0	9.5
2	20	None	0	10.0
3	↓	↓	1	8.5
4			2	6.0
5			3	10.5
6			4	11.0
7			5	10.0
8	↓	↓	6	13.0
9	20	0.5 in.	0	10.0
10	↓	↓	1	8.5
11			2	7.0
12			3	7.5
13			4	15.5
14	↓	↓	6	12.0
15	20	3.0 in.	0	6.0
16	↓	↓	1	6.0
17			2	6.0
18			4	5.5
19	↓	↓	6	5.0

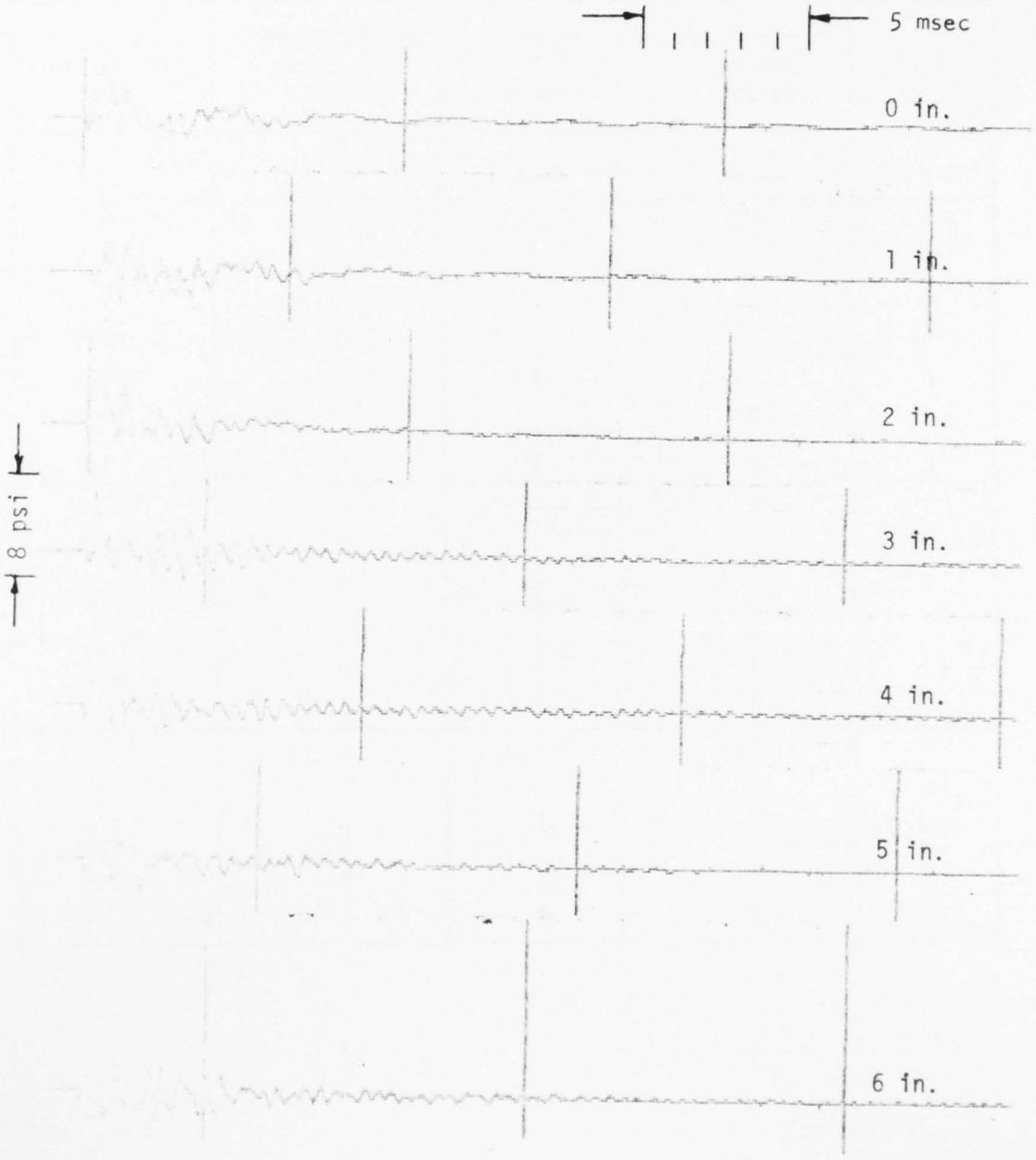

Figure 55. Effect of Piston Position on Pressure History for Complex Closed-Duct Termination; 20 percent Aperture Open Area, no CERCOR

AD-A038 628 ROCKWELL INTERNATIONAL CANOGA PARK CALIF ROCKETDYNE DIV F/G 20/5
PRESSURE DAMPING FOR PULSED ELECTRIC DISCHARGE LASER.(U)
APR 76 R KESSELRING, R MARCH F29601-73-A-0034
UNCLASSIFIED R-9739 AFWL-TR-75-170 NL

2 OF 2
AD A038628

END

DATE FILMED
5-77

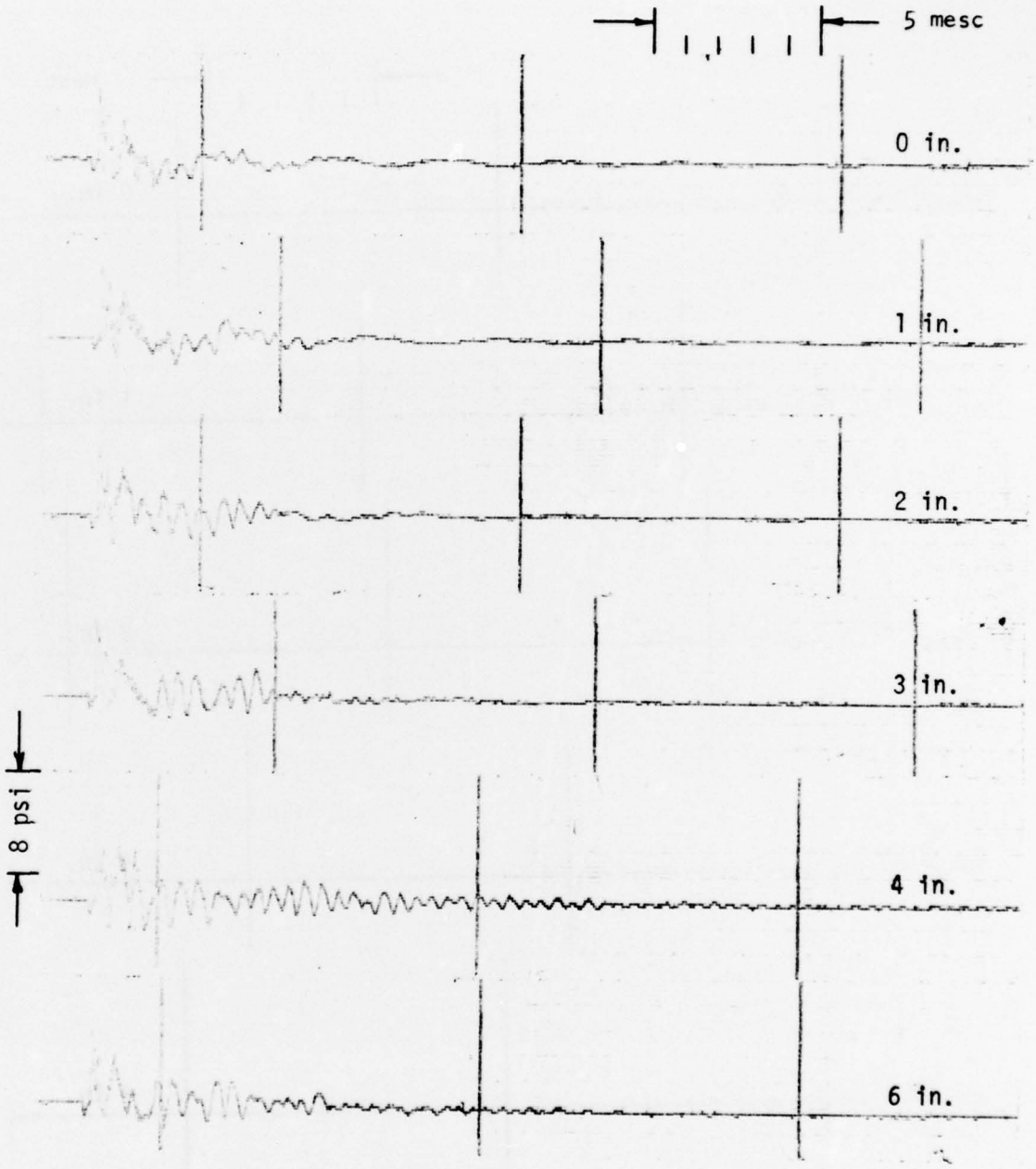

Figure 56. Effect of Piston Position on Pressure History for Complex Closed-Duct Termination; 20-percent Aperture Open Area, 0.5-inch CERCOR

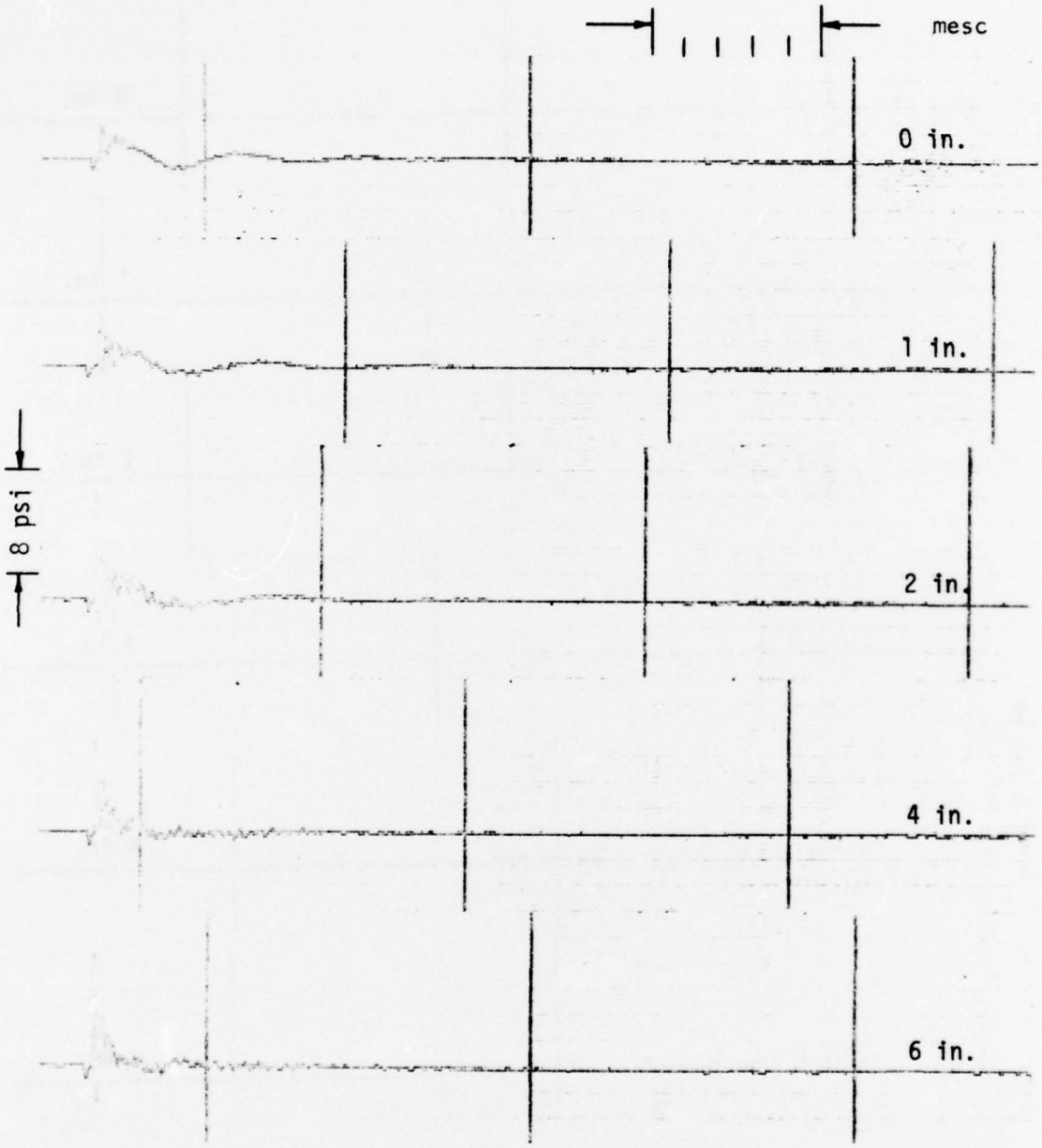

Figure 57. Effect of Piston Position on Pressure History for Complex Closed-Duct Termination; 20-percent Aperture Open Area, 3.0-inch CERCOR

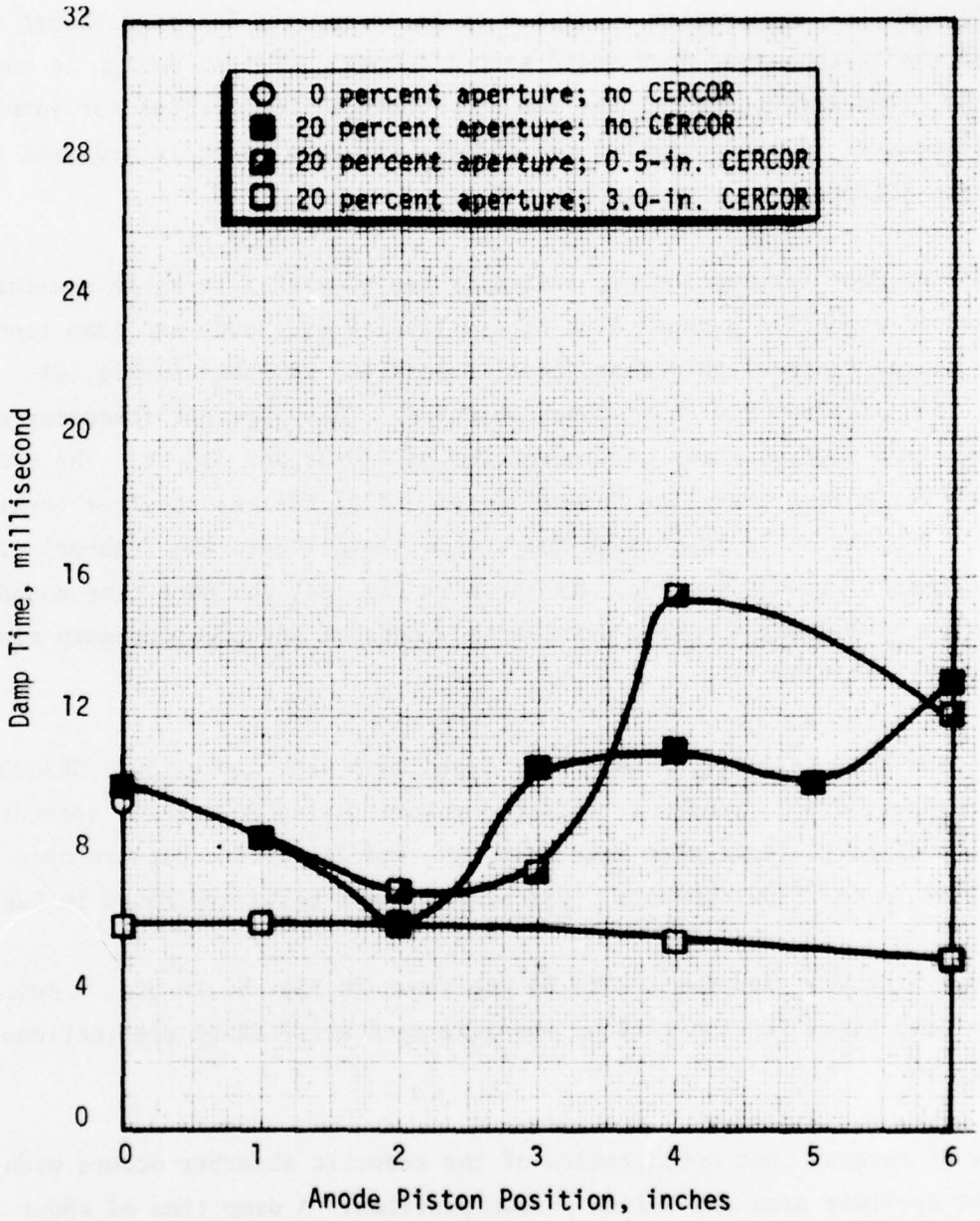

Figure 58. Task 4B Test Results - Effect of Complex Closed-Duct Termination

TASK 4C - PLENUM DUCT TERMINATION

The plenum duct termination consisted of an irregular, T-shaped insert for each end of the 13-inch-long open-ended acoustic model. Detail design is shown in Fig. 59. The insert thus closes the flow channel and provides for turning of an acoustic wave. A photograph of the inserts prior to being joined with the basic acoustic EDL model is shown in Fig. 60.

The plenum duct termination was initially tested with zero anode aperture (solid window) to establish a base value of oscillation frequency and damp time. An oscilloscope trace of this test (test 1, Task 4C) is shown in Fig. 54. An apparent oscillation frequency of 694 Hz was observed. This apparent frequency of 694 Hz results from superposition of frequencies of 570 Hz and 318 Hz. The 570 Hz is calculated for a wave traveling to the closed end of the insert after turning 90 degrees. The 318 Hz is calculated for a wave traveling to the (nearer) closed side of the insert without turning. As shown in Fig. 54, the damp time noted for this duct termination was 73 msec, a value in excess of any previous damp time measured during this contract.

The plenum duct termination was then tested both with and without CERCOR in the flow channels over a range of resonator volumes using 20-percent aperture open area. Additional tests were made using 10- and 34-percent perture open area with no CERCOR in the flow channels. Results of these tests are found in Table 7.

Pressure histories for tests 2 to 34 are shown in Fig. 61 to 65. A comparison of the damp times for the various aperture open area/CERCOR combinations is shown in Fig. 66.

Figure 66 reveals that optimization of the acoustic absorber occurs with a 20-percent aperture area and 3-inch piston position. A damp time of about 14.5 msec is recorded for this configuration. This represents a factor of 5 reduction from the 73-msec damp time recorded with no damping device.

A factor of 9 reduction in damp time is achieved, however, through use of 3.0-inch CERCOR in the flow channels without acoustic resonators. A further reduction (factor of 12) in damp time to 6 msec is noted when CERCOR and a 20-percent open-area acoustic resonator with 2-inch piston position are employed together.

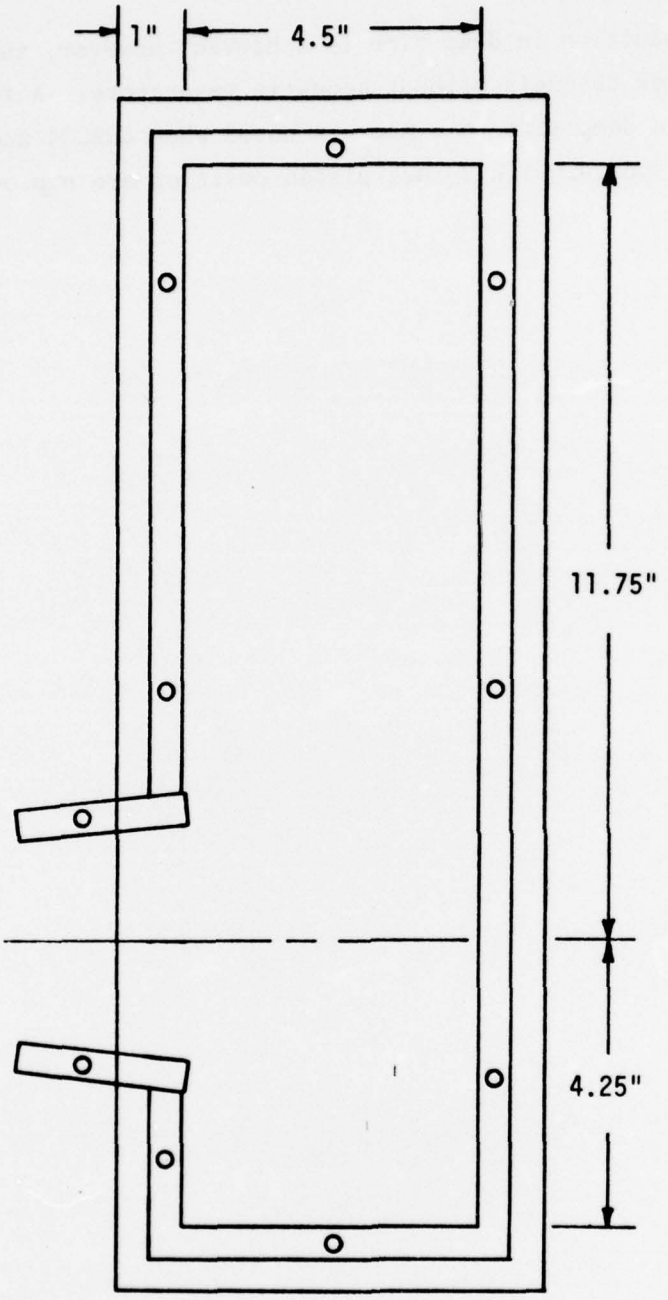

Figure 59. Design of Plenum Duct Termination

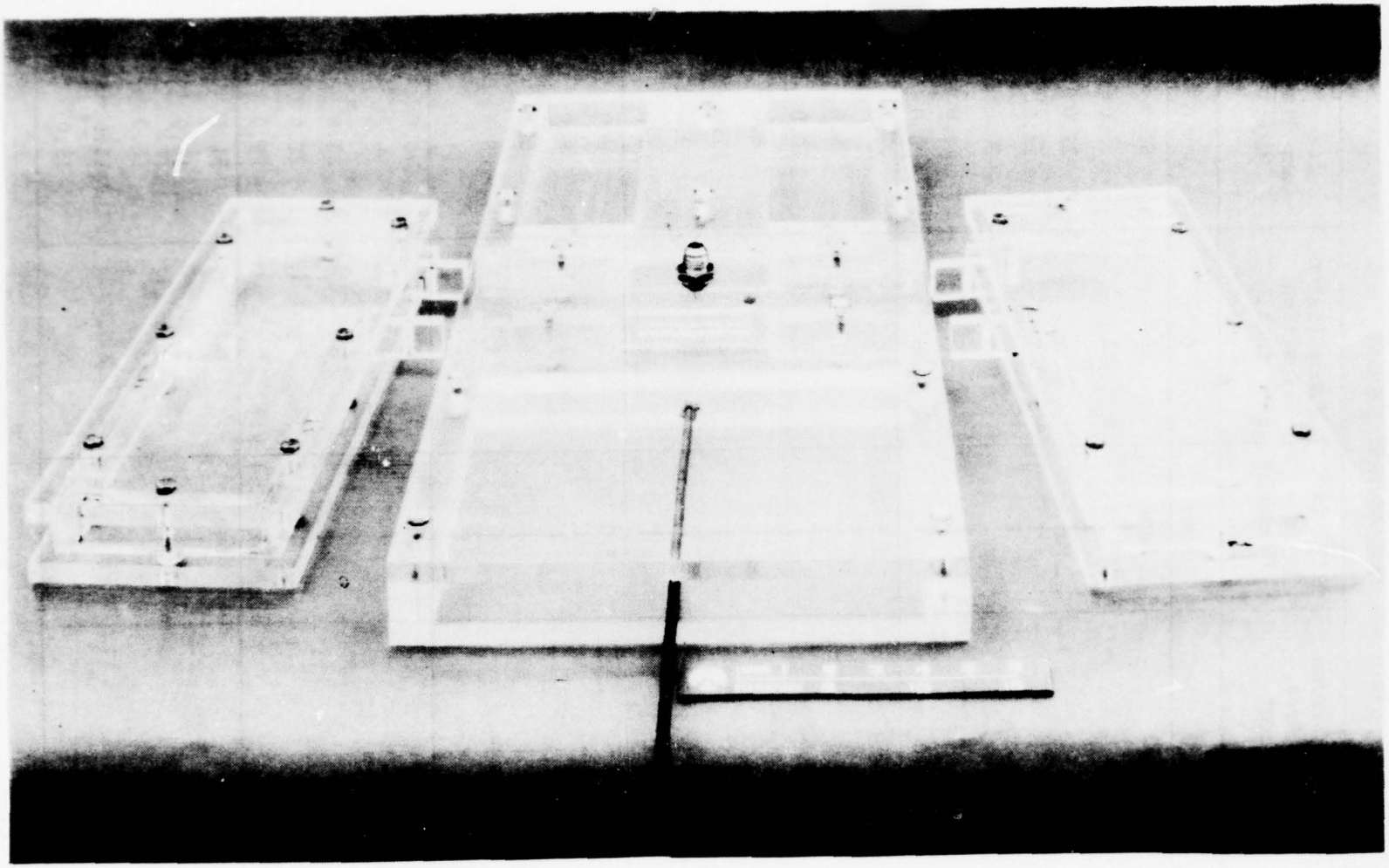

4LE37-4/4/75-S1G

Figure 60. Plenum Duct Termination

TABLE 7. TASK 4C TEST SUMMARY

Test No.	Anode Window Open Area, percent	CERCOR in Channel	Anode Piston Position, inch	Damp Time, msec
1	0	None	0	73.0
2	20	None	0	51.0
3	↓	↓	1	25.0
4			2	22.0
5			3	14.5
6			4	20.0
7			5	15.0
8			6	20.0
9	20	0.5 in.	0	37.0
10	↓	↓	1	18.0
11			2	13.0
12			3	8.0
13			4	11.0
14			5	12.0
15			6	14.0
16	20	3.0 in.	0	9.0
17	↓	↓	1	8.0
18			2	6.0
19			4	8.5
20			6	11.0
21	10	None	0	46.0
22	↓	↓	2	17.5
23			3	23.0
24			4	22.0
25			6	22.0
26	34	None	0	51.5
27	↓	↓	2	19.0
28			3	16.0
29			4	15.5
30			6	15.0

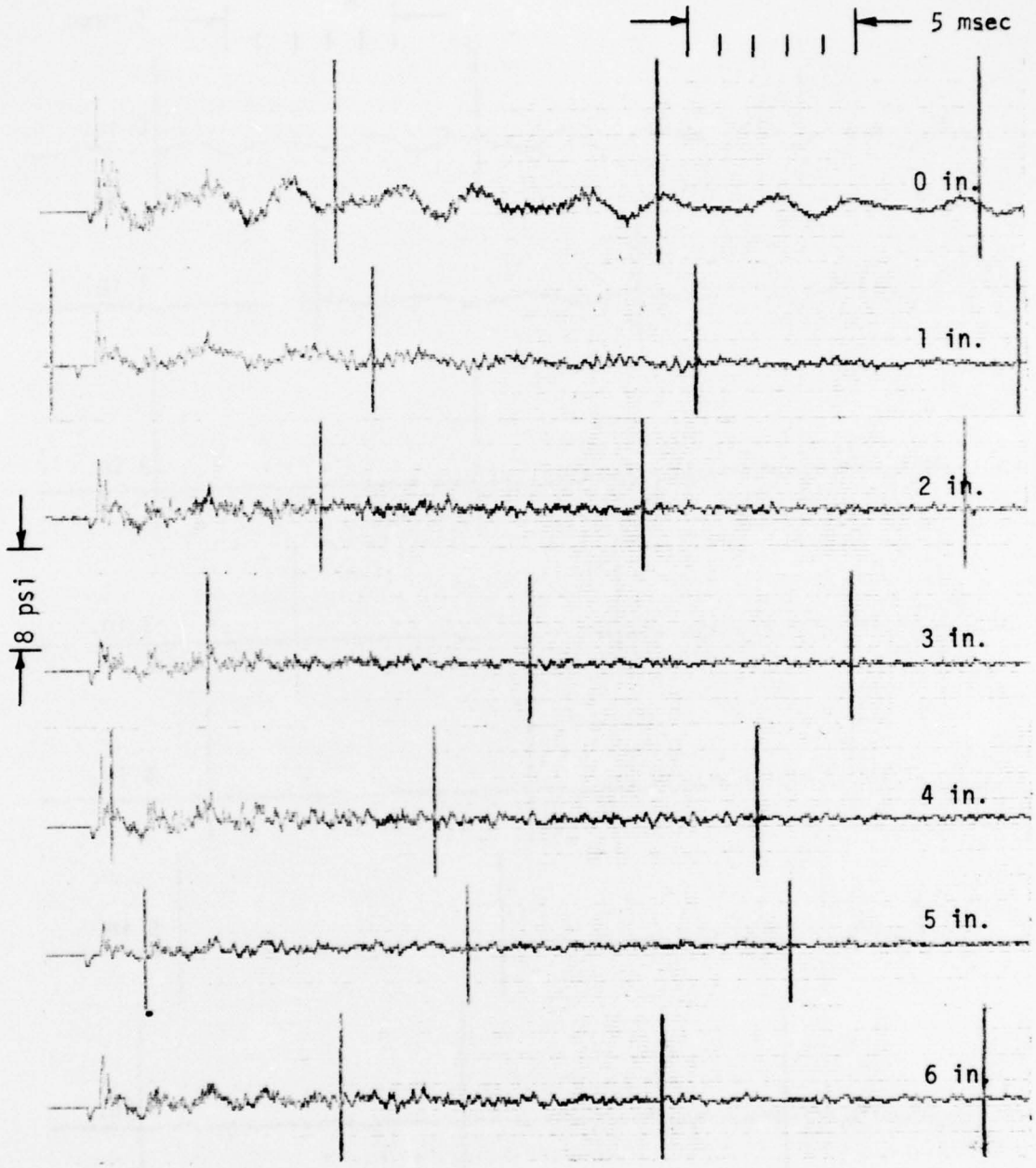

Figure 61. Effect of Piston Position on Pressure History for Plenum Duct Termination; 20-percent Aperture Open Area, no CERCOR

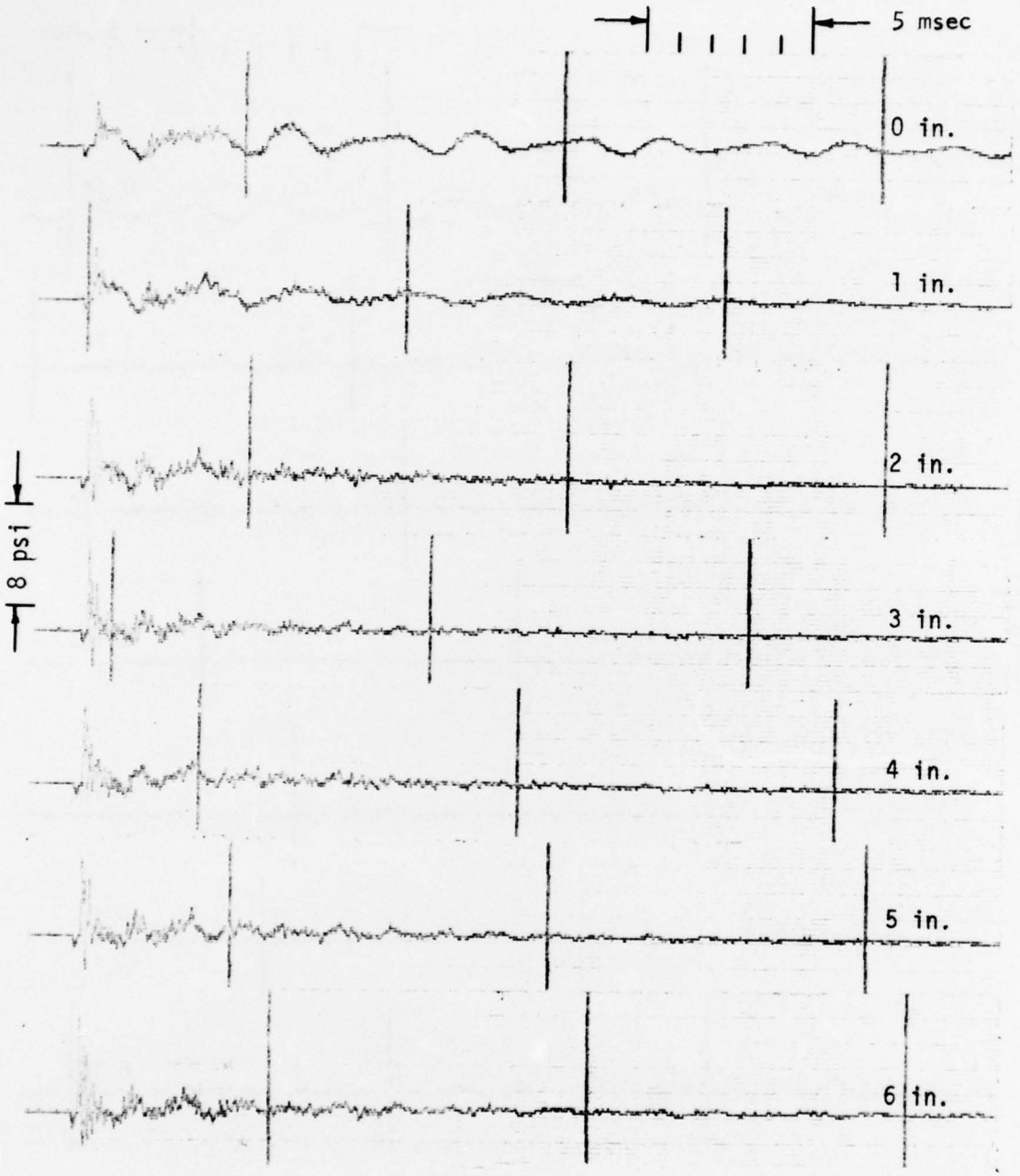

Figure 62. Effect of Piston Position on Pressure History for Plenum Duct Termination; 20-percent Aperture Open Area 0.5-inch CERCOR

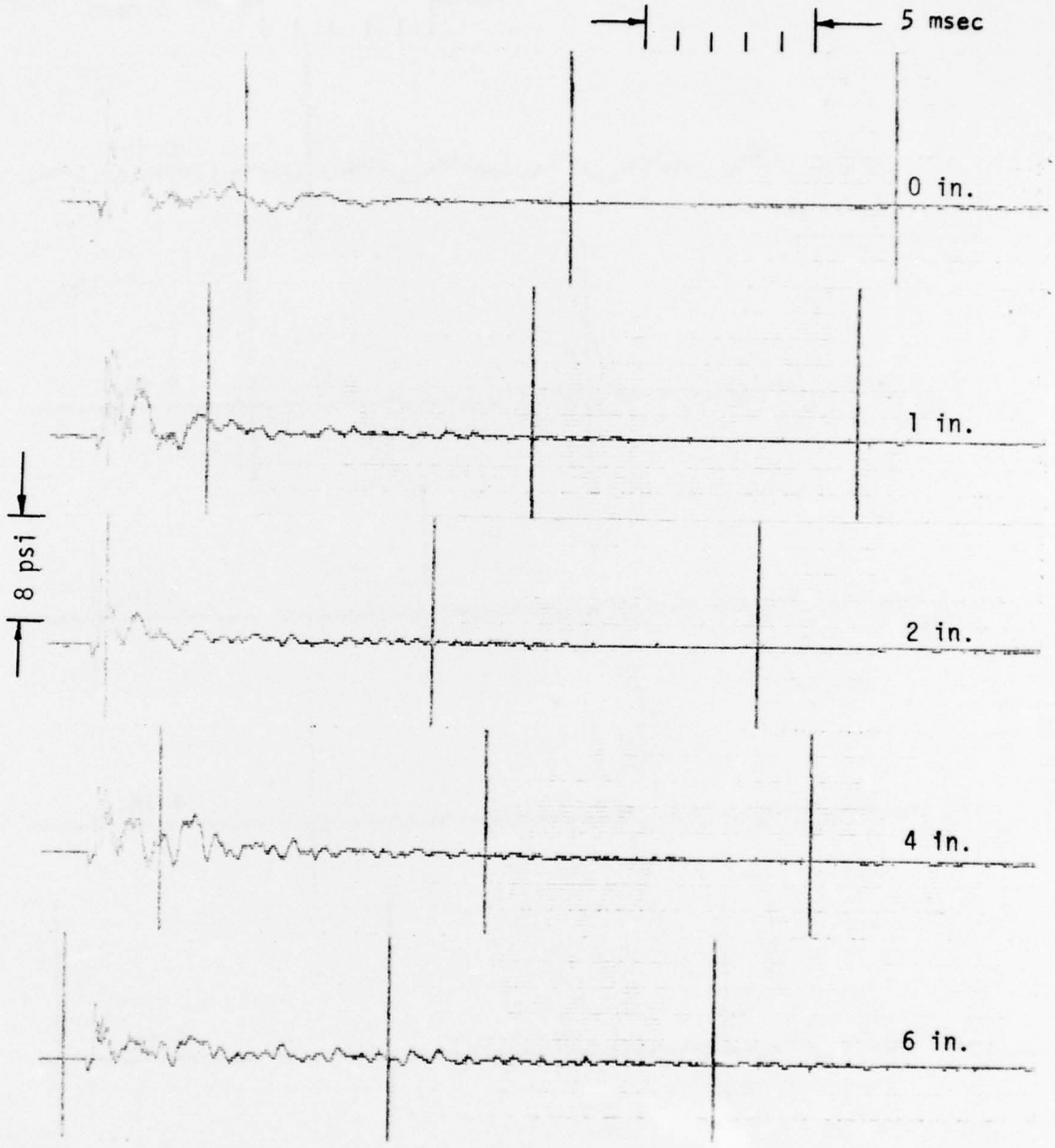

Figure 63. Effect of Piston Position on Pressure History for Plenum Duct Termination; 20-percent Aperture Open Area, 3.0-inch CERCOR

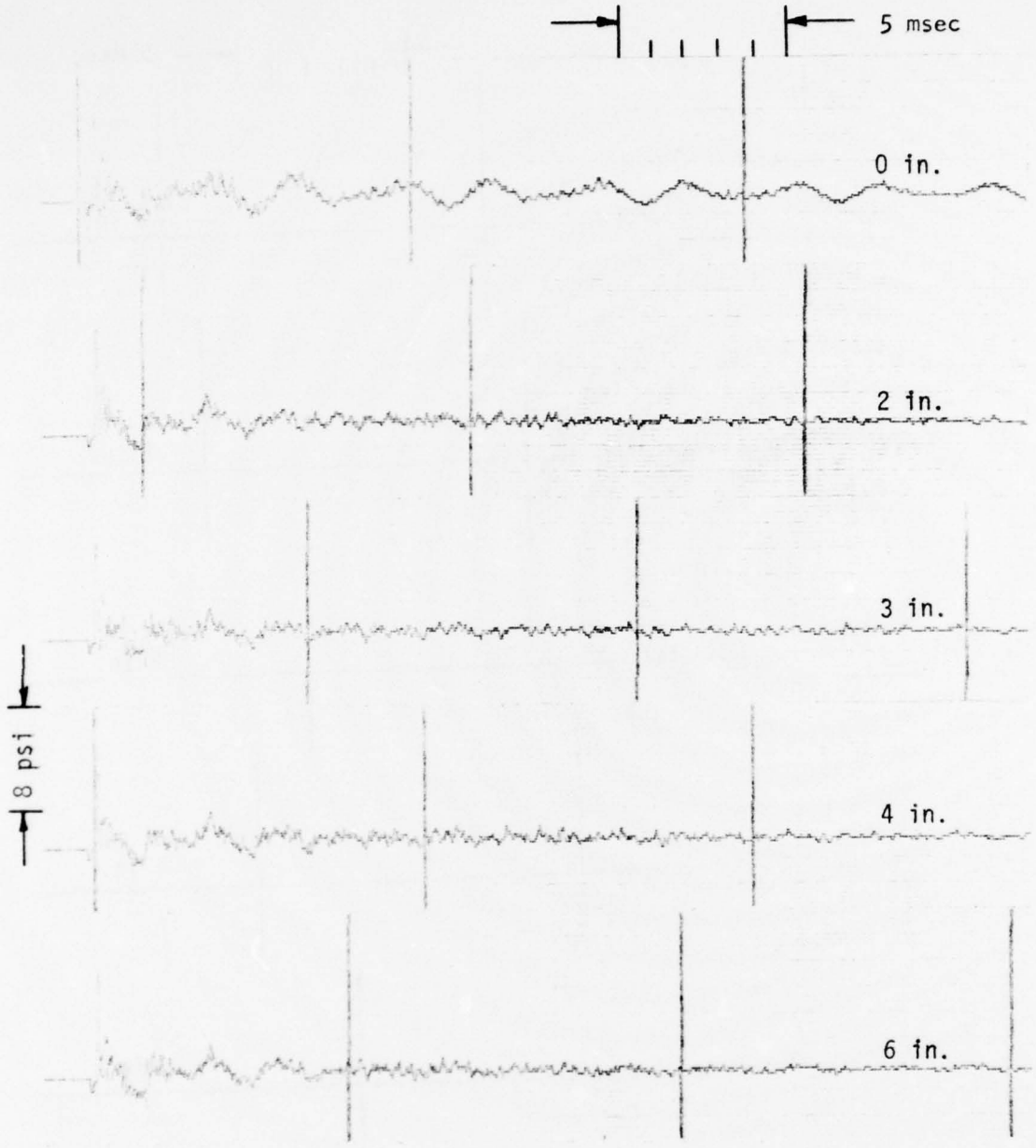

Figure 64. Effect of Piston Position on Pressure History for Plenum Duct Termination; 10-percent Aperture Open Area, no CERCOR

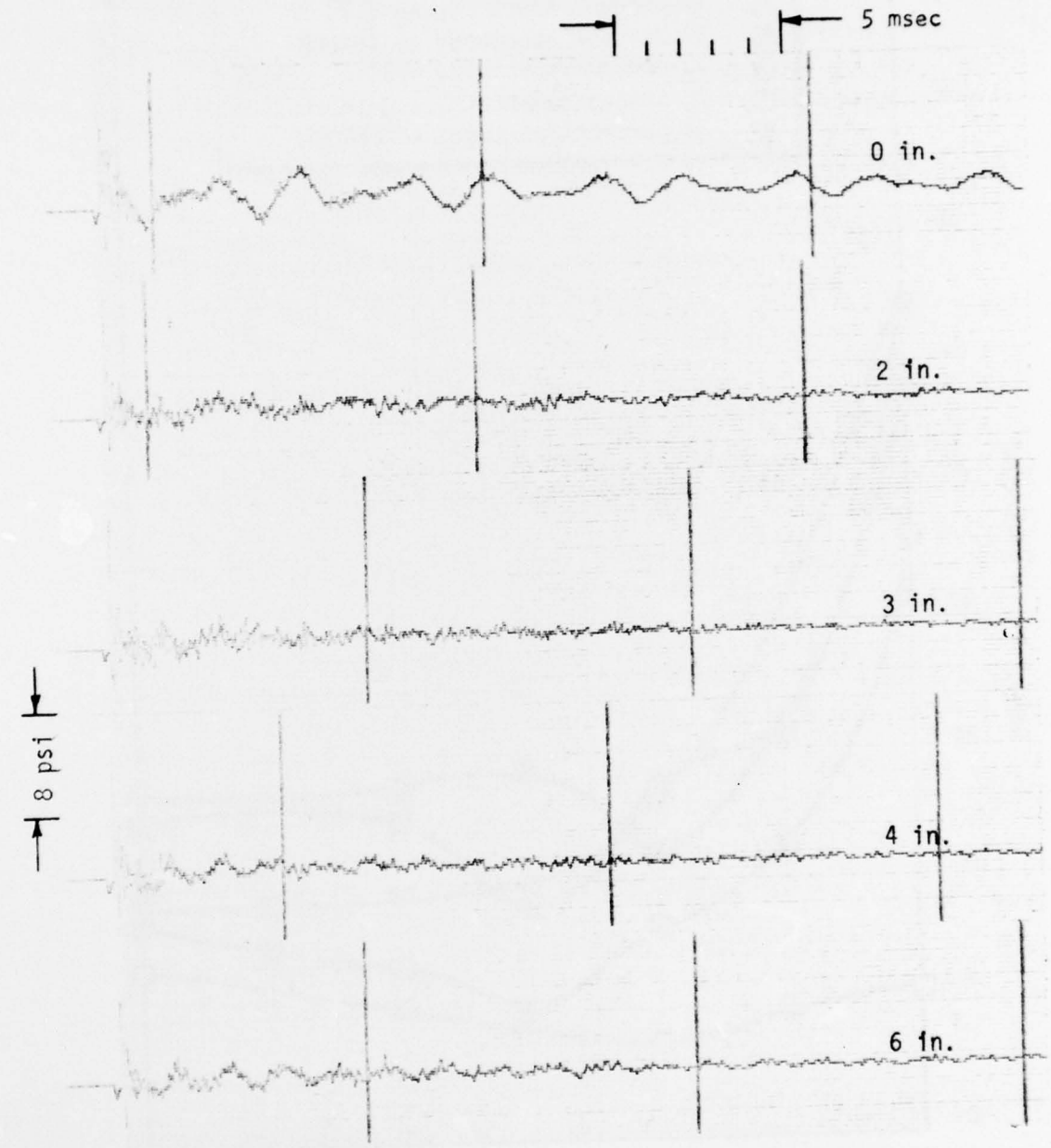

Figure 65. Effect of Piston Position on Pressure History for Plenum Duct Termination; 34-percent Aperture Open Area, no CERCOR

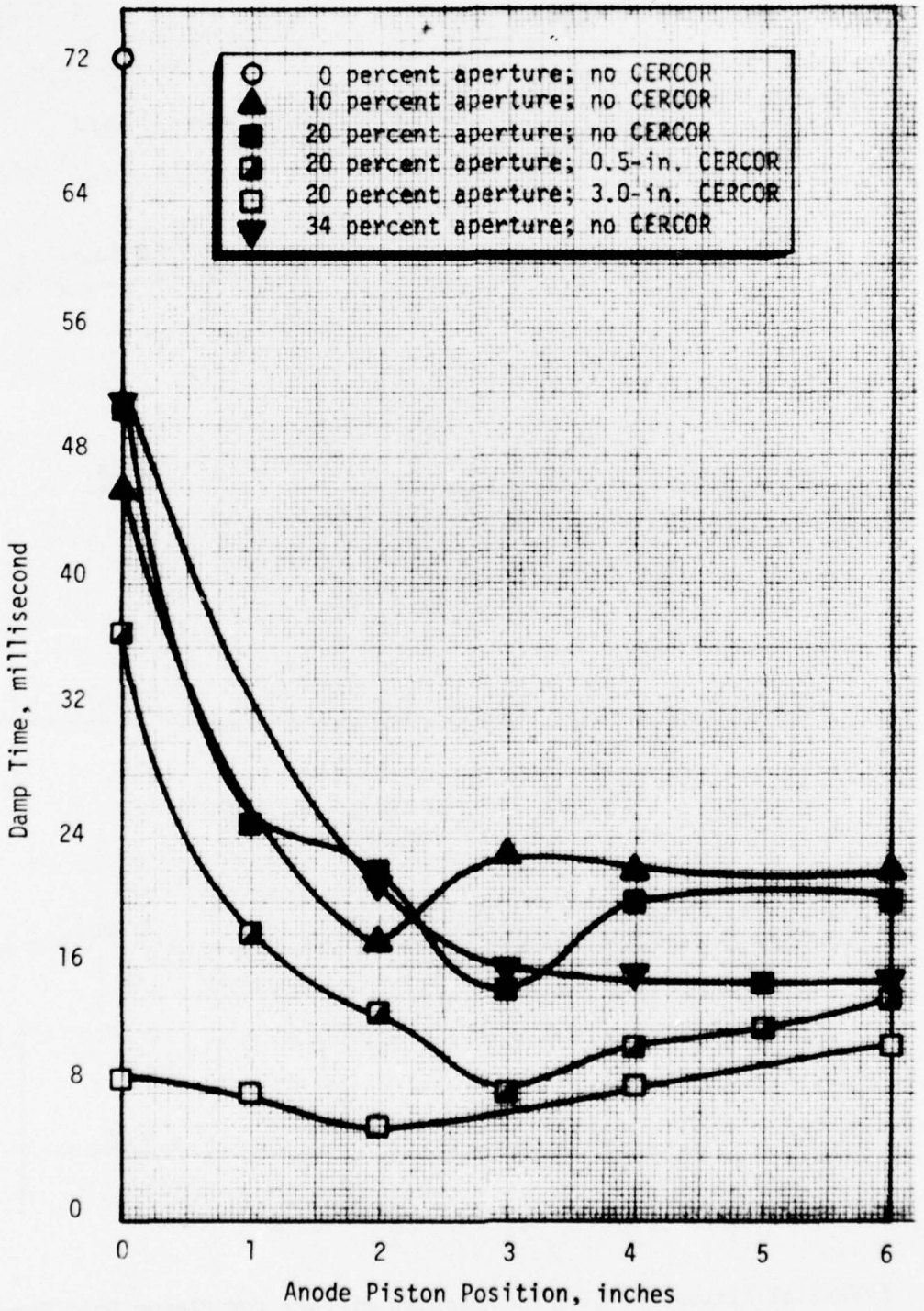

Figure 66. Task 4C Test Results - Effect of Plenum Duct Termination

SECTION VI: TASK 5 - ANALOG MODEL ANALYSIS

SCOPE

A mathematical model developed previously under Ref. 2 was modified to provide accurate representation of disturbance frequencies up to 2500 Hz. This model revision was based upon the experimental results of Tasks 1 through 4 of the subject contract, as well as the experimental results of Ref. 1. The resultant model was used to investigate the effects of high-frequency pressure and temperature oscillations on closed-cycle fluid supply system dynamic performance and control system design. The improved model was used to determine amplitude and depth of penetration of pressure and temperature oscillations into the closed-cycle feed system and to evaluate the effect of attenuation devices and honeycomb flow conditioners on these disturbances.

RESULTS

A high-frequency analog model simulating the plexiglass EDL acoustic model shown in Fig. 20 was constructed. The plexiglass model was first tested under Contract F29601-73-0034-0003 (Ref. 1) with several geometric variations: (1) both with and without CERCOR inserts, (2) various acoustic aperture areas and resonator volumes, and (3) both with and without 3-foot long flow ducts on either side of the 13-inch-long model. The modeling technique used to develop the analog model was evaluated through comparison of similar analytical and experimental tests. The high-frequency analog model simulated the 1/8 grain explosive charge set off in the cavity. The frequency and amplitude of the resultant pressure oscillations observed in the analog model were then compared with experimental pressure histories.

The analog computer model consists of a 9-lump parameter representation, of which the lasing cavity was 3 lumps and the CERCOR inserts 3 lumps on each side. Each lump consists of mass and energy continuity with both linear and nonlinear flow resistance between nodes. In addition, descriptions of an acoustic absorber and the inlet and exit flow ducts were included, employing the modal analysis technique (as opposed to lumped parameter technique) which includes all resonant modes up to

2500 Hz. The absorber description is connected to the lasing cavity by a nonlinear flow resistance representing the aperture. The flow ducts, containing linear resistance, interface on either side of the 13-inch-long model section (Fig. 20).

A comparison of the analytical and experimental pressure histories is shown in Fig. 67 through 73. With no flow ducts, no CERCOR, and no acoustic absorber, good agreement between the experimental data and the analog model was observed (Fig. 67). Frequencies were duplicated to within 7.5 percent and damp times to within 14 percent. Figure 68 shows the effect of adding a 5-inch-long anode absorber with 76-percent aperture open area, and Fig. 69 and 70 show the effect of CERCOR addition, the former configurations all resulting in good agreement with the analog model. The addition of 3-foot-long flow ducts (Fig. 71 through 73) substantially changed the damping characteristics but, again, reasonable analog model simulation was achieved, i.e., the dominant frequency was duplicated within 8 percent and damp times within 10 percent. The damp times obtained from the analog model are compared in Fig. 74 to damp times from Lucite model test data obtained in Ref. 1 with various anode piston positions and an absorber open area of 76 percent. Again, acceptable comparison between the analog model and the test data is shown. The maximum deviation in damp time was 20 percent with the exception of the furthest (10-inch) anode piston position.

It was concluded that the high-frequency analog modeling technique is acceptable, and represents a tool that can be used to evaluate high-frequency pulse characteristics in an EDL closed-cycle fluid supply system.

A schematic of a typical closed-cycle fluid supply system is shown in Fig. 75. It contains a compressor, which circulates a laser gas mixture of He, N_2 and CO_2. A monopropellant hydrazine gas generator provides high temperature gas to drive the turbocompressor. The cavity exit heat exchanger is used to remove the heat released due to lasing inefficiency, while the inlet heat exchanger is used to remove the heat of compression. During lasing, the nominal fluid pressures are: (1) at the inlet of the upstream flow duct, P_{14} = 16.5 psia (2) at the cavity entrance, P_{L4} = 15 psia, and (3) at the exit of the downstream flow duct, P_{01} = 13.0. The analog model was first run as a continuous wave system to establish

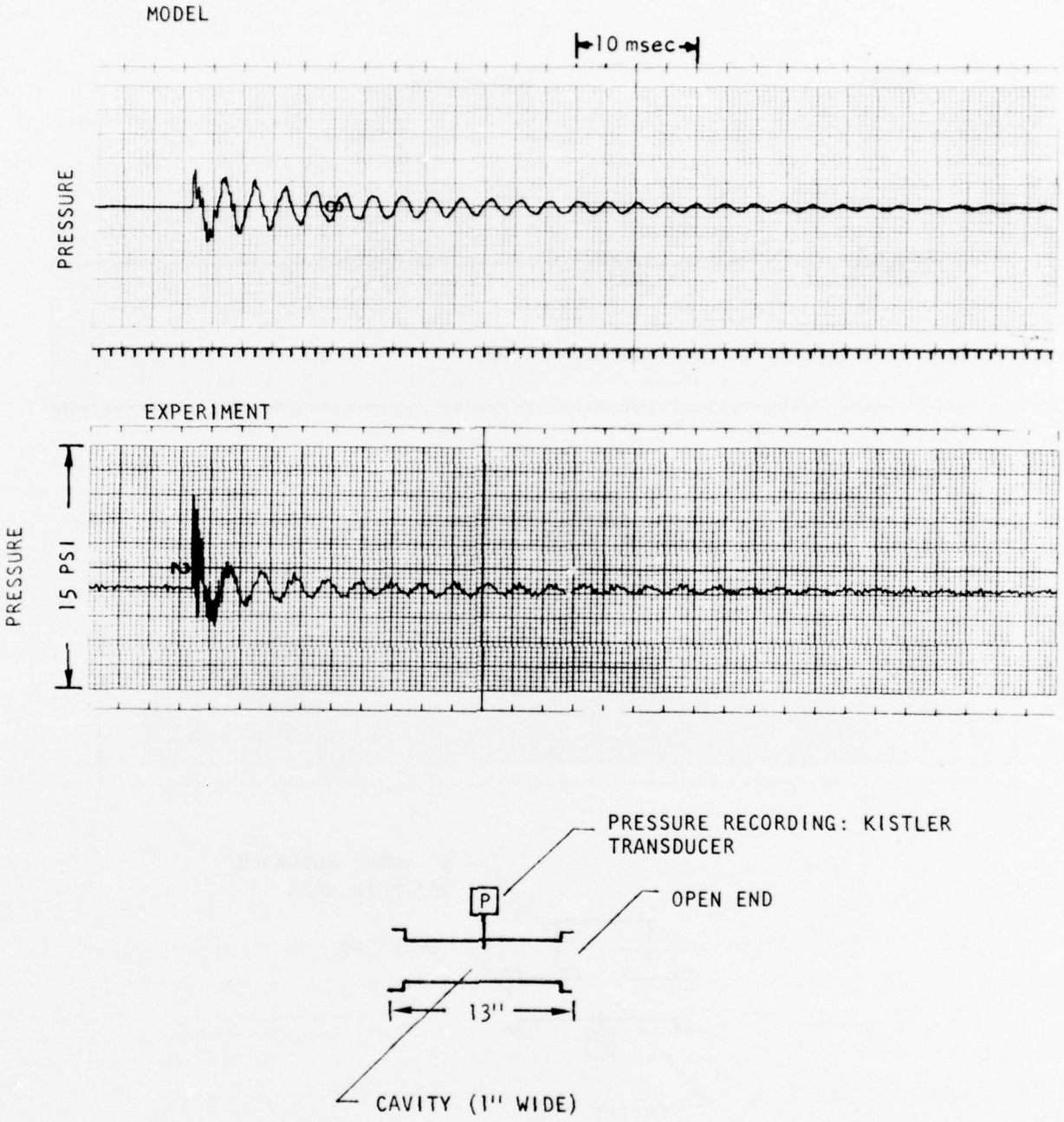

Figure 67. Pressure Response to Pulse (Open-Ended Cavity)

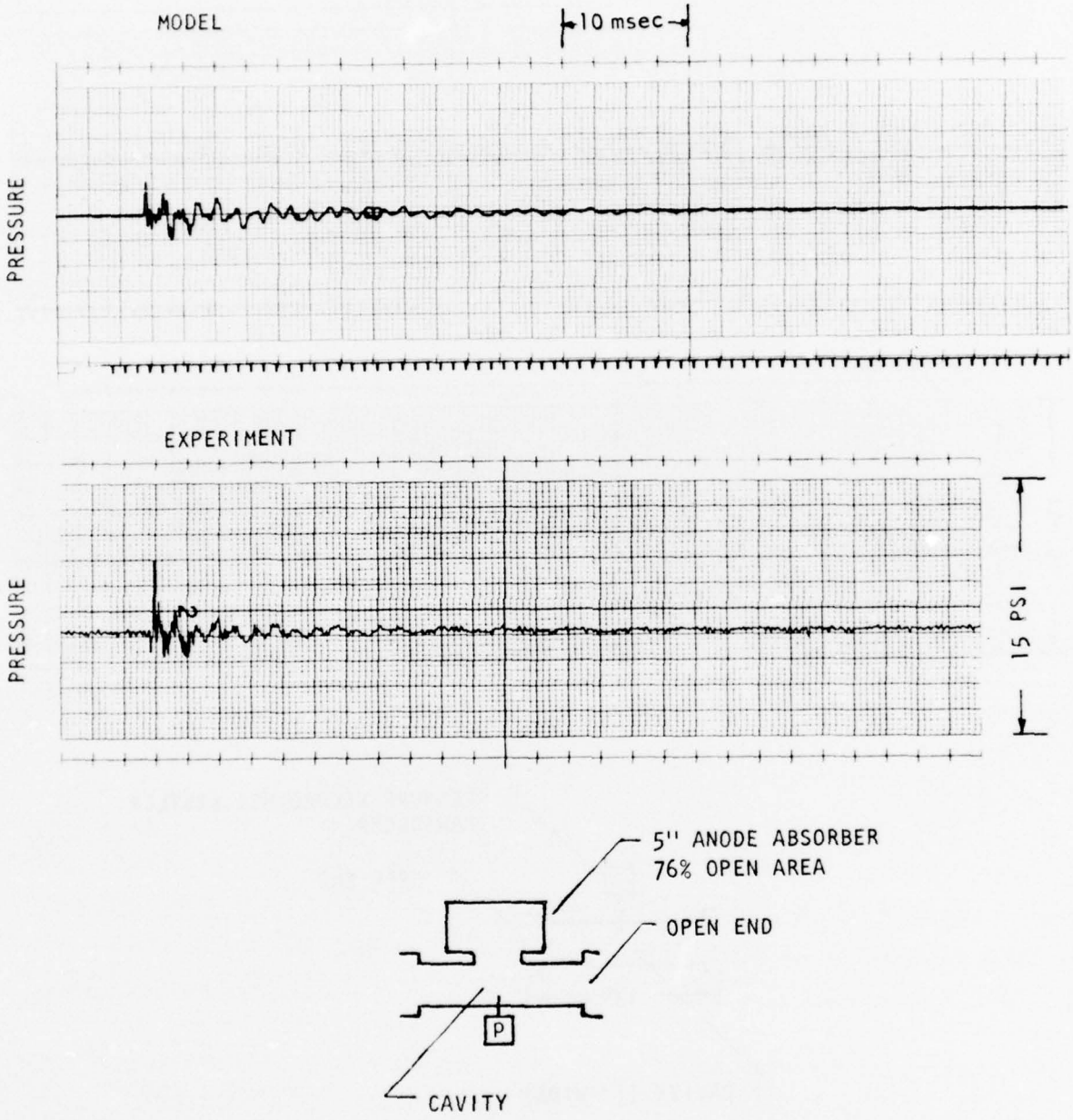

Figure 68. Pressure Response to Pulse (Open-Ended Cavity with Anode Absorber)

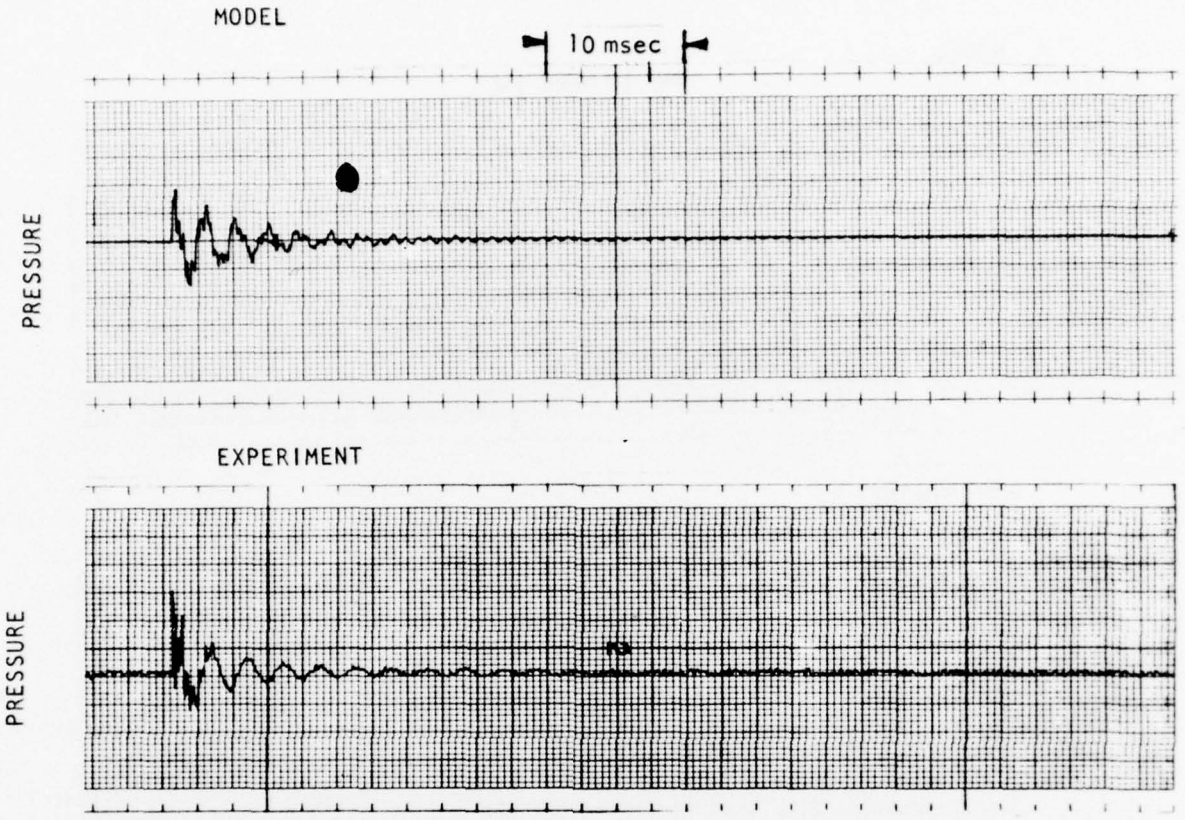

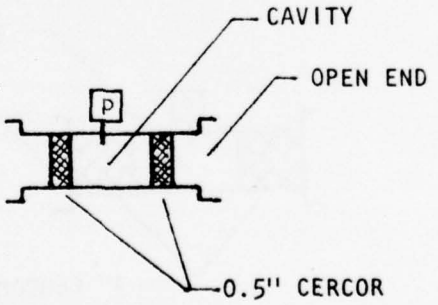

Figure 69. Pressure Response to Pulse (Open-Ended Cavity with 0.5-inch CERCOR)

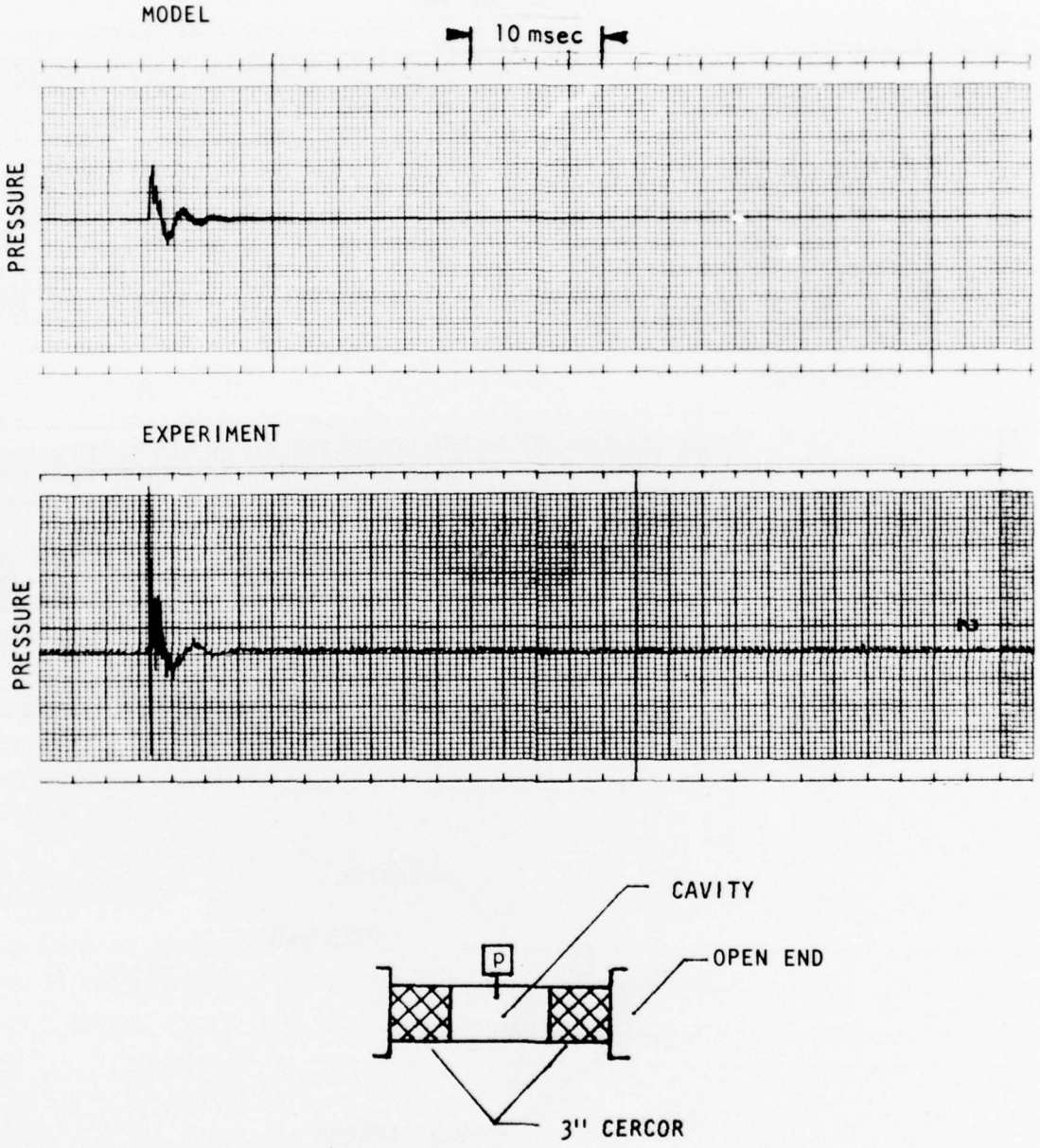

Figure 70. Pressure Response to Pulse (Open-Ended Cavity with 3-inch CERCOR)

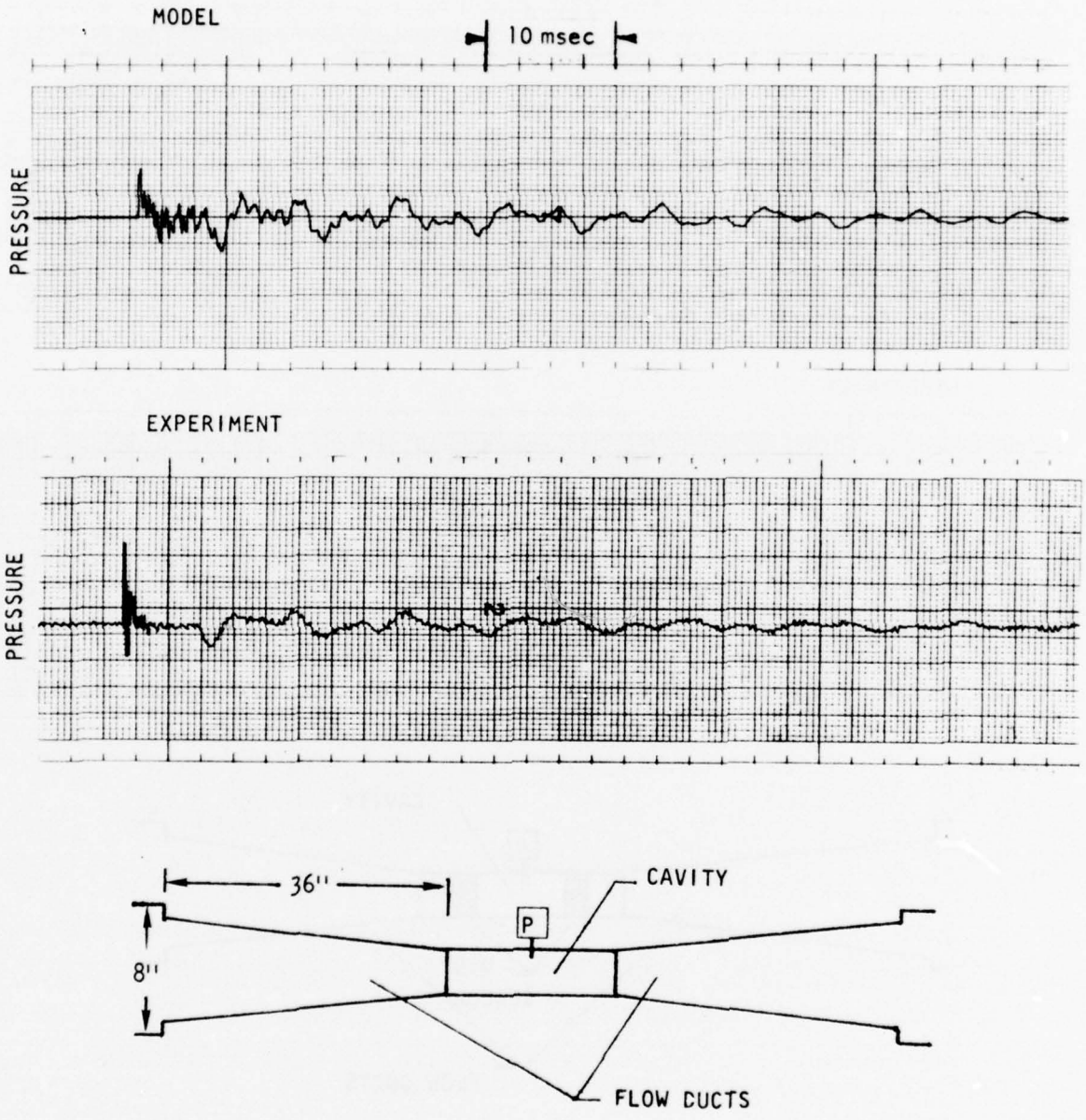

Figure 71. Pressure Response to Pulse (Open-Ended Flow Ducts on Either End of Cavity)

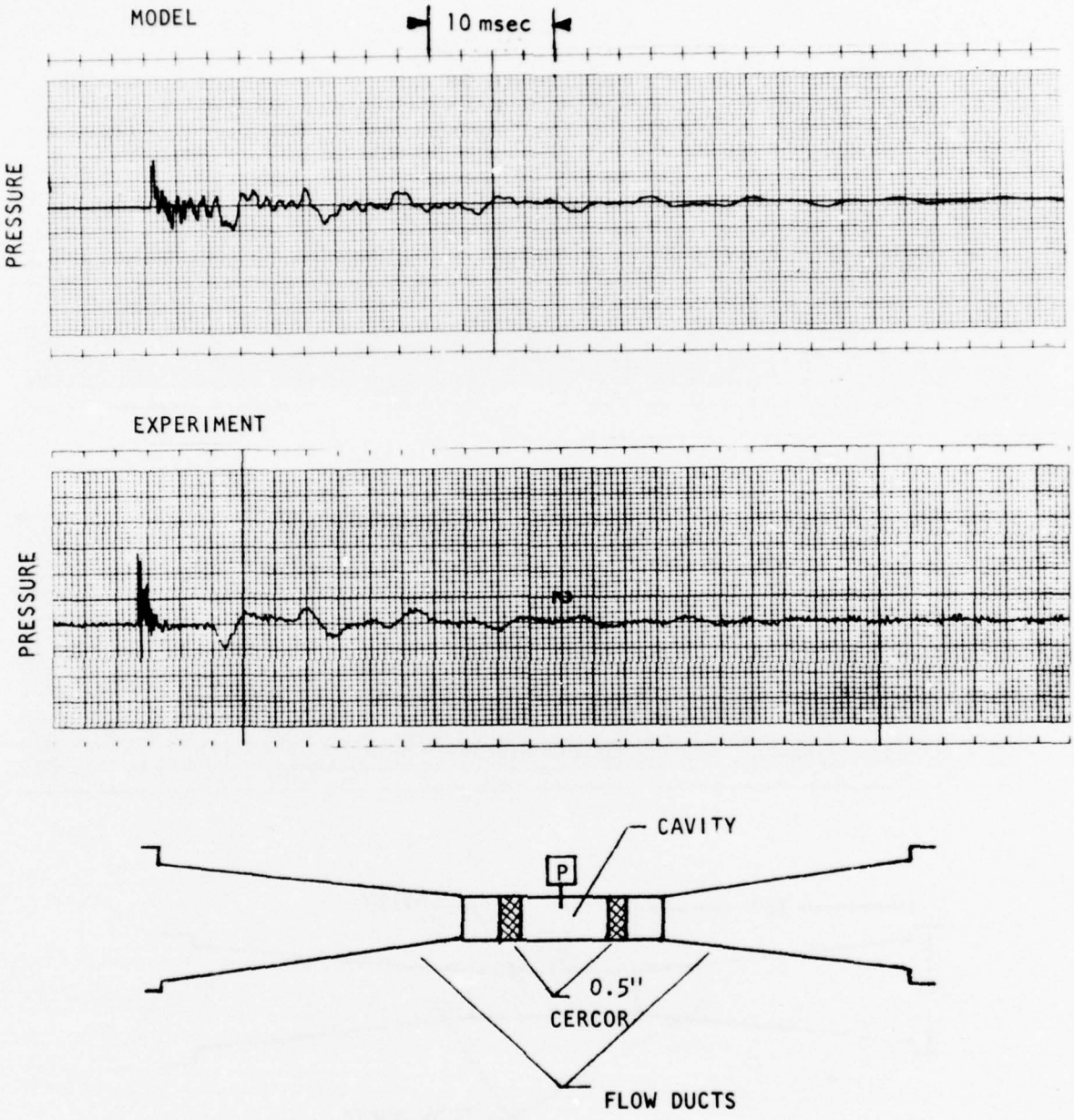

Figure 72. Pressure Response to Pulse (Open-Ended Flow Ducts on Either End of Cavity with 0.5-inch CERCOR)

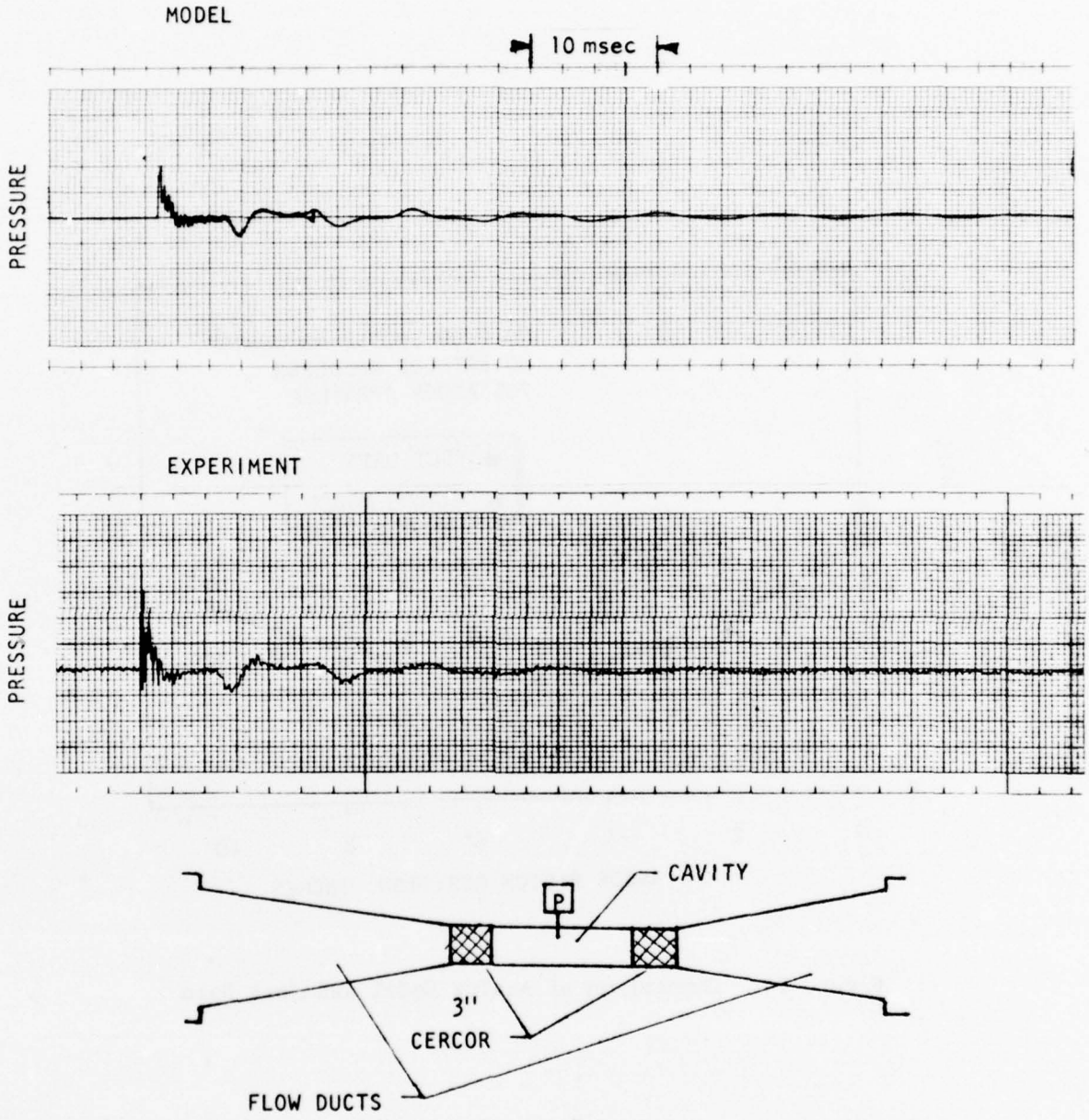

Figure 73. Pressure Response to Pulse (Open-Ended Flow Ducts on Either End of Cavity with 3-inch CERCOR)

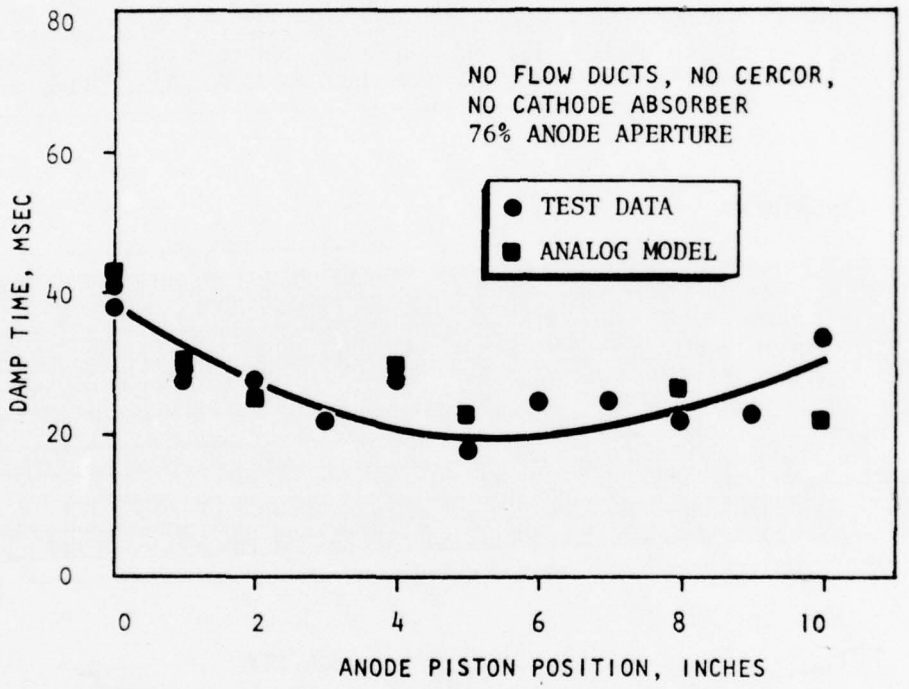

Figure 74. Comparison of Analog Model and Test Data

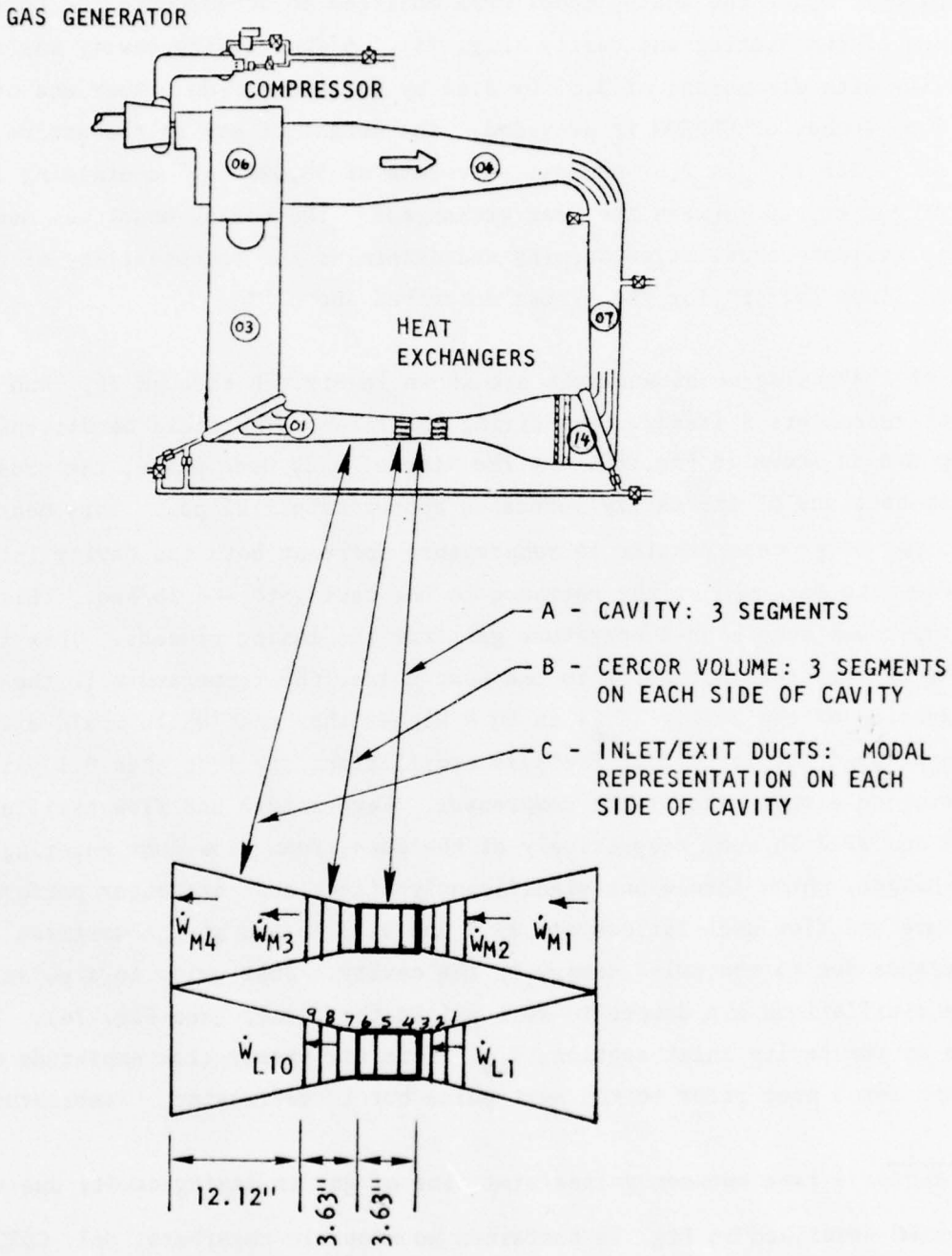

Figure 75. High-Frequency Analog Model

nominal operating characteristics. The high-frequency section (between the two heat exchangers) was modeled using the techniques proved satisfactory above. The equations comprising the analog model were modified to accommodate the physical dimensions of the ducting and cavity (Fig. 75). A dual lasing cavity was simulated, each cavity with dimensions of 3.63 by 3.63 by 59 inches. On either end of the cavity 3.63 inches of CERCOR is provided. The weight of gas in the entire loop volume of 75,253 $in.^3$ is 2.67 pounds. A volume of 36,086 $in.^3$ containing 1.22 pounds of gas exists between the heat exchangers. The analog model was used primarily to evaluate oscillation damping and determine the acceptability of a 1.25 idealized flush factor* for the system described above.**

Results of the analog model analysis are shown in Fig. 76 through 79. Run 030 (Fig. 76) represents a steady-state firing condition. The fluid conditions around the loop are as shown in Fig. 80. At the time of a 20 μsec pulse, the pressure in the three sections of the cavity increases approximately 22 psi. This nearly constant volume process results in temperature spike at both the cavity inlet and exit. Flowrate reverses at the entrance to the cavity to -64 lb/sec. This flow carries upstream some high-temperature gas from the lasing process. This is evidenced by the fact that prior to the next pulse, the temperature in the downstream section of the cavity (T_{L6}) is 50 R higher than that which would exist if the flowrate had not reversed. Pressure oscillations are less than 0.1 psi in the ducting on either side of the compressor. Temperature and flow oscillations are ±9 R and ±2.7 lb/sec, respectively at the downstream flow duct entering the heat exchanger, which should not significantly affect heat exchanger performance. Temperature and flow oscillations are ±5 R and ±1.3 lb/sec at the upstream flow duct entrance due to the pulse energy in the cavity. Just prior to a pulse, pressure oscillations are damped to ±0.6 psi in the cavity (see Fig. 76). Temperature at the cavity inlet section, T_{L4}, is fairly steady (low amplitude oscillation) for 1 msec prior to the next pulse but is decreasing. Temperature at

*Flush factor - time between pulses/stay time of gas in lasing cavity due to flow only.

**The system described in Fig. 75 contained no acoustic absorbers, only CERCOR. This was occasioned by the fact that for the majority of tests in Tasks 1-4, the use of 3.0-inch CERCOR by itself resulted in a damp time better than, or comparable to, the damp time observed through the use of acoustic absorbers alone.

the cavity exit section, T_{L6}, has a somewhat larger amplitude oscillation, ±10 R, while decreasing prior to the next pulse. Flowrate oscillations within the cavity remain large, ±6 lb/sec prior to a pulse, due to the low cavity flow impedance. Based upon the temperature and pressure oscillations shown in Fig 76* and discussed above, density variations of from 2 to 5 percent are expected to exist in the two axes normal to the laser beam when a flush factor of 1.25, ie., 3.6 msec between pulses, is employed.

Run 032 (Fig 77*) represents a steady-state firing with the exit CERCOR removed in an attempt to reduce pressure and temperature oscillations in the cavity (by minimizing flowrate reversal). Pressure oscillations in the cavity just prior to a pulse were worsened, ±1.0 psi, along with increased temperature and flowrate oscillations. The initial pressure, flowrate, and temperature spikes resulting from a pulse were comparable to Run 030 (with CERCOR on both ends of the cavity).

Run 033 (Fig 78*) shows the effects of an increased idealized flush factor of 1.5, i.e., 4.28 msec between pulses, to evaluate the improvement in damping just prior to a pulse. Pulse power was not increased. In general, cavity temperature just prior to a pulse was reduced closer to the nominal value. Pressure in the cavity indicated no damping improvement, due to reflection of a pressure wave off the heat exchanger at the time of the pulse.

Run 034 (Fig 79*) shows the effect of a mis-pulse, i.e., 7.1 msec separating two successive pulses. Pressure oscillations in the cavity were damped to ±0.3 psi, during the missed pulse elapsed time. Temperature throughout the cavity was reduced to the nominal value prior to the next pulse. A total of 5.0 msec was required for the exit cavity section temperature to reduce to within 5 R of the nominal inlet temperature (this represents a flush factor of 1.75).

It is concluded that the subsonic, pulsed wave EDL, closed-cycle fluid supply system investigated in this report (Fig. 75) can provide a spatial cavity density distribution prior to each pulse within ±2 to ±5 percent in the two axes normal to the beam, using idealized flush factors of 1.25 to 1.75. These disturbances result from the temporal pressure and temperature variations following each pulse, rather than the spatial fluid properties supplied by the closed-cycle system.

*Figures 76, 77, 78, and 79 are foldouts and appear at the end of this report.

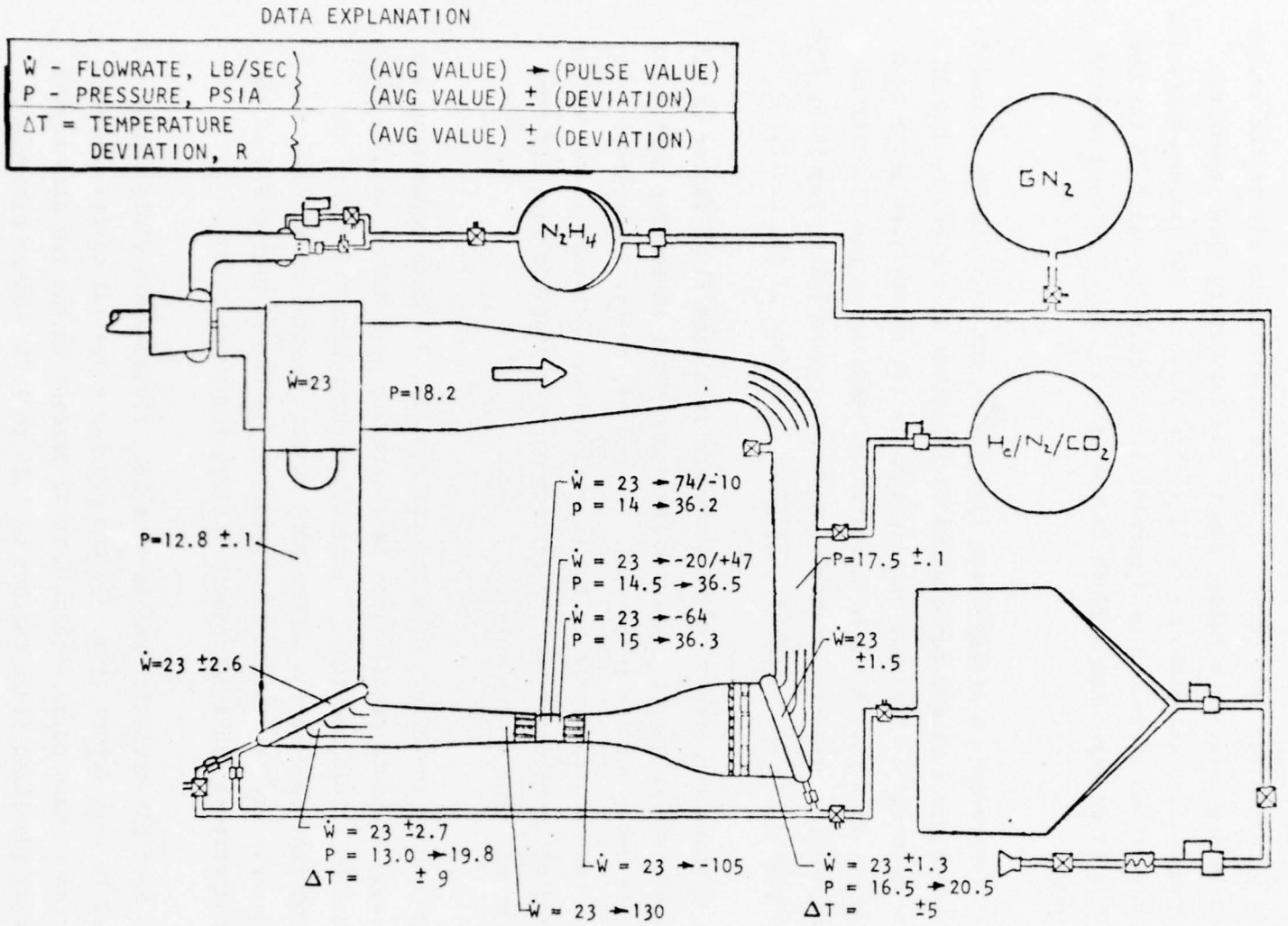

Figure 80. Closed-Cycle FSS - Steady State Firing, Run 030

SECTION VII: CONCLUSIONS

The objective of this program was to further investigate the use of acoustic absorbers and honeycomb flow conditioners as attenuation devices in a pulsed electric discharge laser.

Previous data obtained using the Kirtland 50-kW device* indicated a predominant pressure oscillation frequency of about 883 Hz. Decay of this predominant frequency was found to be essentially achieved within 2.5 msec of pulse initiation (a factor of 5 reduction in amplitude being reached at that time). Damping of the complex pressure wave to a factor of 7 reduction in amplitude was found to occur within about 53 msec (39 to 95 msec range) for the Kirtland 50-kW device. Interferometry, however, suggested damping to acceptable beam quality in 4 msec.

The following conclusions were drawn from the results described previously in this report.

Task 1: An analysis of the AFWL data and the Rocketdyne acoustic model data obtained in Ref.1 led to the conclusion that laser cavity modes (2 to 3 kHz) exert relatively little influence in the attenuation of the pressure oscillation. The predominant frequency apparent in the data (<1 kHz) is most probably related to flow channel modes. The method of determining damp time by measuring the time required for the peak-to-peak pressure oscillation to fall to one-seventh of its average initial amplitude is concluded to be satisfactory for further application.

Task 2: It was concluded that there is no measurable effect of cavity throughflow on the damping characteristics, at least over the range ($0 < \text{Mach No.} < 0.100$) investigated.

Task 3: For a ductless EDL acoustic model with a predominant frequency of 484 Hz, optimum damping was achieved using a 20-percent aperture and a 2-inch piston position. A factor of 8 reduction in damp time (from 33 to 4 msec) was noted.

*This device contained absorbers at the end of its flow ducts.

The addition of CERCOR in the flow channel did not improve the damping characteristics of the 20-percent aperture absorber; a 3.0-inch CERCOR thickness resulted in a factor of 5.5 reduction in damp time (from 33 to 6 msec). However, the damping characteristics of an off-optimum (34 percent) aperture open-area absorber were significantly improved with CERCOR added to the flow channel. Simultaneous use of the optimum absorber configuration and the 3.0-inch CERCOR did not result in an improvement over the absorber alone, a factor of 6.5 reduction in damp time (from 33 to 5 msec) being obtained.

The addition of CERCOR directly behind the aperture in the resonator volume itself was also found to result in no improvement in the damping characteristics over the 20-percent aperture absorber with or without CERCOR in the flow channel. Indeed, with either no CERCOR or 0.5-inch CERCOR in the flow channels, damping was worsened by the addition of CERCOR in the resonator volume. Consequently, it is concluded that the addition of CERCOR in the resonator volume does not appear at all attractive in the case of the 20-percent aperture open-area absorber.

Task 4A: For a close-ended, 13-inch-long EDL acoustic model with a predominant frequency of 1044 Hz, optimum damping was achieved with a 20 percent aperture and 0-inch piston position. A factor of 2.3 reduction in damp time (from 27 to 12 msec) was noted. The acoustic absorber alone is much less effective in this case than a CERCOR thickness of 3.0 inches in damping the pressure oscillation. The 3.0-inch CERCOR results in a factor of 13 reduction in damp time (from 27 to 2 msec). Simultaneous use of 3-inch CERCOR and absorber shows no improvement over the use of CERCOR alone.

Task 4B: For an open-ended, 13-inch-long EDL acoustic model containing an array of rods partially blocking the flow area, and having a predominant frequency of 304 Hz, optimum damping with a 20-percent aperture was achieved at a piston position of 2 inches. A factor of 1.6 reduction in damp time (from 9.5 to 6 msec) was noted. Use of 3.0-inch CERCOR instead resulted in an identical amplitude reduction. No significant advantage was observed in the simultaneous use of absorber and CERCOR.

The fact that neither optmization of the acoustic absorber nor use of the CERCOR flow conditioner improved damp time by any more than 4 or 5 msec leads one to conclude that the solid rods in the duct inserts (heat exchanger tube simulants) provide a very significant amount of damping by themselves.

Task 4C: The plenum duct termination in the EDL acoustic model resulted in simultaneously occuring frequencies of 570 and 318 Hz which appeared as a predominant frequency of 694 Hz. Optimization of the acoustic absorber occurred with a 20-percent aperture area and a 3-inch piston position. A factor of 5 reduction in damp time (from 73 to 14.5 msec) was noted.

A factor of 9 reduction in damp time (from 73 to 8 msec) was achieved, however, through use of a 3.0-inch CERCOR without acoustic resonators. A further reduction (factor of 12) in damp time to 6 msec is noted when CERCOR and a 20-percent aperture acoustic resonator with 2-inch piston position are employed together.

Based on the results of Tasks 1 through 4, an acoustic resonator having an aperture open area of 20 percent and a piston position of about 2 inches appears optimum from a damping standpoint over a range of EDL duct geometry variations. In some cases, however, such an absorber will not be as effective as the use of 3.0-inch CERCOR inserts in the flow channel immediately upstream and downstream of the lasing cavity. The use of such inserts involves a pressure drop penalty though that may be undesirable. Such use of flow conditioners may, however, be unnecessary unless it is clearly shown that the damping provided by the acoustic resonator itself is insufficient to damp the density oscillations to the point where beam quality is acceptable for the flush factors desired.

Task 5: It was concluded, based on the dynamic computer model with nonoptimized damping, that a subsonic, pulsed wave EDL, closed-cycle fluid supply system can provide a spatial cavity density distribution prior to each pulse within ±2 to ±5 percent in two axes normal to the beam, using idealized flush factors of 1.25 to 1.75. These disturbances result from the temporal pressure and temperature variations following each pulse, rather than from the spatial fluid properties supplied by the closed-cycle system.

REFERENCE

1. Nestlerode, J. A. R. C. Kesselring, and C. L. Oberg: Acoustic Damping for Pulsed Electric Discharge Lasers, Final Report, AFWL-TR-74-128, Air Force Weapons Laboratory, Kirtland AFB, NM, June 1974.

2. Marcy, R.: Closed-Cycle Fluid Supply System, Final Report, AFWL-TR-74234, Air Force Weapons Laboratory, Kirtland AFB, NM, November 1974.

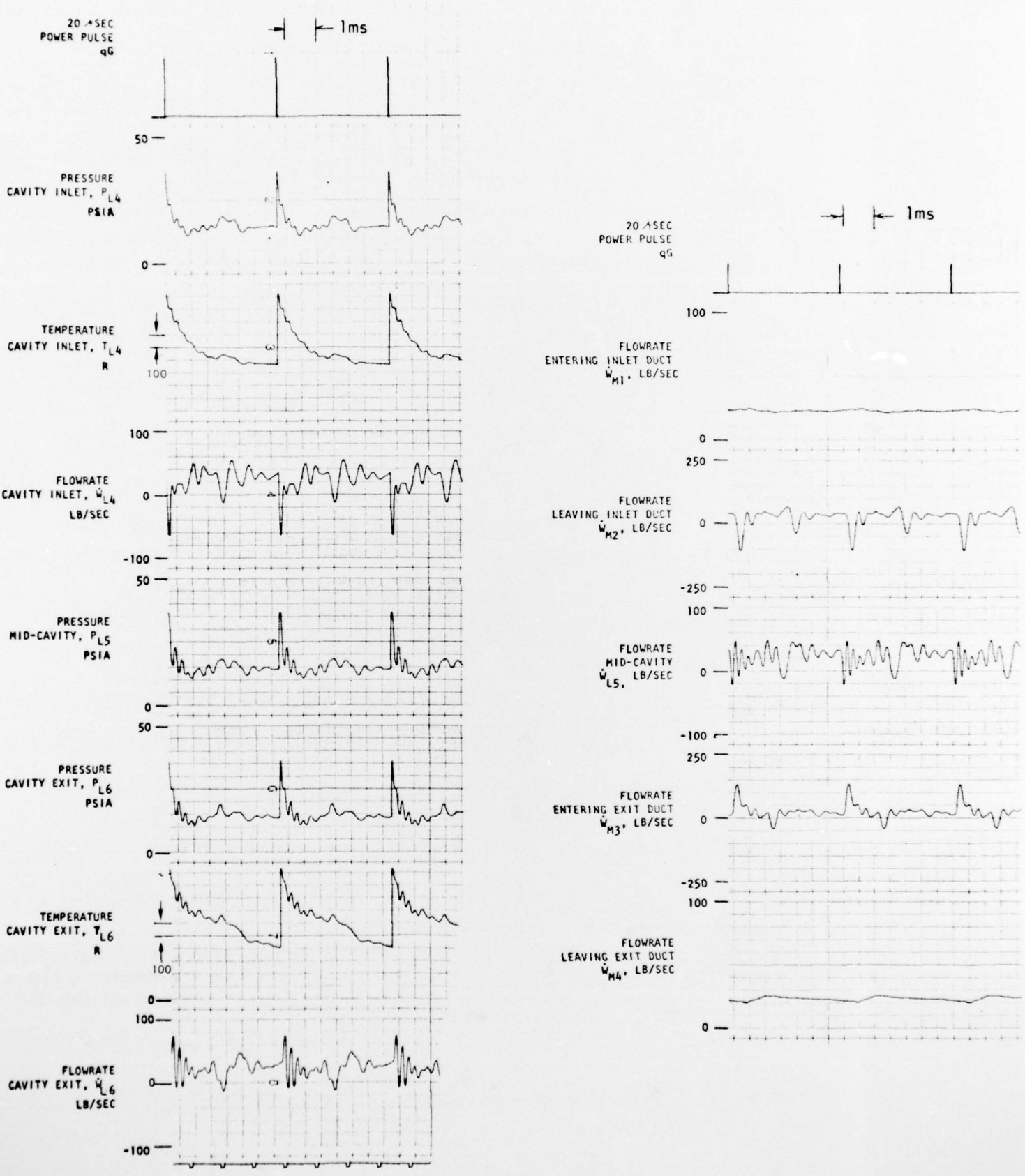
20 μSEC
POWER PULSE
qG
1ms
50
PRESSURE
CAVITY INLET, P_{L4}
PSIA
0
TEMPERATURE
CAVITY INLET, T_{L4}
R
100
100
FLOWRATE
CAVITY INLET, $\dot{W}_{L4}$
LB/SEC
0
-100
50
PRESSURE
MID-CAVITY, P_{L5}
PSIA
0
50
PRESSURE
CAVITY EXIT, P_{L6}
PSIA
0
TEMPERATURE
CAVITY EXIT, T_{L6}
R
100
0
100
FLOWRATE
CAVITY EXIT, $\dot{W}_{L6}$
LB/SEC
0
-100
20 μSEC
POWER PULSE
qG
1ms
100
FLOWRATE
ENTERING INLET DUCT
$\dot{W}_{M1}$, LB/SEC
0
250
FLOWRATE
LEAVING INLET DUCT
$\dot{W}_{M2}$, LB/SEC
0
-250
100
FLOWRATE
MID-CAVITY
$\dot{W}_{L5}$, LB/SEC
0
-100
250
FLOWRATE
ENTERING EXIT DUCT
$\dot{W}_{M3}$, LB/SEC
0
-250
100
FLOWRATE
LEAVING EXIT DUCT
$\dot{W}_{M4}$, LB/SEC
0

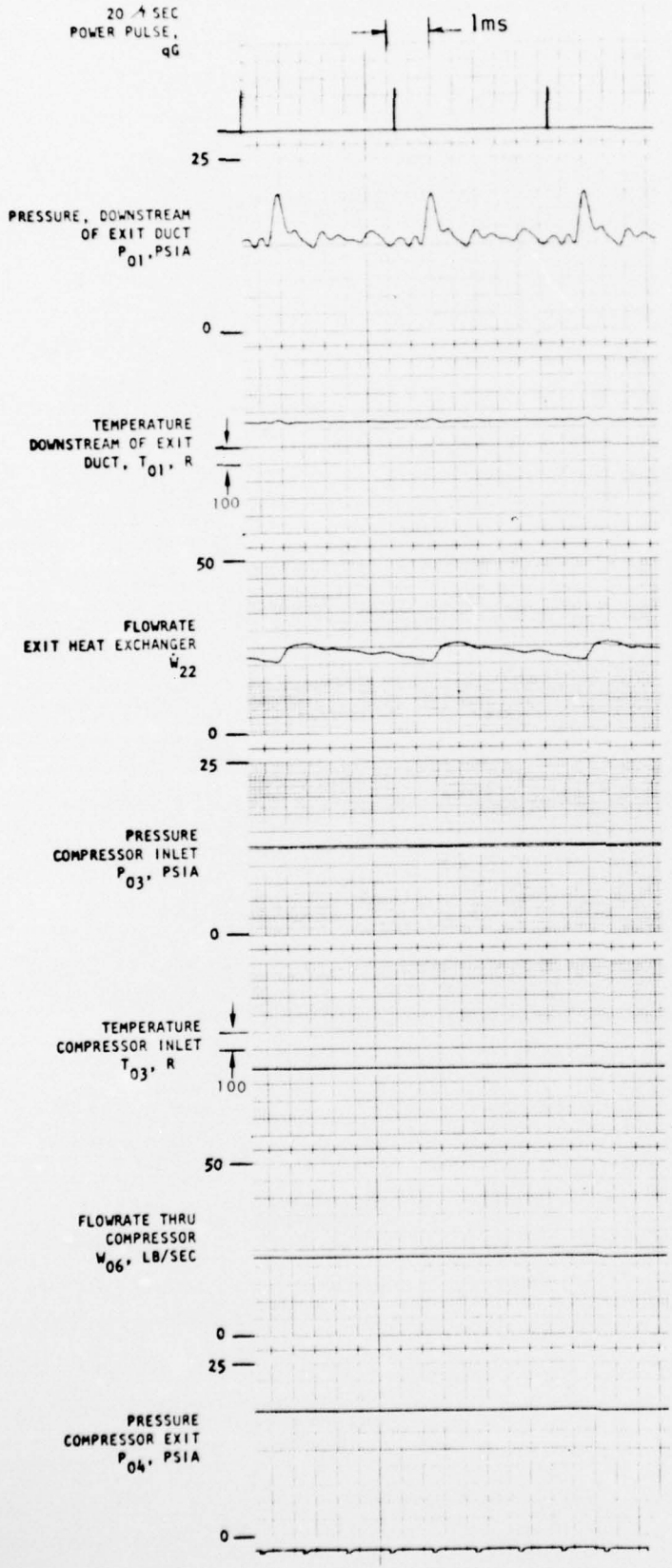
20 μ SEC
POWER PULSE,
qG
1ms
25
PRESSURE, DOWNSTREAM
OF EXIT DUCT
P01, PSIA
0
TEMPERATURE
DOWNSTREAM OF EXIT
DUCT, T01, R
100
50
FLOWRATE
EXIT HEAT EXCHANGER
Ẇ22
0
25
PRESSURE
COMPRESSOR INLET
P03, PSIA
0
TEMPERATURE
COMPRESSOR INLET
T03, R
100
50
FLOWRATE THRU
COMPRESSOR
W06, LB/SEC
0
25
PRESSURE
COMPRESSOR EXIT
P04, PSIA
0

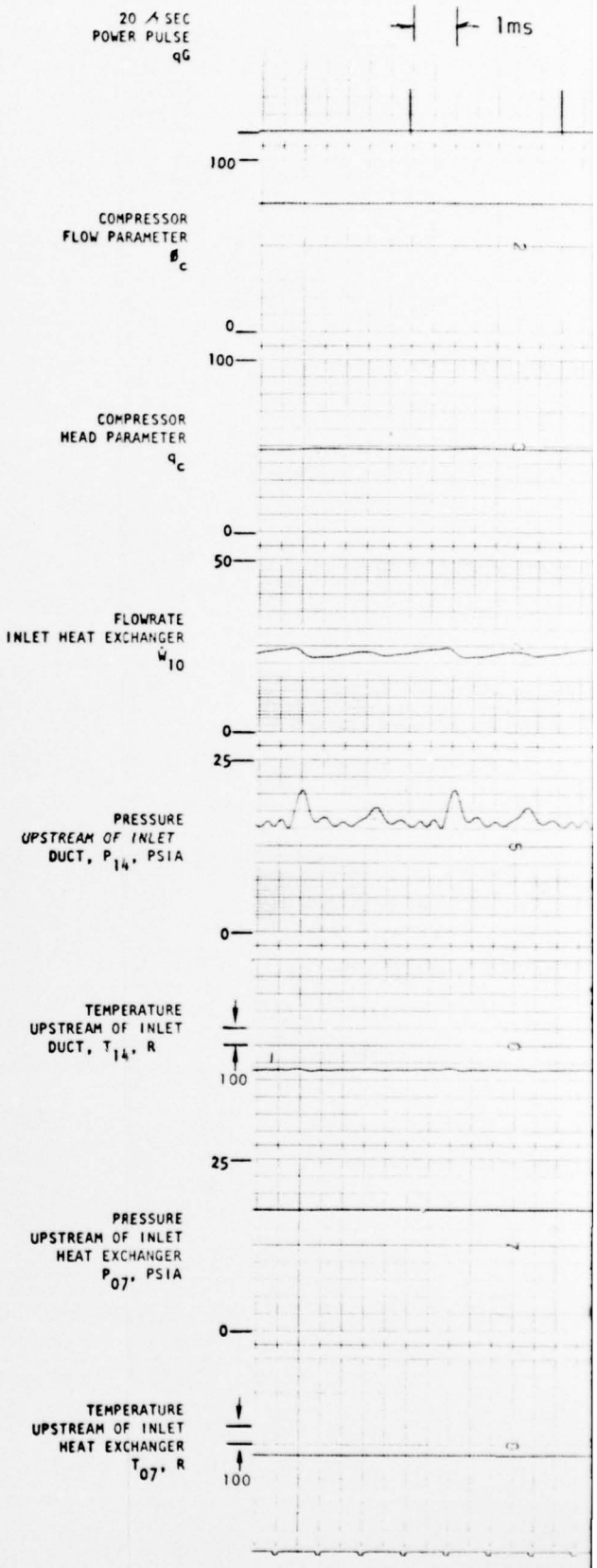
20 μ SEC
POWER PULSE
qG
1ms
100
COMPRESSOR
FLOW PARAMETER
Ø c
0
100
COMPRESSOR
HEAD PARAMETER
qc
0
50
FLOWRATE
INLET HEAT EXCHANGER
Ẇ10
0
25
PRESSURE
UPSTREAM OF INLET
DUCT, P14, PSIA
0
TEMPERATURE
UPSTREAM OF INLET
DUCT, T14, R
100
25
PRESSURE
UPSTREAM OF INLET
HEAT EXCHANGER
P07, PSIA
0
TEMPERATURE
UPSTREAM OF INLET
HEAT EXCHANGER
T07, R
100

1 2

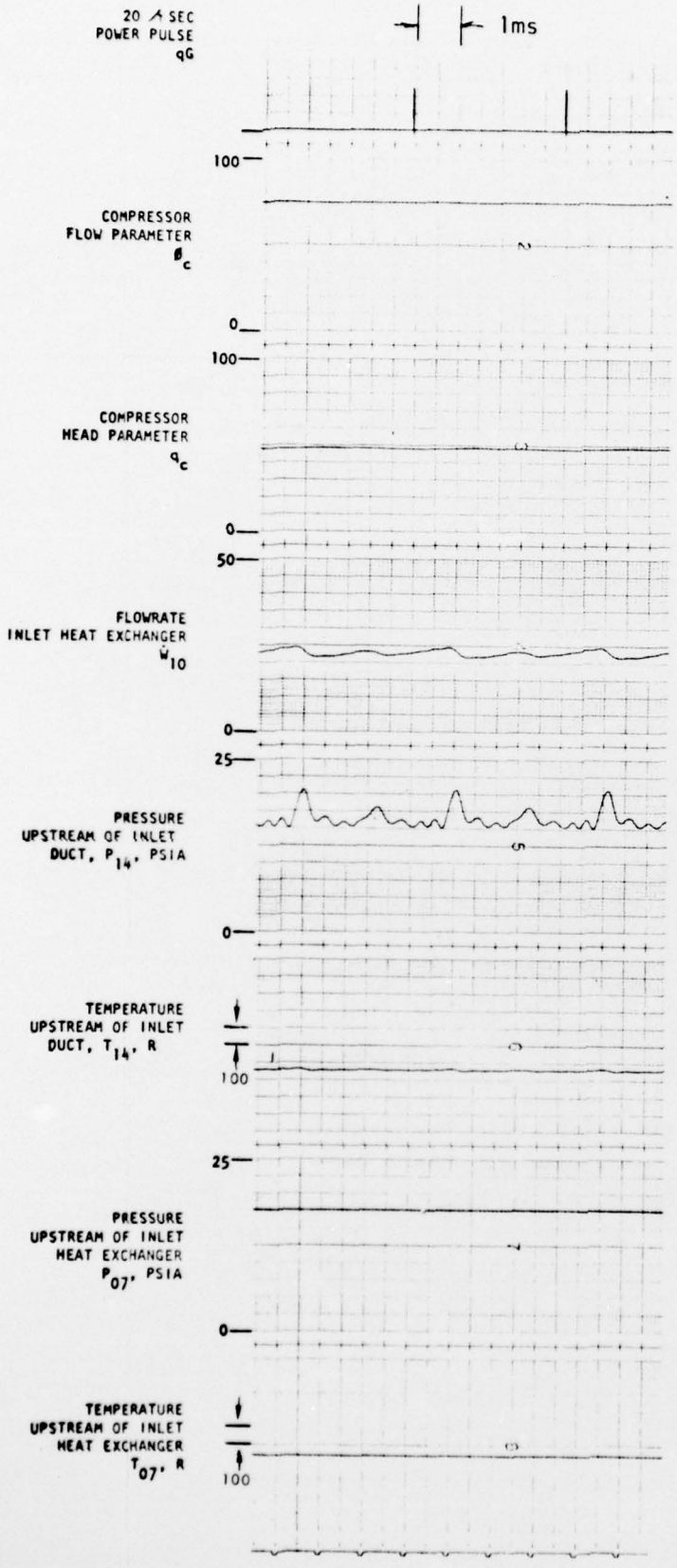

Figure 76. Steady-State Firing - Run 030

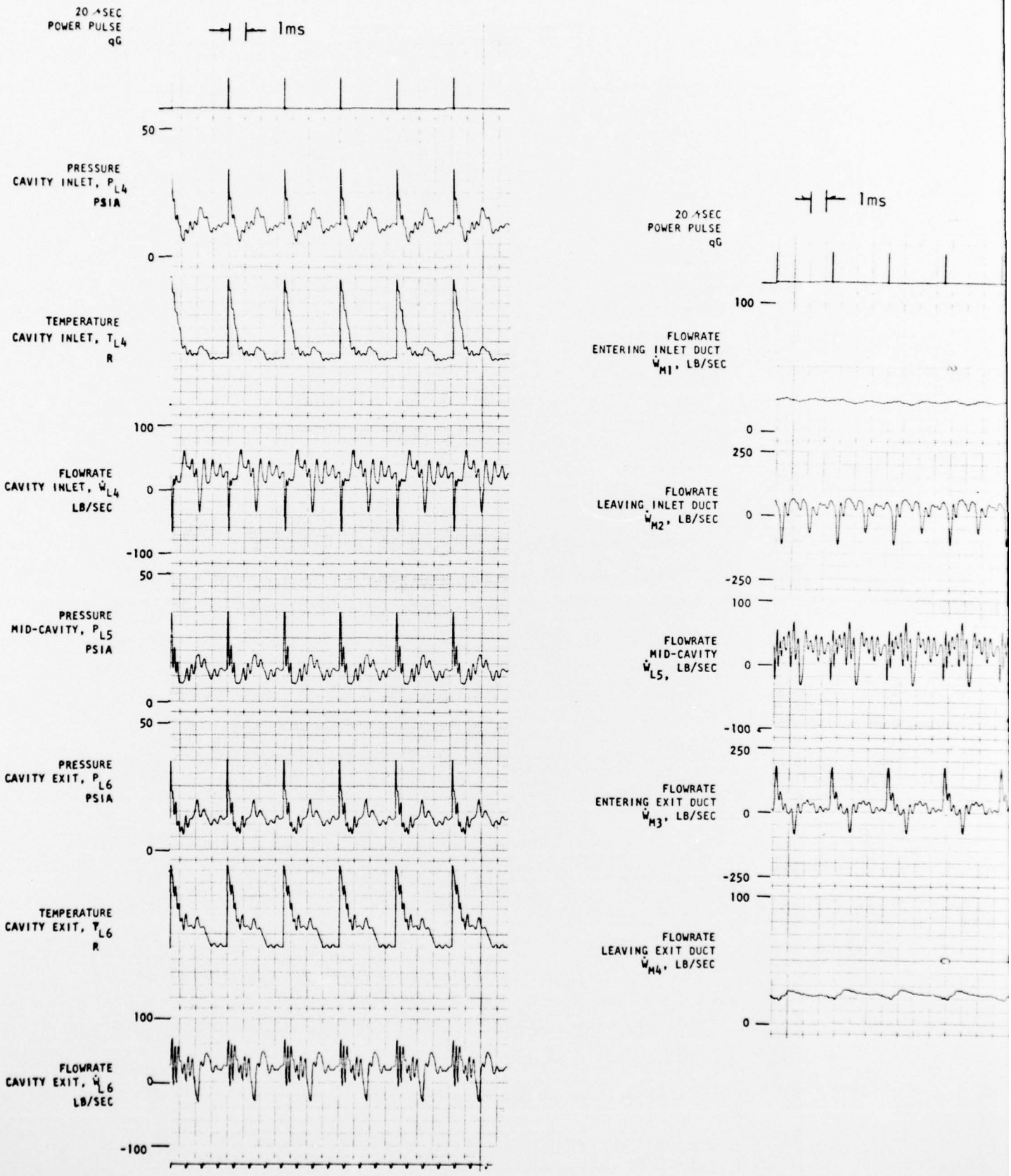
20 μSEC
POWER PULSE
qG
1ms
50
PRESSURE
CAVITY INLET, P_{L4}
PSIA
0
TEMPERATURE
CAVITY INLET, T_{L4}
R
100
FLOWRATE
CAVITY INLET, $\dot{W}_{L4}$
LB/SEC
0
-100
50
PRESSURE
MID-CAVITY, P_{L5}
PSIA
0
50
PRESSURE
CAVITY EXIT, P_{L6}
PSIA
0
TEMPERATURE
CAVITY EXIT, T_{L6}
R
100
FLOWRATE
CAVITY EXIT, $\dot{W}_{L6}$
LB/SEC
0
-100
20 μSEC
POWER PULSE
qG
1ms
100
FLOWRATE
ENTERING INLET DUCT
$\dot{W}_{M1}$, LB/SEC
0
250
FLOWRATE
LEAVING INLET DUCT
$\dot{W}_{M2}$, LB/SEC
0
-250
100
FLOWRATE
MID-CAVITY
$\dot{W}_{L5}$, LB/SEC
0
-100
250
FLOWRATE
ENTERING EXIT DUCT
$\dot{W}_{M3}$, LB/SEC
0
-250
100
FLOWRATE
LEAVING EXIT DUCT
$\dot{W}_{M4}$, LB/SEC
0

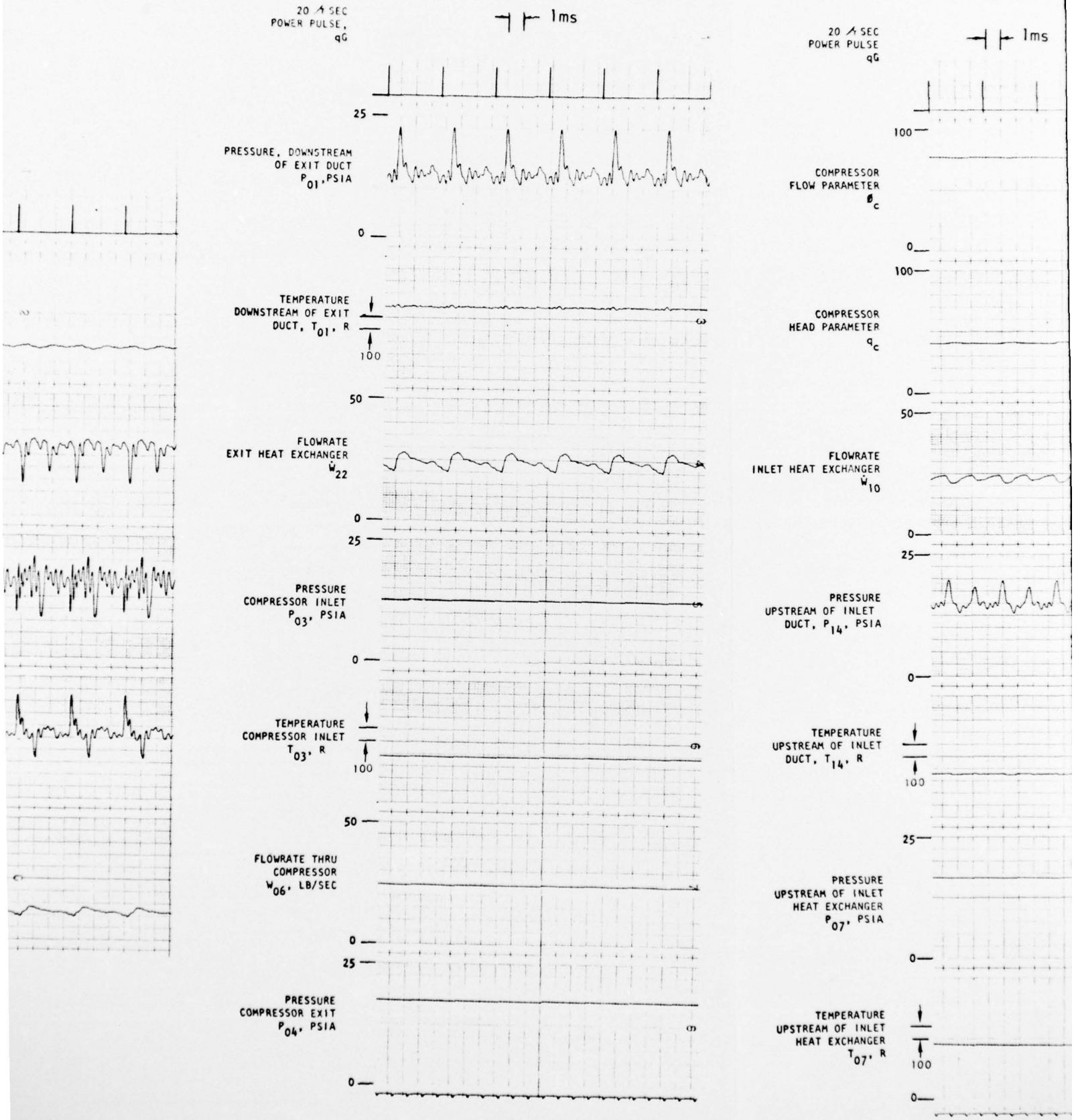
20 ⌇ SEC
POWER PULSE,
qG
1ms
25
PRESSURE, DOWNSTREAM
OF EXIT DUCT
P01, PSIA
0
TEMPERATURE
DOWNSTREAM OF EXIT
DUCT, T01, R
100
50
FLOWRATE
EXIT HEAT EXCHANGER
Ẇ22
0
25
PRESSURE
COMPRESSOR INLET
P03, PSIA
0
TEMPERATURE
COMPRESSOR INLET
T03, R
100
50
FLOWRATE THRU
COMPRESSOR
W06, LB/SEC
0
25
PRESSURE
COMPRESSOR EXIT
P04, PSIA
0
20 ⌇ SEC
POWER PULSE
qG
1ms
100
COMPRESSOR
FLOW PARAMETER
Ø c
0
100
COMPRESSOR
HEAD PARAMETER
qc
0
50
FLOWRATE
INLET HEAT EXCHANGER
Ẇ10
0
25
PRESSURE
UPSTREAM OF INLET
DUCT, P14, PSIA
0
TEMPERATURE
UPSTREAM OF INLET
DUCT, T14, R
100
25
PRESSURE
UPSTREAM OF INLET
HEAT EXCHANGER
P07, PSIA
0
TEMPERATURE
UPSTREAM OF INLET
HEAT EXCHANGER
T07, R
100
0

2

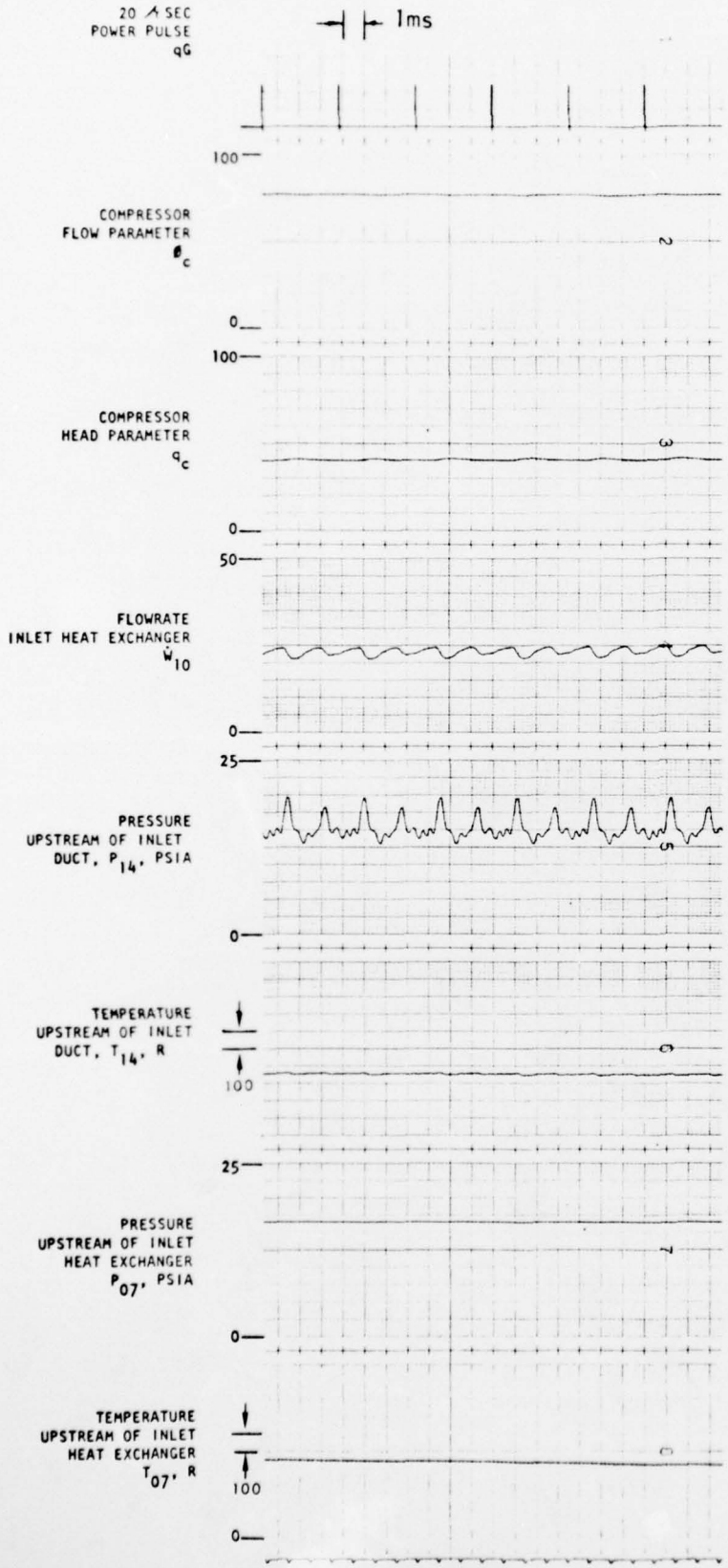

Figure 77. Steady-State Firing (Downstream CERCOR Removed) Run 032

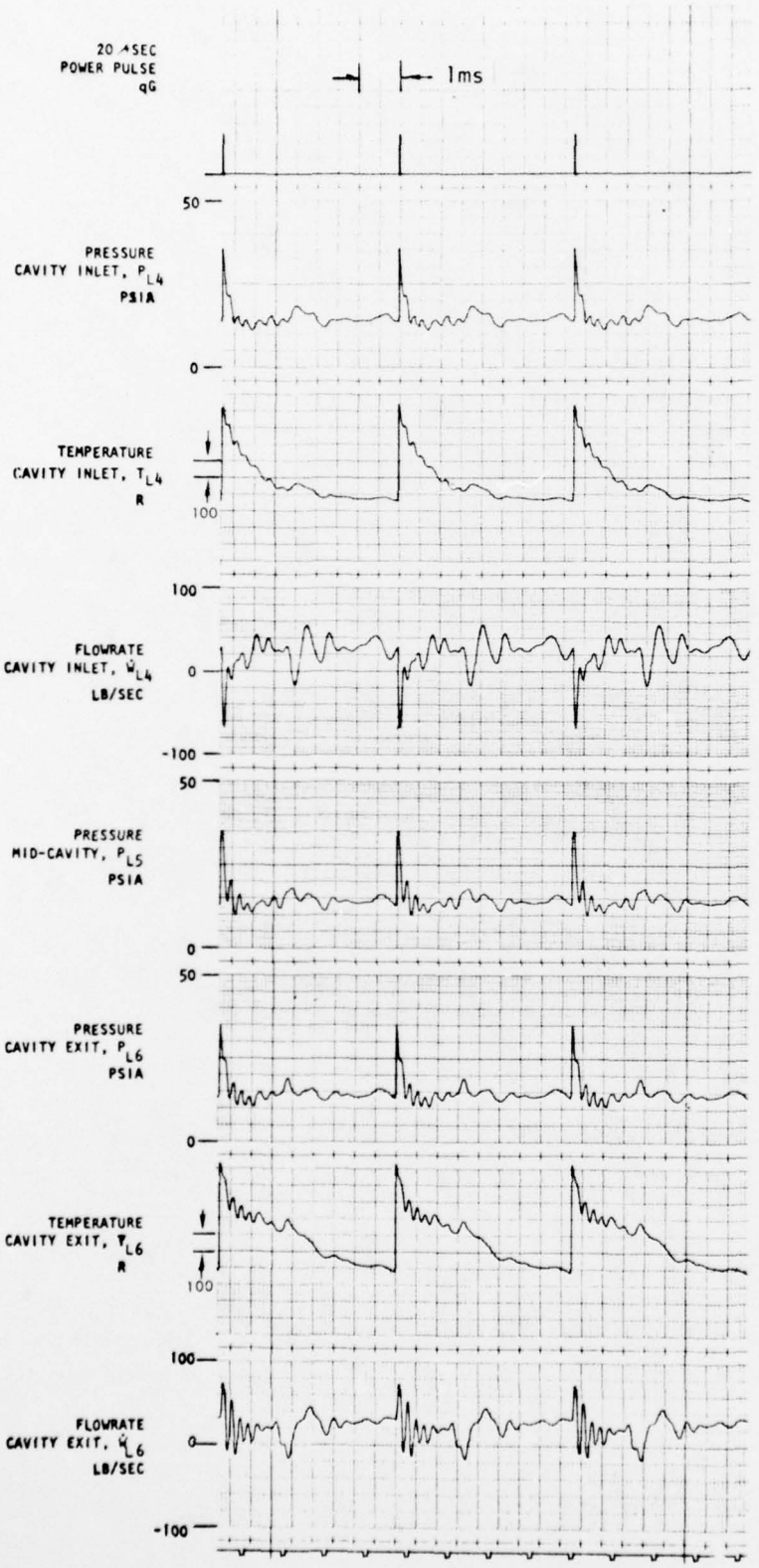
20 ASEC
POWER PULSE
qG
1ms
50
PRESSURE
CAVITY INLET, P_{L4}
PSIA
0
TEMPERATURE
CAVITY INLET, T_{L4}
R
100
100
FLOWRATE
CAVITY INLET, $\dot{W}_{L4}$
LB/SEC
0
-100
50
PRESSURE
MID-CAVITY, P_{L5}
PSIA
0
50
PRESSURE
CAVITY EXIT, P_{L6}
PSIA
0
TEMPERATURE
CAVITY EXIT, T_{L6}
R
100
100
FLOWRATE
CAVITY EXIT, $\dot{W}_{L6}$
LB/SEC
0
-100

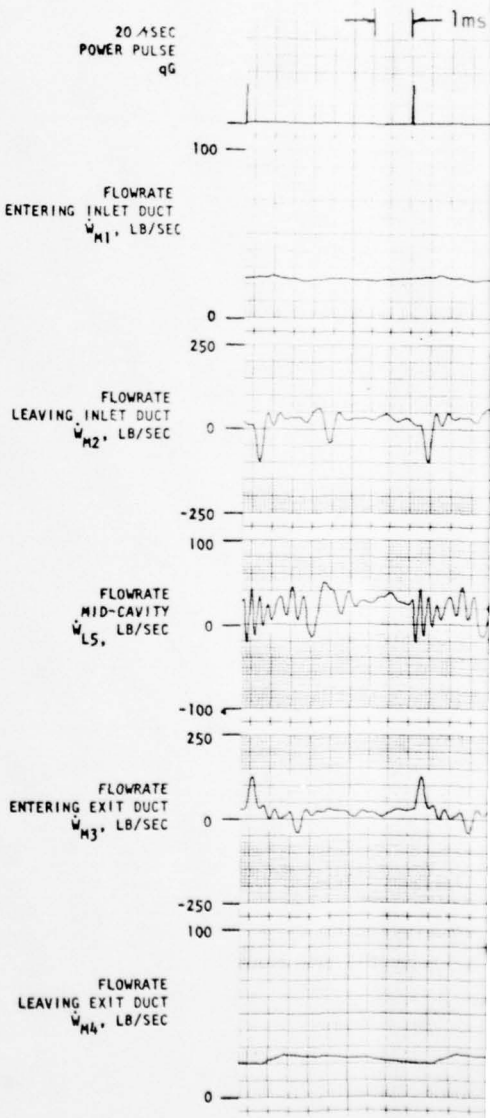
20 ASEC
POWER PULSE
qG
1ms
100
FLOWRATE
ENTERING INLET DUCT
$\dot{W}_{M1}$, LB/SEC
0
250
FLOWRATE
LEAVING INLET DUCT
$\dot{W}_{M2}$, LB/SEC
0
-250
100
FLOWRATE
MID-CAVITY
$\dot{W}_{L5}$, LB/SEC
0
-100
250
FLOWRATE
ENTERING EXIT DUCT
$\dot{W}_{M3}$, LB/SEC
0
-250
100
FLOWRATE
LEAVING EXIT DUCT
$\dot{W}_{M4}$, LB/SEC
0

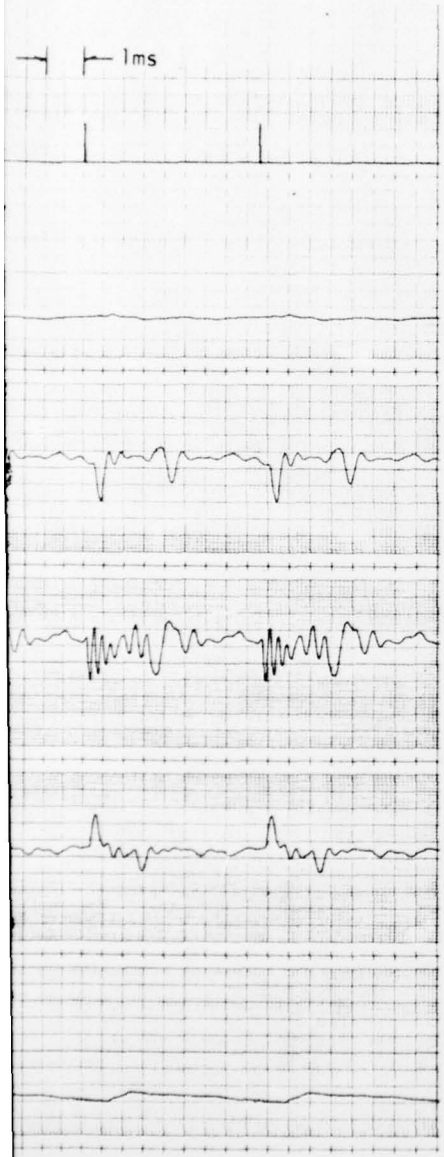
1ms

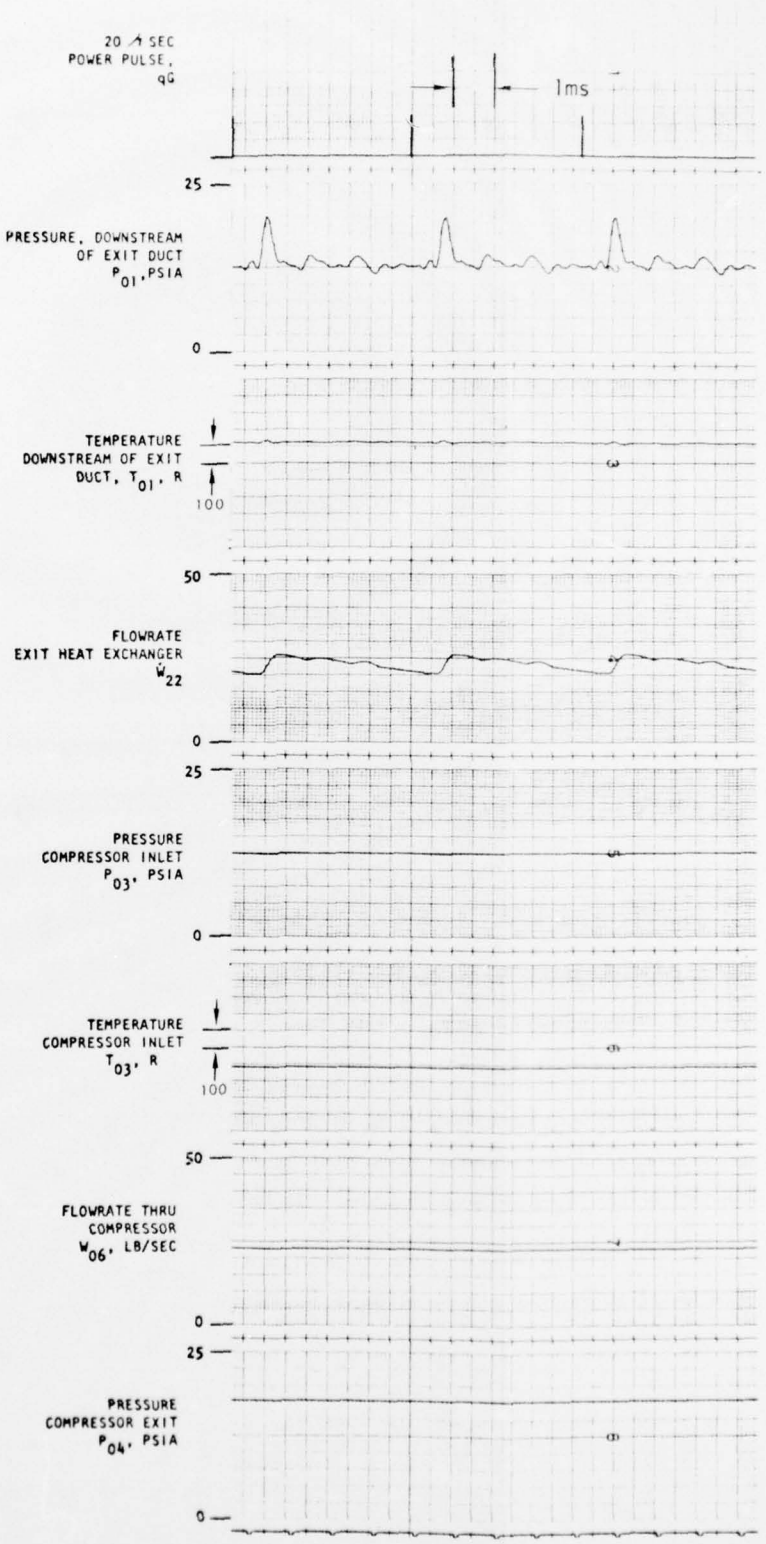
20 A SEC
POWER PULSE,
qG
1ms
25
PRESSURE, DOWNSTREAM
OF EXIT DUCT
P01, PSIA
0
TEMPERATURE
DOWNSTREAM OF EXIT
DUCT, T01, R
100
50
FLOWRATE
EXIT HEAT EXCHANGER
W22
0
25
PRESSURE
COMPRESSOR INLET
P03, PSIA
0
TEMPERATURE
COMPRESSOR INLET
T03, R
100
50
FLOWRATE THRU
COMPRESSOR
W06, LB/SEC
0
25
PRESSURE
COMPRESSOR EXIT
P04, PSIA
0

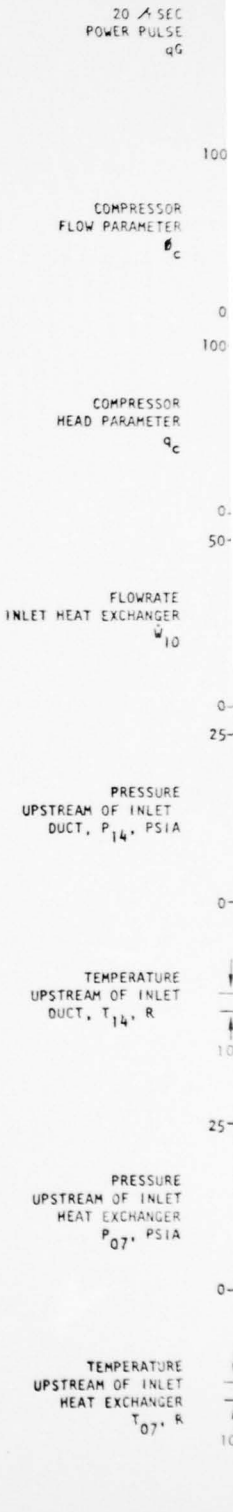
20 A SEC
POWER PULSE
qG
100
COMPRESSOR
FLOW PARAMETER
Ø c
0
100
COMPRESSOR
HEAD PARAMETER
ψc
0
50
FLOWRATE
INLET HEAT EXCHANGER
W10
0
25
PRESSURE
UPSTREAM OF INLET
DUCT, P14, PSIA
0
TEMPERATURE
UPSTREAM OF INLET
DUCT, T14, R
25
PRESSURE
UPSTREAM OF INLET
HEAT EXCHANGER
P07, PSIA
0
TEMPERATURE
UPSTREAM OF INLET
HEAT EXCHANGER
T07, R

2

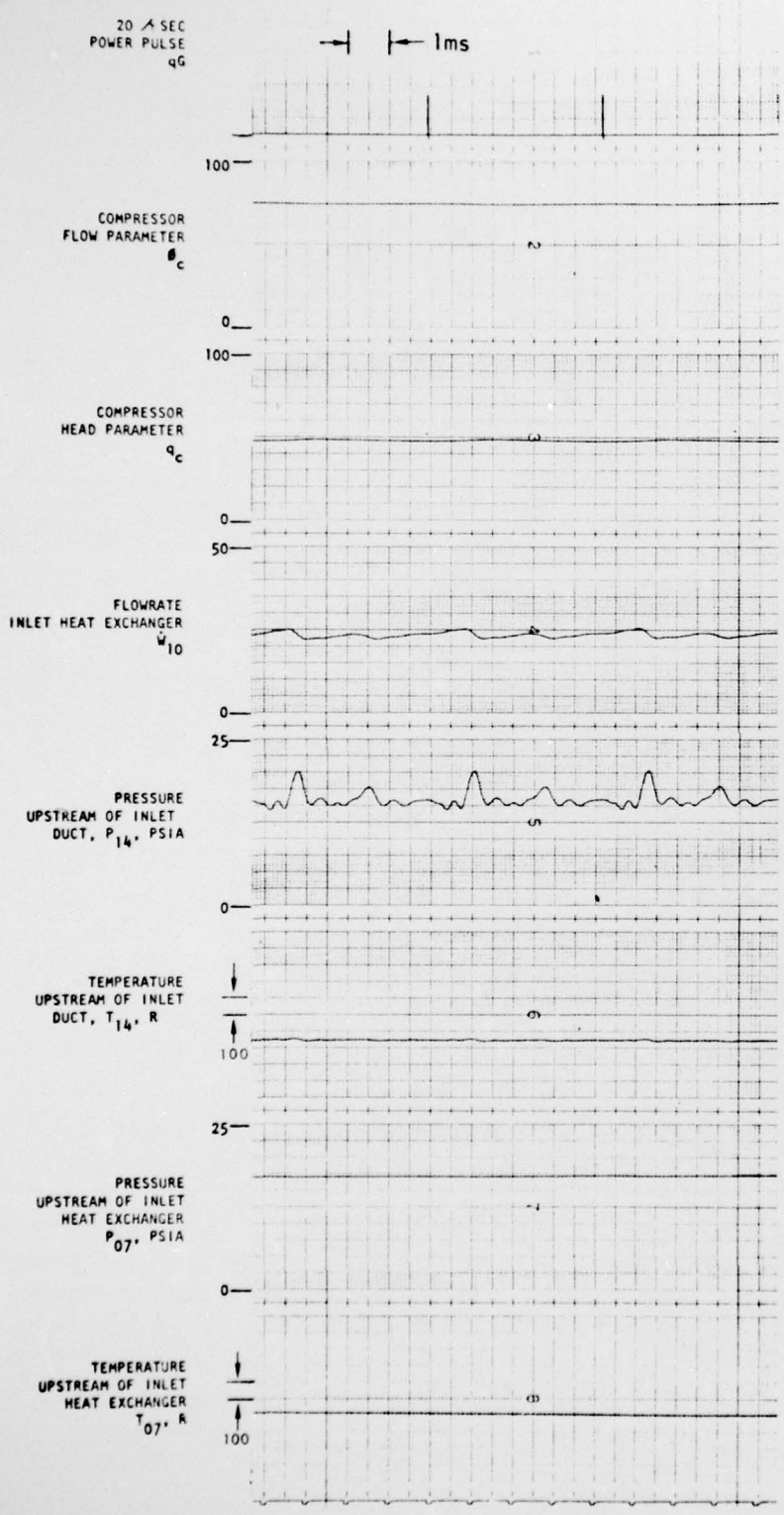

Figure 78. Steady-State Firing, Flush Factor Increased to 1.5, Run 033

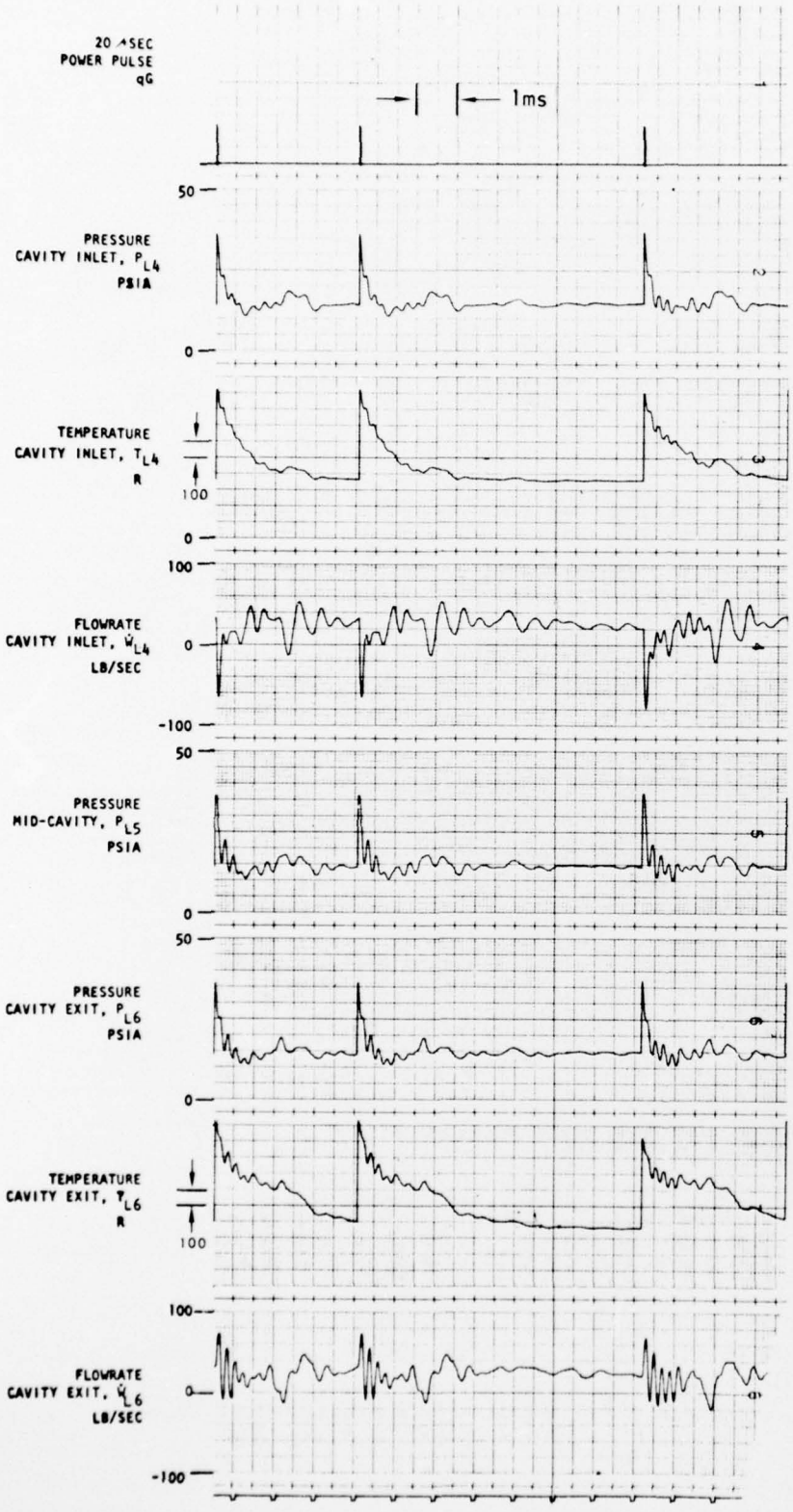
20 μSEC
POWER PULSE
qG
1ms
50
PRESSURE
CAVITY INLET, P_{L4}
PSIA
0
TEMPERATURE
CAVITY INLET, T_{L4}
R
100
0
100
FLOWRATE
CAVITY INLET, $\dot{W}_{L4}$
LB/SEC
0
-100
50
PRESSURE
MID-CAVITY, P_{L5}
PSIA
0
50
PRESSURE
CAVITY EXIT, P_{L6}
PSIA
0
TEMPERATURE
CAVITY EXIT, T_{L6}
R
100
100
FLOWRATE
CAVITY EXIT, $\dot{W}_{L6}$
LB/SEC
0
-100

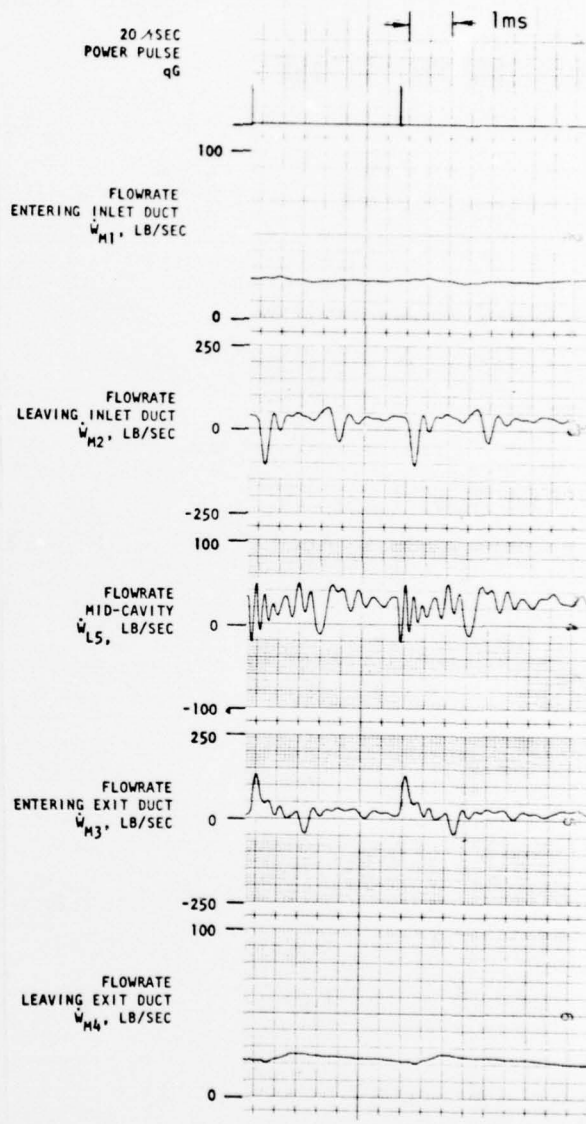
20 μSEC
POWER PULSE
qG
1ms
100
FLOWRATE
ENTERING INLET DUCT
$\dot{W}_{M1}$, LB/SEC
0
250
FLOWRATE
LEAVING INLET DUCT
$\dot{W}_{M2}$, LB/SEC
0
-250
100
FLOWRATE
MID-CAVITY
$\dot{W}_{L5}$, LB/SEC
0
-100
250
FLOWRATE
ENTERING EXIT DUCT
$\dot{W}_{M3}$, LB/SEC
0
-250
100
FLOWRATE
LEAVING EXIT DUCT
$\dot{W}_{M4}$, LB/SEC
0

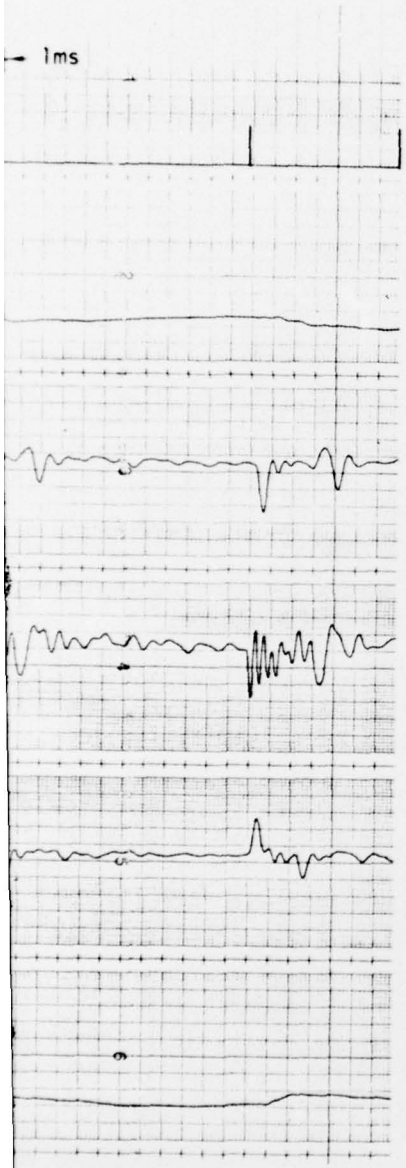
1ms

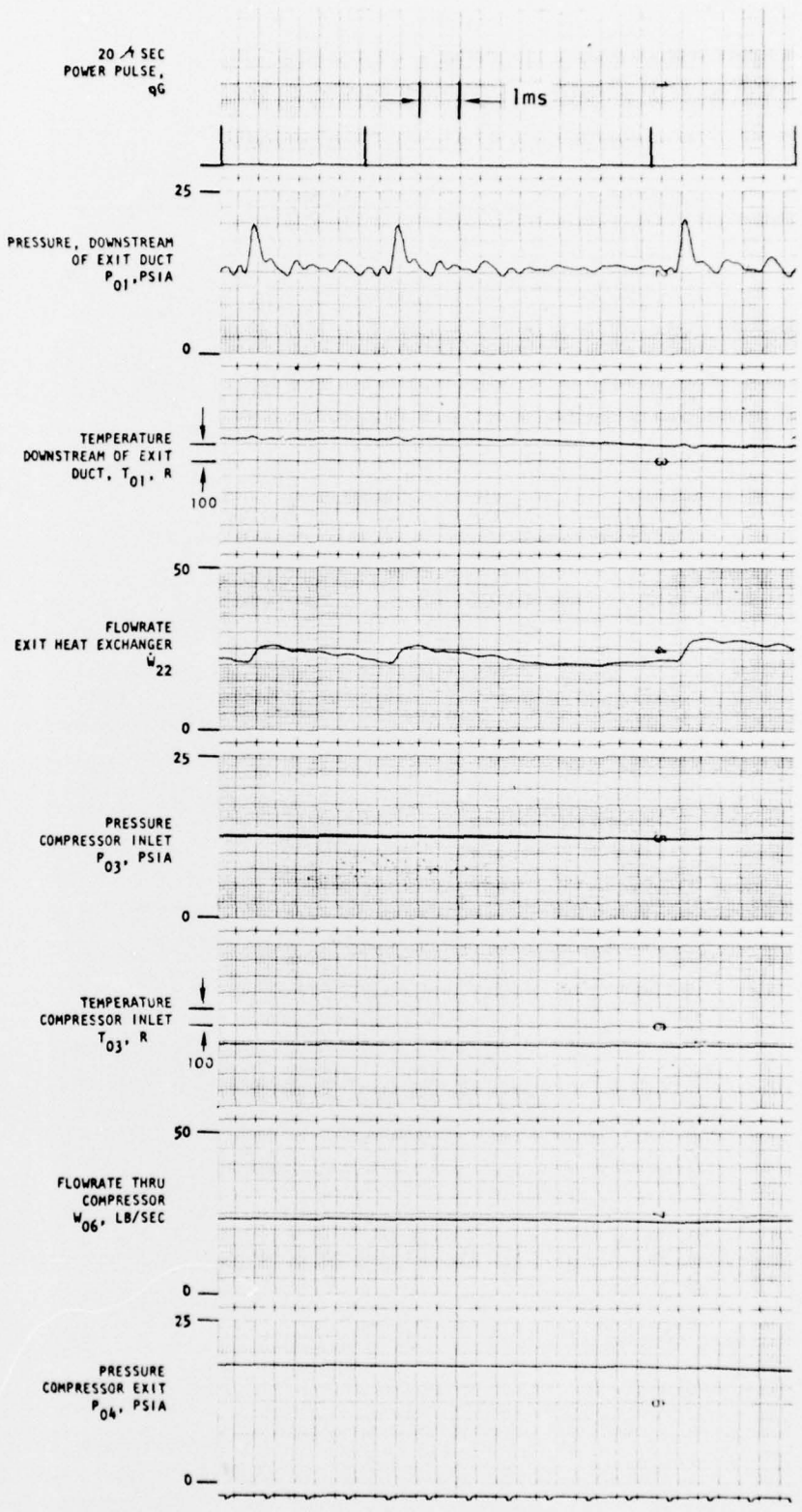
20 A SEC
POWER PULSE,
qG
1ms
25
PRESSURE, DOWNSTREAM
OF EXIT DUCT
P01, PSIA
0
TEMPERATURE
DOWNSTREAM OF EXIT
DUCT, T01, R
100
50
FLOWRATE
EXIT HEAT EXCHANGER
W22
0
25
PRESSURE
COMPRESSOR INLET
P03, PSIA
0
TEMPERATURE
COMPRESSOR INLET
T03, R
100
50
FLOWRATE THRU
COMPRESSOR
W06, LB/SEC
0
25
PRESSURE
COMPRESSOR EXIT
P04, PSIA
0

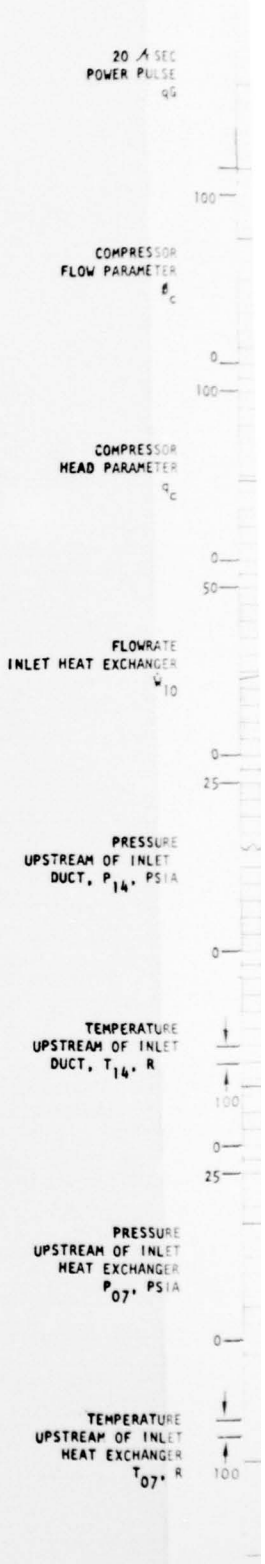
20 A SEC
POWER PULSE
qG
100
COMPRESSOR
FLOW PARAMETER
0
100
COMPRESSOR
HEAD PARAMETER
0
50
FLOWRATE
INLET HEAT EXCHANGER
W10
0
25
PRESSURE
UPSTREAM OF INLET
DUCT, P14, PSIA
0
TEMPERATURE
UPSTREAM OF INLET
DUCT, T14, R
100
0
25
PRESSURE
UPSTREAM OF INLET
HEAT EXCHANGER
P07, PSIA
0
TEMPERATURE
UPSTREAM OF INLET
HEAT EXCHANGER
T07, R
100

2

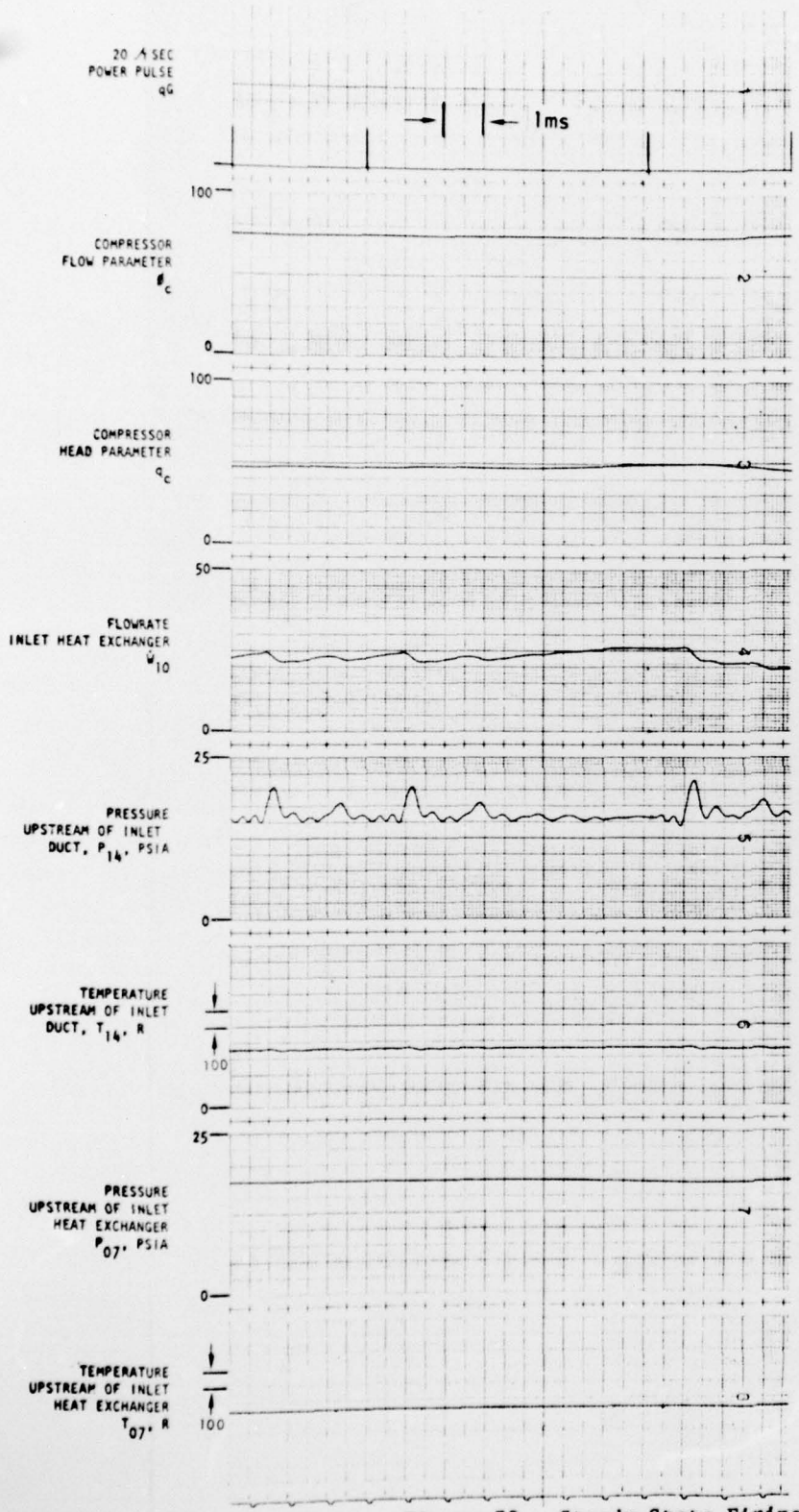

Figure 79. Steady-State Firing With Missed Pulse, Run 034